論文 / 著書情報
Article / Book Information

題目(和文)	担子菌シイタケ遺伝子の5'及び3'制御領域に存在するピリミジン/プリンに富む配列の構造と機能に関する研究
Title(English)	Studies on Structure and Function of Pyrimidine/Purine-Biased Sequences Originated from the 5'- and 3'-Regulatory Regions of Basidiomycete <I>Lentinus edodes</I> Genes
著者(和文)	山崎丘
Author(English)	TAKASHI YAMAZAKI
出典(和文)	学位:理学博士, 学位授与機関:東京工業大学, 報告番号:乙第3454号, 授与年月日:2000年6月30日, 学位の種別:論文博士, 審査員:
Citation(English)	Degree:Doctor of Science, Conferring organization: Tokyo Institute of Technology, Report number:乙第3454号, Conferred date:2000/6/30, Degree Type:Thesis doctor, Examiner:
学位種別(和文)	博士論文
Type(English)	Doctoral Thesis

Studies on Structure and Function of Pyrimidine/Purine-Biased Sequences Originated from the 5'- and 3'-Regulatory Regions of Basidiomycete *Lentinus edodes* Genes

Takashi Yamazaki

2000

Department of Life Science
Graduate School of Bioscience and Biotechnology
Tokyo Institute of Technology

Contents

Chapter 1

General introduction

The predominant and normal state of DNA is a duplex, right-handed B-DNA. However, the pyrimidine/purine (CT/AG)-biased sequences having a mirror repeat sequence have been known to form an intramolecular triplex structure (also called H-DNA) (Fig. 1.1, Wells *et al.*, 1988; Mirkin *et al.*, 1987; Shimizu *et al.*, 1990). An intramolecular triplex structure induced by a mirror repeat sequence can be formed with a portion of the CT-rich strand folded back and Hoogsteen base-paired in the major groove of the Watson-Crick double helix under highly negative superhelical density (Hanvey *et al.*, 1988; Wells *et al.*, 1988; Mirkin *et al.*, 1987; Shimizu *et al.*, 1990, see Fig. 1.1). The stability of the intramolecular triplex structure depends on the length of the mirror repeat, with longer repeats having greater stability for non-B conformations (Murchie and Lilley, 1992; Lyamichev *et al.*, 1989; Kohwi-Shigematsu and Kohwi, 1991), and the length of the DNA sequence between the two halves of the repeat is another important factor in stability, with a 3 ~ 6 bp loop region being most favored (Shimizu *et al.*, 1989). The canonical triplex structures are formed by the protonated CGC^+ base triads and the TAT base triads at low pH (Fig. 1.2). The cytosine residues protonated at low pH are necessary for stabilizing the CGC^+ base triads. The CGC^+ and TAT base triads consist of the canonical Watson-Crick G·C and A·T base pairs with attached thymine and protonated cytosine by the Hoogsteen base pairing.

As depicted in Fig. 1.3, two isomers, H-y5 and H-y3 are possible for an intramolecular triplex structure induced by the CT/AG-biased sequences having a mirror repeat sequence. In the former, the 5' half of the mirror repeat of the pyrimidine strand is the third strand, which interacts with the purine strand by

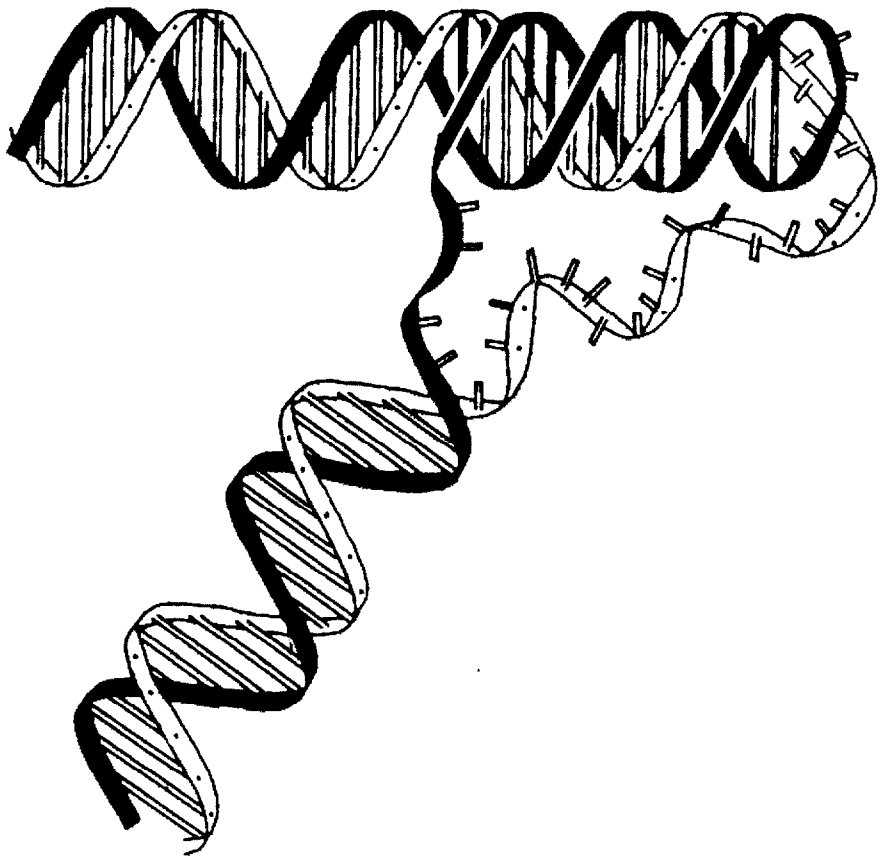

Figure 1.1 Model for an intramolecular triplex structure

DNA strands containing the pyrimidine-rich and purine-rich sequences are shown by black and white lines, respectively.

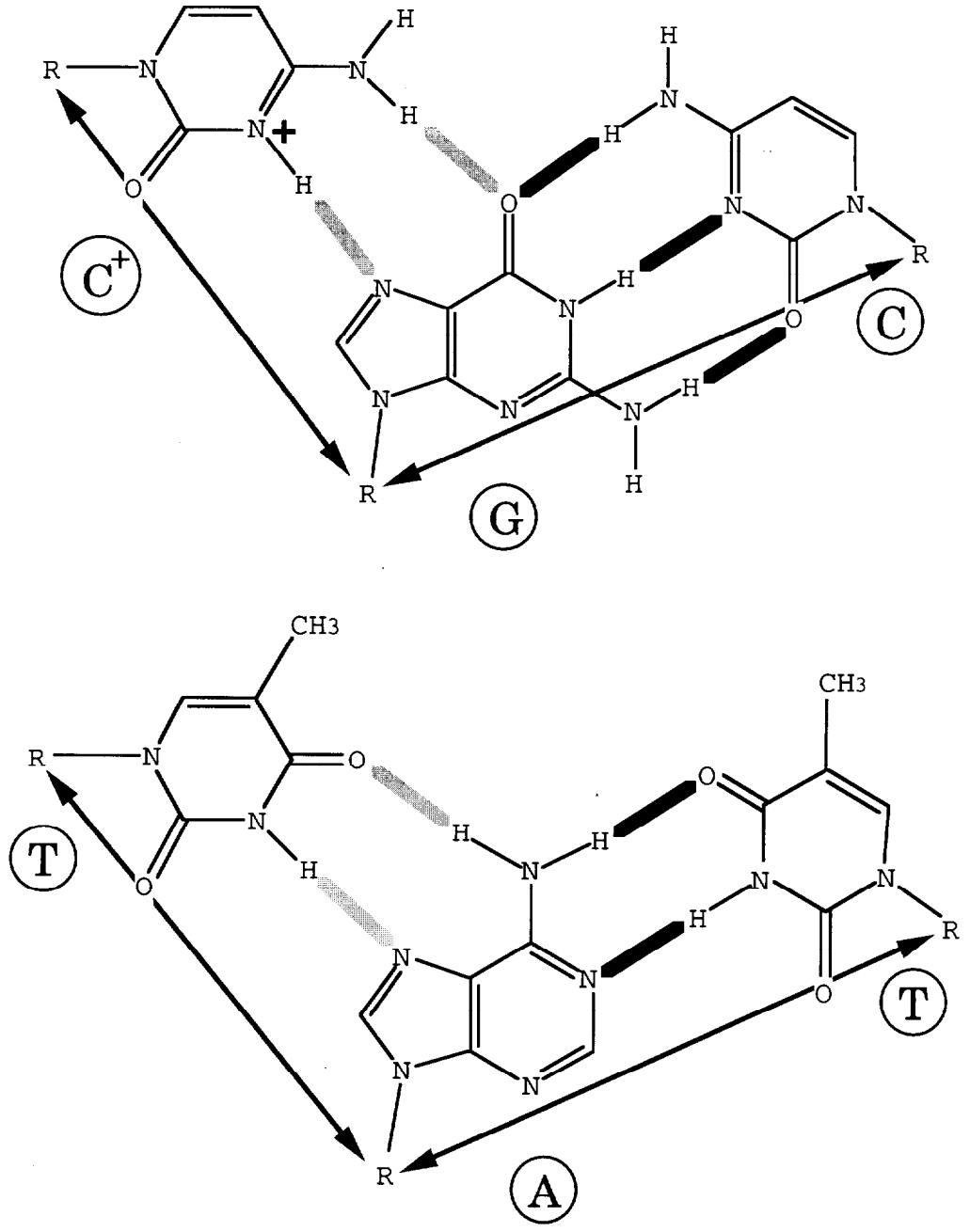

Figure 1.2 The CG·C$^+$ and TA·T base triads

The CT/AG-biased sequence having a mirror repeat sequence enable the specific association. The protonated site is marked by plus. The thick black and gray lines show the canonical Watson-Crick base pairing and the Hoogsteen base pairing, respectively. The two base-triads are isomorphous; the respective distances between glycosil bonds (arrows) are equal.

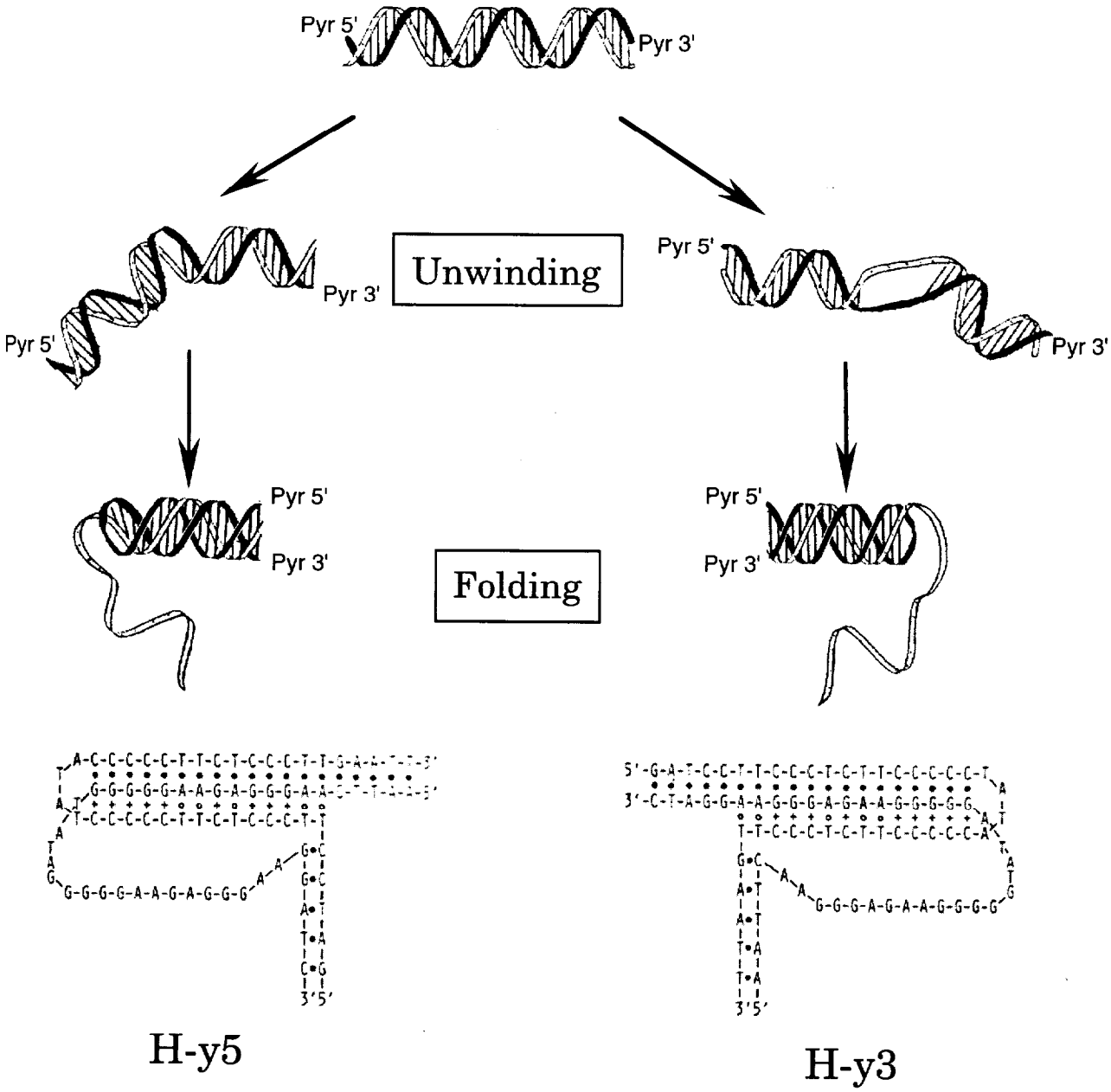

Figure 1.3 Representation of the formation of two possible isomers of an intramolecular triplex

Pyrimidine-rich strands and purine-rich strands are shown by black and white, respectively. The Watson-Crick base pairing (•), Hoogsteen base pairing (A∘T and C+G) are shown.

Hoogsteen base pairing, and in the latter, the 3' half of that of the pyrimidine strand is the third strand. It has been reported by analysis of chemical modification patterns of several CT/AG-biased sequences that only H-y3 isomer was formed by short CT/AG-biased sequences (< 40 bp), that is, specifically the 3' half of the mirror repeat of the pyrimidine strand was the third strand and the 5' half of that of the purine strand was unpaired (Hanvey *et al.*, 1988). It has been proposed that H-y3 formation requires a wide range of base-pair opening compared to that of H-y5 and it depends on sequences in the central region of CT/AG-biased sequences, in other words, between the two halves of mirror repeat whether an intramolecular triplex structure forms H-y5 or H-y3 isomer (Shimizu *et al.*, 1994). For example, if the sequence between two halves of mirror repeat is abundant in C and/or G residues (Shimizu *et al.*, 1994) or certain metal ions (Mg^{++}, Zn^{++}, Mn^{++} and Ca^{++}) are present at low pH (Kang *et al.*, 1992), an intramolecular triplex structure tends to form H-y5 isomer because the central interruption sequence of the mirror repeat (the loop) are more stabilized by GC base pairs or metal ions binding and it is difficult to open the Watson-Crick double helix widely (See Fig. 1.3).

Genomes of higher eukaryotes often contain CT/AG-biased sequences upstream as well as in coding regions of genes (Wells *et al.*, 1988). Some CT/AG-biased sequences have the capability of adopting non-B conformations, and in particular, an intramolecular triplex. These sequences have been postulated to play a role in regulation of replication (Baran *et al.*, 1991; Brinton *et al.*, 1991) and gene expression (Kohwi and Kohwi-Shigematsu, 1991), and in recombination (Weinreb *et al.*, 1990).

The pyrimidine-rich sequences found in the region around the transcriptional initiation site(s) of genes are called CT-motifs. The transcriptional initiation sites of various fungal genes, especially basidiomycetous fungal genes are often found in or near the CT-motifs (Gurr *et al.*, 1988). Table 1.1 summarizes the CT-motifs found in the 5'-promoter regions of basidiomycetous fungal genes. Besides core promoter

Table 1.1 CT-motifs found in the 5'-promoter regions of the basidiomycetous fungal genes.

Species	Gene	CT-motif	Position	CT : AG	Reference
A. bisporus	*gdhA*	TCTCTCAATCTTACCCCTCTCTTTTCTTCCCTTC	-48 → -15	31 : 3	Schaap, *et al.* 1996
	gdhB	CCTCCTCACTCCTCTCTTGTTATCCCCGCTCTCCCCTC	-60 → -23	34 : 4	Kersten, *et al.* 1999
	pkiA	TCCTCCATTCCACATCTCTCTCCTC	-35 → -11	22 : 3	(X97579)
C. cinereus	β1-tubulin gene	CCCTTTCTATTTCCTATCCCCT	-182 → -161	20 : 2	(AB000116)
	eln2	CCCCTCTCCCCTATTCGTTTTCCCCCTCCTCCCATTTCCC	-233 → -194	37 : 3	(AB013443)
		TTCCTTCATCTTCCCTC	-22 → -6	16 : 1	
	ras	TCTTCTTTCTTTCCCAAATCTTTTTCTTCTCTTTC	-55 → -21	32 : 3	Ishibashi and Shishido, 1993
	TRP1	CCTTTCTTTCCTTACCCC	-111 → -94	17 : 1	Skrzynia, *et al.* 1989
C. hirsutus	*ras*	CCTCTCCTCCCTCCCATTCCCGCCCTTC	-65 → -38	26 : 2	Our unpublished data
		CCCCCCTCCACCTCCTCCTCC	-32 → -12	20 : 1	
L. edodes	*mfbA*	CCTTTCTCTCTTATCTCT	-239 → -222	17 : 1	Kondoh, *et al.* 1995
		TCCTTTGCATCGCTGTTTTCCC	-195 → -174	17 : 5	
	priA	TTTCATCTCTCTCCCTCTCCTCTCTT	-85 → -60	25 : 1	Kajiwara, *et al.* 1992
	priB	CTCTCCCTCGTTTCTCCTCT	-109 → -90	19 : 1	Endo, *et al* . 1994
	ras	TTCTACCCGCTTTTCCCATCTTCCCCTTTA~	-165 → -104	55 : 7	Hori, et al. 1991
		~TTCTTTGGTTGTCCTTCTTCTTCTTCTTTTCC			
	uck1	TCATCCTCTTGTACCTCCTTCTCGTCCTC	-46 → -18	25 : 4	Kaneko, *et al* . 1998
S. commune	*bar1*	TCCCCTCCGCTACTTCCTCCTCCCTCT	-175 → -149	25 : 2	Wendland and Kothe, 1996
	G-protein	TCTCTCCTTTGTTCTCCTCCCCGCGCCCCT~	-92 → -50	38 : 5	(AF157495)
	α subunit gene	~CCGCTGCCCTCTC			
	laccase gene	TTTCCCTTCTCGCCTCCTT	-73 → -55	18 : 1	(AB015758)
	sc3	CCCTTCCTTCCTTCGCTATCCTTCCTT	-41 → -15	25 : 2	Schuren and Wessels, 1990
	sc4	TCTTTGCTCTTCACCCCGCTTCTC	-40 → -17	21 : 3	Schuren and Wessels, 1990
	sc6	CTTTTCCTGACTTGCTTTTCGTTCT	-38 → -14	21 : 4	(AJ007504)

Positions of the 5' end of CT-motifs are given in bp from the A (+1) of the translation initiation codon.
For references, accession No. in parentheses are shown for the sequence data reported only in the DDBJ/EMBL/GenBank Nucleotide Sequence Databases.

elements such as GC box, CAAT box and TATA box, CT-motifs have been postulated to function as one of the promoter components in fungal genes. However, structure-biological function relationships have not been well studied for these sequences.

Here, to clarify the functional role for the expression of transgenes in basidiomycetes, the author studied the CT/AG-biased sequences having a mirror repeat sequence originated from the 5'- and 3'-regulatory regions of genes isolated from one of the most popular basidiomycetes *L. edodes*. The non-B, unusual structures formed in the CT/AG-biased sequences were analyzed, suggesting that the mirror repeat plays an important role for expression of the promoter activity toward a transgene in basidiomycetes. This is the first report showing that a non-B, unusual DNA structure induced by the CT/AG-biased sequences having a mirror repeat sequence, possibly an intramolecular triplex structure, are responsible for the expression of the promoter activity of basidiomycetous fungal gene *in vivo*.

Chapter 2

Promoters of *L. edodes ras* and *priA* genes and their use for construction of novel heterologous protein expression vectors in basidiomycetous fungi

2.1 Introduction

Our group has previously isolated the *ras* and *priA* genes from one of the most popular edible basidiomycetes, *L. edodes* (Hori *et al.*, 1991; Kajiwara *et al.*, 1992). The *Le. ras* gene was transcribed at similar higher levels during vegetative growth and all stages of fruiting development (Hori *et al.*, 1991). An analysis of the nucleotide sequence of the *Le.ras* promoter revealed that the promoter region contains a CAAT box (Breathnach and Chambon, 1981), a CACCC box (Myers *et al.*, 1986b), two consecutive TATAAA boxes (Breathnach and Chambon, 1981) and a 62-bp CT-motif (Gurr *et al.*, 1988) in 5' to 3' order (Fig. 2.1). On the other hand, the *priA* gene was actively transcribed in earlier developmental stages of fruiting (Kajiwara *et al.*, 1992) and the *priA* promoter region was shown to contain a GGGCGG box (Kadonaga *et al.*, 1986), CCAAT box, TATAAA box and a 26-bp CT-motif in 5' to 3' order (Fig. 2.2). Primer extension analysis revealed that transcription of the *Le. ras* gene and the *priA* gene start from three (one major and two alternative) and two transcriptional initiation sites, respectively. Interestingly, one major transcriptional initiation site of the *Le.ras* gene and the downstream transcription initiation site of the *priA* gene are within the CT-motif (Kajiwara and Shishido, 1992; Kajiwara *et al.*, 1992). In this chapter, the *Le.ras* and *priA* promoter activities were assessed in the rapidly growing basidiomycete *Coprinus cinereus* by using the manganese (II) peroxidase (MnP) gene derived from *P. ostreatus* as a reporter gene.

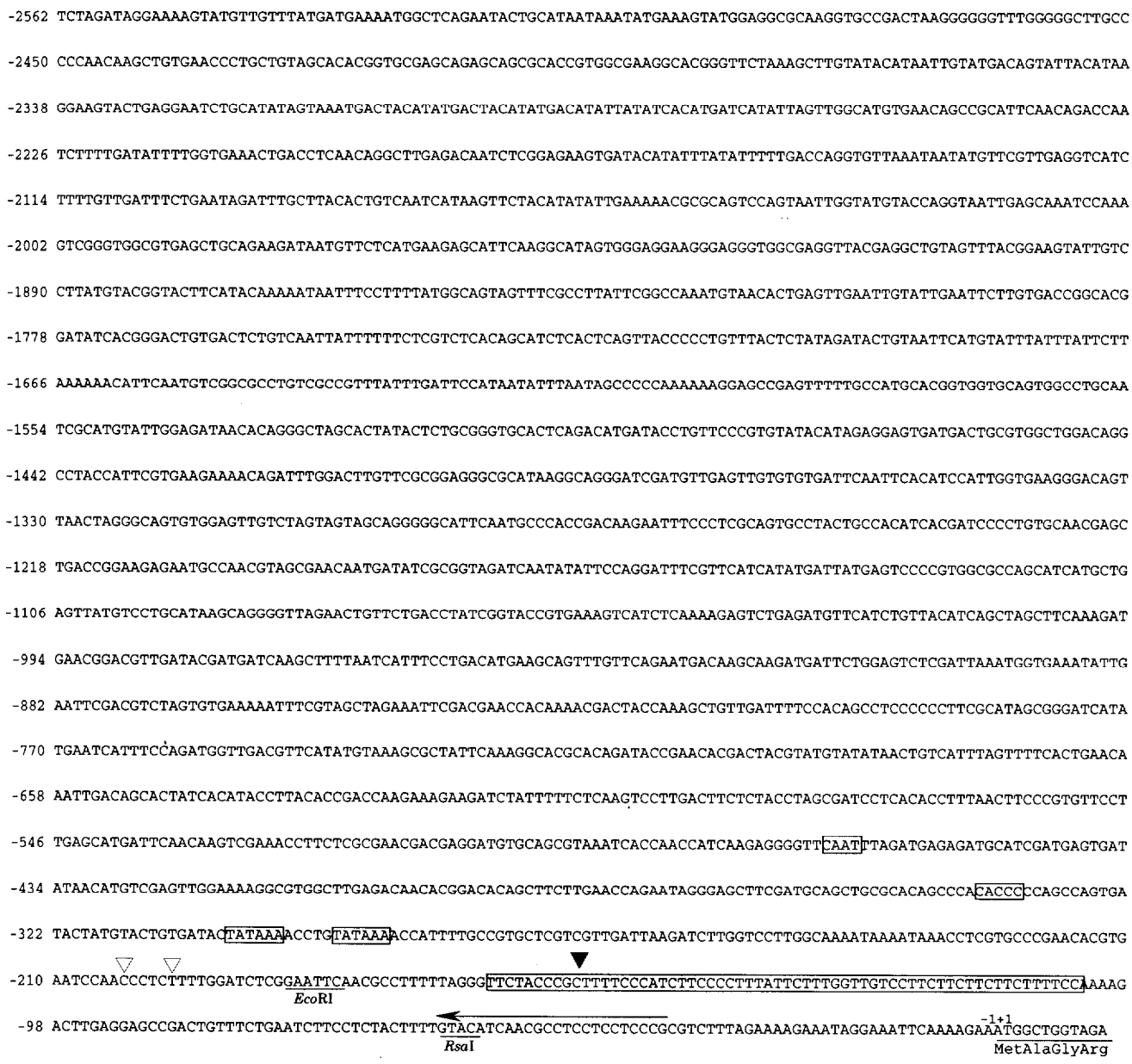

Figure 2.1 The nucleotide sequence of the 5'-promoter region of the *L. edodes ras* gene

The 62-bp CT-motif, CAAT box, CACCC box, TATAAA boxes are boxed. The mirror repeat sequences involved in the formation of the deduced intramolecular triplex structure are shaded (see Chapters 3 and 6). Major and two alternative transcriptional initiation sites are indicated by closed and open arrowheads, respectively. The complementary sequence to the primer used for the construction of pLC1 is shown by a horizontal long arrow. The nucleotide sequence coordinats are presented on the left-hand side. The start codon assigned the +1 coordinates. Restriction sites used for an isolation of the CT-motif are also shown (see Chapter 3). The sequence data will appear in the DDBJ/EMBL/GenBank nucleotide sequence databases under accession No. D10987.

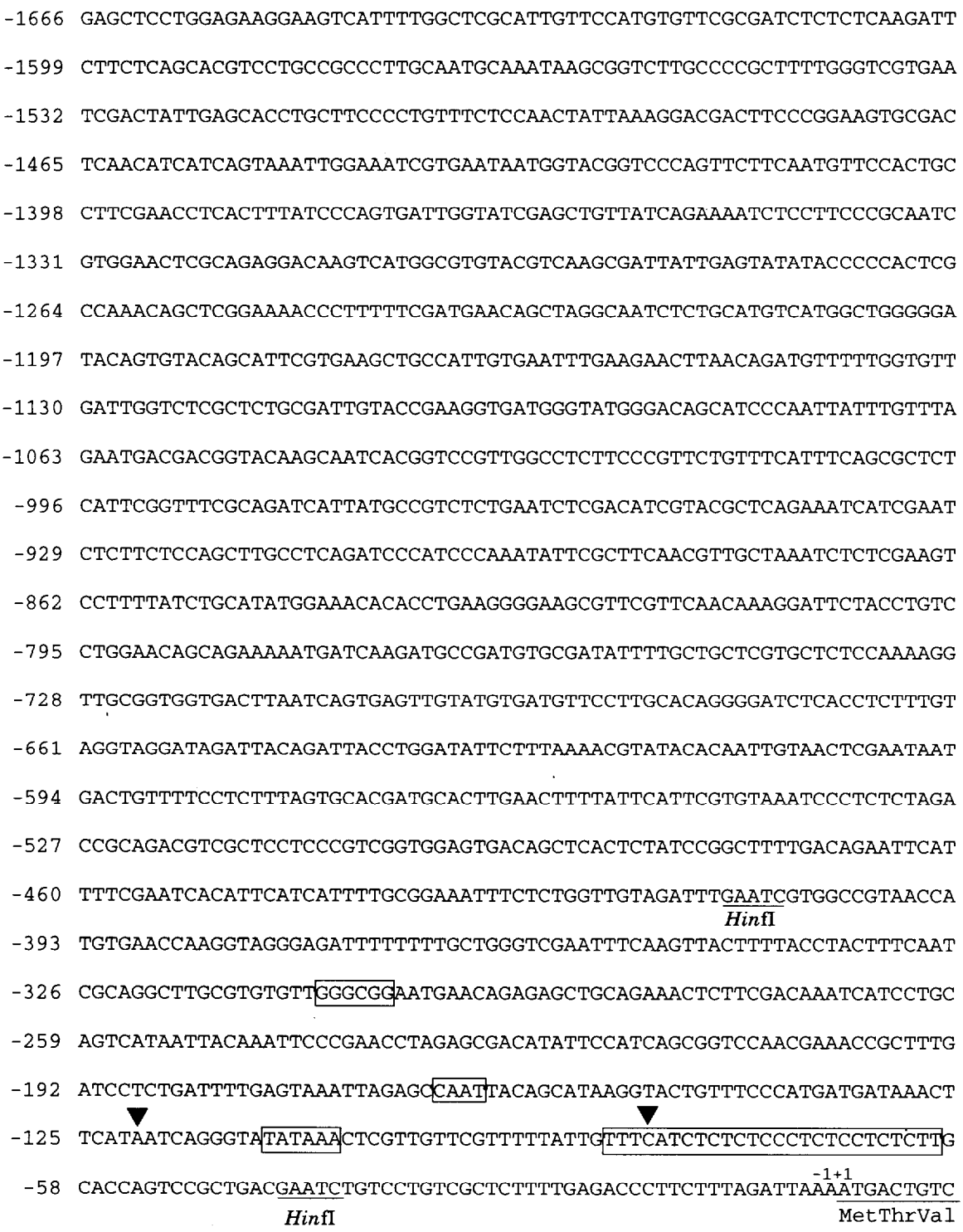

Figure 2.2 The nucleotide sequence of the 5'-promoter region of the *L. edodes priA* gene

GGGCGG box, CAAT box, TATAAA boxes and the 26-bp CT-motif are boxed. The mirror repeat sequences involved in the formation of the deduced intramolecular triplex structure are shaded (see Chapter 4 and 6). Two alternative transcriptional initiation sites are indicated by closed arrowheads. The *Hin*fI sites used for the construction of pLC2 is shown. The nucleotide sequence coordinates are presented on the left-hand side. The start codon assigned the +1 coordinates. The sequence data will appear in the DDBJ/EMBL/GenBank nucleotide sequence databases under accession No. X60956.

2.2 Materials and methods

2.2.1 Strains and media

C. cinereus monokaryotic strain LT2-44 (*trp1-1, trp1-6*), kindly provided by Dr. S. Yanagi of NFRI at Tsukuba (originally provided by Dr. L.A. Casselton of University of Oxford), was used as the recipient in transformation experiments. *P. ostreatus* IFO30160, a dikaryotic strain, was from the culture collection of the Institute of Fermentation Osaka. MYG medium (1 % malt extract, 0.4 % yeast extract, 0.4 % glucose, pH 5.6) containing 100 μg of tryptophan per ml, when required, was used for the growth of *C. cinereus* and *P. ostreatus*. Regeneration medium (pH 6.0) used for *C. cinereus* protoplasts contained 171 g sucrose, 5 g glucose, 2 g asparagine, 40 μg thiamin, 1 g KH_2PO_4, 2.25 g $Na_2HPO_4 \cdot 12H_2O$, 1.5 g NH_4Cl, 0.29 g Na_2SO_4, 0.25 g $MgSO_4 \cdot 7H_2O$, 5 g soluble starch per 1 liter. Construction, propagation, and amplification of recombinant plasmids were carried out in *Escherichia coli* JM109 (Yanisch-Perron *et al.*, 1985). *E. coli* was cultured in LB medium.

2.2.2 Plasmid construction

pLC1 was previously constructed (Kajiwara, 1993) and pLC2 was constructed as follows. The 0.37-kb *Hin*fI fragment containing the *priA* core promoter elements was ligated to the *Bam*HI adaptor (5'-CCGGATCCGG) and inserted into the *Bam*HI site of pBR322. In this plasmid, the orientation of the *priA* core promoter elements are contrary to the tetracycline-resistance gene (*tet*) of pBR322. The recombinant plasmid was partially digested with *Bam*HI to convert the DNA to a linear form and recircularized by self-ligation after the ends had been filled-up. By these treatments, the junction between the 5'-regulatory sequence of the *priA* basal promoter and pBR322 sequence converted to be *Bam*HI-uncleavable sequence. pLC1 was digested with *Bam*HI and *Hin*dIII and the 1.2-kb *Bam*HI - *Hin*dIII fragment containing the *priA* terminator sequence (Fig. 2.3) was

inserted between the *Bam*HI and *Hin*dIII sites of the pBR322 derivative containing the *priA* basal promoter sequence, yielding pLC2. Plasmid pMOSBlue-*mnp*, containing the 1274-bp sequence of MnP cDNA (*mnp*c) (Fig. 2.4) derived from *P. ostreatus* IFO30160 between *Xba*I and *Bam*HI sites on pMOSBlue T-vector (Amersham), was digested with *Xba*I and ligated to *Bam*HI adaptor (5'-CCGGATCCGG) after filling up the ends. Thus the *P. ostreatus mnp*c was obtained as a 1.3-kb *Bam*HI fragment and inserted into the *Bam*HI *site* of pLC1 and pLC2, yielding pLC1-mnp and pLC2-mnp (Fig. 2.5). Plasmid pCc1001 used for co-transformation with pLC1-mnp or pLC2-mnp is the pUC9-based vector carrying the 6.5-kb *Pst*I genomic fragment containing *C. cinereus* tryptophan synthetase gene (*TRP1*) (Binninger *et al.*, 1987).

2.2.3 Transformation of *C. cinereus*

Oidia (~ 10^9 cells) were harvested from a single plate culture of LT2-44 and germinated at 30°C for 48 ~ 60 h without shaking in 30 ml of MYG medium supplemented with tryptophan. The cells were harvested by centrifugation at 750 × g for 5 min at room temperature and washed once with 10 ml of MM buffer (0.5 M mannitol in 50 mM maleate, pH 5.5). The washed cells were suspended in 1 ml of the MM buffer containing 10 mg of Novozyme 234 (Calbiochem) and 1 mg of Chitinase-RS (Pias Co., Japan) and incubated at 30°C for 2 h. The protoplasts were separated from cell debris by filtering through 60 μm pore nylon mesh, washed once with 10 ml of MM buffer and once with 10 ml of MMC (MM containing 50 mM $CaCl_2$), and resuspended in 1 ml of MMC to give 1 ~ 2 × 10^8 cells per 1 ml. Transformations were essentially carried out as described by Binninger *et al.* (1987). To 200 μl of protoplast suspension were added 20 μl of plasmid DNA (4 μg) in TE buffer (10 mM Tris-HCl, 1 mM EDTA, pH 8.0) and 50 μl of PEG solution (25% PEG4000, 50 mM $CaCl_2$ in 10 mM Tris-HCl pH 7.5) in 15 ml polypropylene conical tubes. The tubes were placed in ice for 20 min and then 2 ml of PEG was

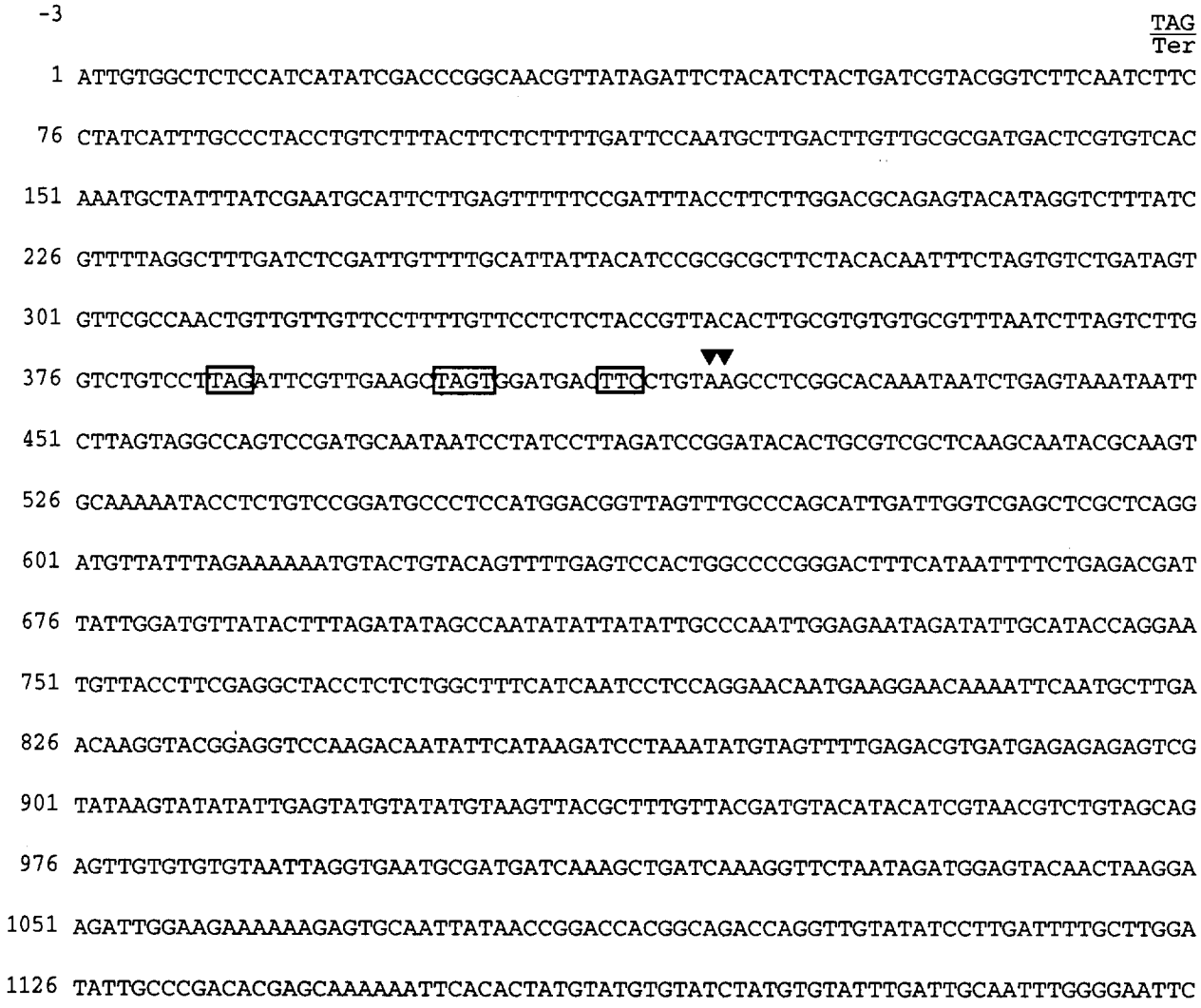

Figure 2.3 The nucleotide sequence of the terminator region of the *L. edodes priA* gene

Transcriptional termination signals and poly (A) addition signals in *S. cerevisiae* are boxed. The termination codon (Ter) of the *priA* gene is shown. The poly (A) addition sites are indicated by closed arrowheads. The nucleotide sequence coordinats are presented on the left-hand side. The nucleotide next to the termination codon of the *priA* gene is assigned the +1 coordinate. The sequence data will appear in the DDBJ/ EMBL/GenBank nucleotide sequence databases under accession No. DX60956.

```
-30 GTCTTACCGCAGTCGCATCCCTACATCGCAATGACCTTTGCTTCGCTTTCTGCGCTCGTC
                                    MetThrPheAlaSerLeuSerAlaLeuVal   10

 31 CTTGTCTTCGCTGTGACTGTCCAAGTCGCTCAAGCCGTATCTTTGCCTCAGAAACGCGCA
    LeuValPheAlaValThrValGlnValAlaGlnAlaValSerLeuProGlnLysArgAla   30

 91 ACTTGTGCTGGTGGACAAGTTACCGCCAACGCGGCCTGTTGTGTTCTGTTCCCGCTCATG
    ThrCysAlaGlyGlyGlnValThrAlaAsnAlaAlaCysCysValLeuPheProLeuMet   50

151 GAAGACCTGCAGAAGAACCTGTTCGACGACGGCGCATGCGGCGAAGATGCCCATGAAGCC
    GluAspLeuGlnLysAsnLeuPheAspAspGlyAlaCysGlyGluAspAlaHisGluAla   70

211 CTTCGCCTGACCTTCCACGACGCTATTGGATTCTCTCCTTCCAGGGGTGTTATGGGAGGC
    LeuArgLeuThrPheHisAspAlaIleGlyPheSerProSerArgGlyValMetGlyGly   90

271 GCCGATGGCTCTGTCATCACATTCTCCGATACTGAGGTCAACTTCCCAGCCAACCTCGGT
    AlaAspGlySerValIleThrPheSerAspThrGluValAsnPheProAlaAsnLeuGly  110

331 ATTGACGAGATCGTCGAGGCTGAGAAACCGTTCCTTGCAAGGCACAACATCTCCGCAGGC
    IleAspGluIleValGluAlaGluLysProPheLeuAlaArgHisAsnIleSerAlaGly  130

391 GATTTGGTTCACTTCGCCGGCACCCTCGCTGTTACCAACTGTCCTGGTGCTCCACGAATC
    AspLeuValHisPheAlaGlyThrLeuAlaValThrAsnCysProGlyAlaProArgIle  150

451 CCGTTCTTCTTAGGTCGCCCTCCTGCCAAGGCCGCATCACCCATTGGATTGGTTCCGGAA
    ProPhePheLeuGlyArgProProAlaLysAlaAlaSerProIleGlyLeuValProGlu  170

511 CCATTCGATACCATTACAGATATCCTGGCCCGAATGGATGACGCTGGATTCGTCTCTGTC
    ProPheAspThrIleThrAspIleLeuAlaArgMetAspAspAlaGlyPheValSerVal  190

571 GAGGTTGTCTGGCTTCTTTCCGCCCACTCTGTCGCTGCAGCTGACCATGTTGACGAAACT
    GluValValTrpLeuLeuSerAlaHisSerValAlaAlaAlaAspHisValAspGluThr  210

631 ATTCCTGGAACGCCGTTCGACTCAACGCCAAACCTTTTCGATTCACAAATCTTCATCGAG
    IleProGlyThrProPheAspSerThrProAsnLeuPheAspSerGlnIlePheIleGlu  230

691 ACGCAACTCCGTGGAATTTCCTTCCCAGGCACTGGTGGGAATCACGGCGAAGTACAATCC
    ThrGlnLeuArgGlyIleSerPheProGlyThrGlyGlyAsnHisGlyGluValGlnSer  250

751 CCACTCAAGGGTGAAATGAGACTCCAGTCAGATCACTTGTTCGCTCGAGACGATAGGACA
    ProLeuLysGlyGluMetArgLeuGlnSerAspHisLeuPheAlaArgAspAspArgThr  270

811 TCCTGCGAATGGCAGTCCATGACTAATGATCAACAGAAGATCCAAGACCGCTTTTCCGAC
    SerCysGluTrpGlnSerMetThrAsnAspGlnGlnLysIleGlnAspArgPheSerAsp  290

871 ACACTGTTCAAGATGTCGATGCTTGGACAGAACCAGGACGCCATGATCGATTGCTCCGAT
    ThrLeuPheLysMetSerMetLeuGlyGlnAsnGlnAspAlaMetIleAspCysSerAsp  310

931 GTCATCCCTGTCCCCGCTGCCCTTGTAACCAAACCCCATCTCCCCGCCGGGAAGAGTAAG
    ValIleProValProAlaAlaLeuValThrLysProHisLeuProAlaGlyLysSerLys  330

991 ACCGACGTTGAACAAGCCTGTGCCACCGGCGCCTTCCCAGCCCTCGGTGCTGACCCTGGC
    ThrAspValGluGlnAlaCysAlaThrGlyAlaPheProAlaLeuGlyAlaAspProGly  350

1051 CCAGTCACCTCTGTTCCTCGTGTCCCACCTGCGTAAGCAAAGTGGACGATGTGACTATAT
     ProValThrSerValProArgValProProAla***                         361
```

Figure 2.4 The nucleotide sequence of the *P. ostreatus* MnP cDNA (*mnpc*) and the deduced amino acid sequence

Isolation of *mnpc* and determination of the DNA sequence were done by Asada *et al.* (1995). The nucleotide sequence coordinates and amino acid sequence coordinates are presented on the left-hand side and right-hand side, respectively. The start codon assigned the +1 coordinates. The sequence data will appear in the DDBJ/EMBL/GenBank nucleotide sequence data bases under accession No. U21878 and U21879.

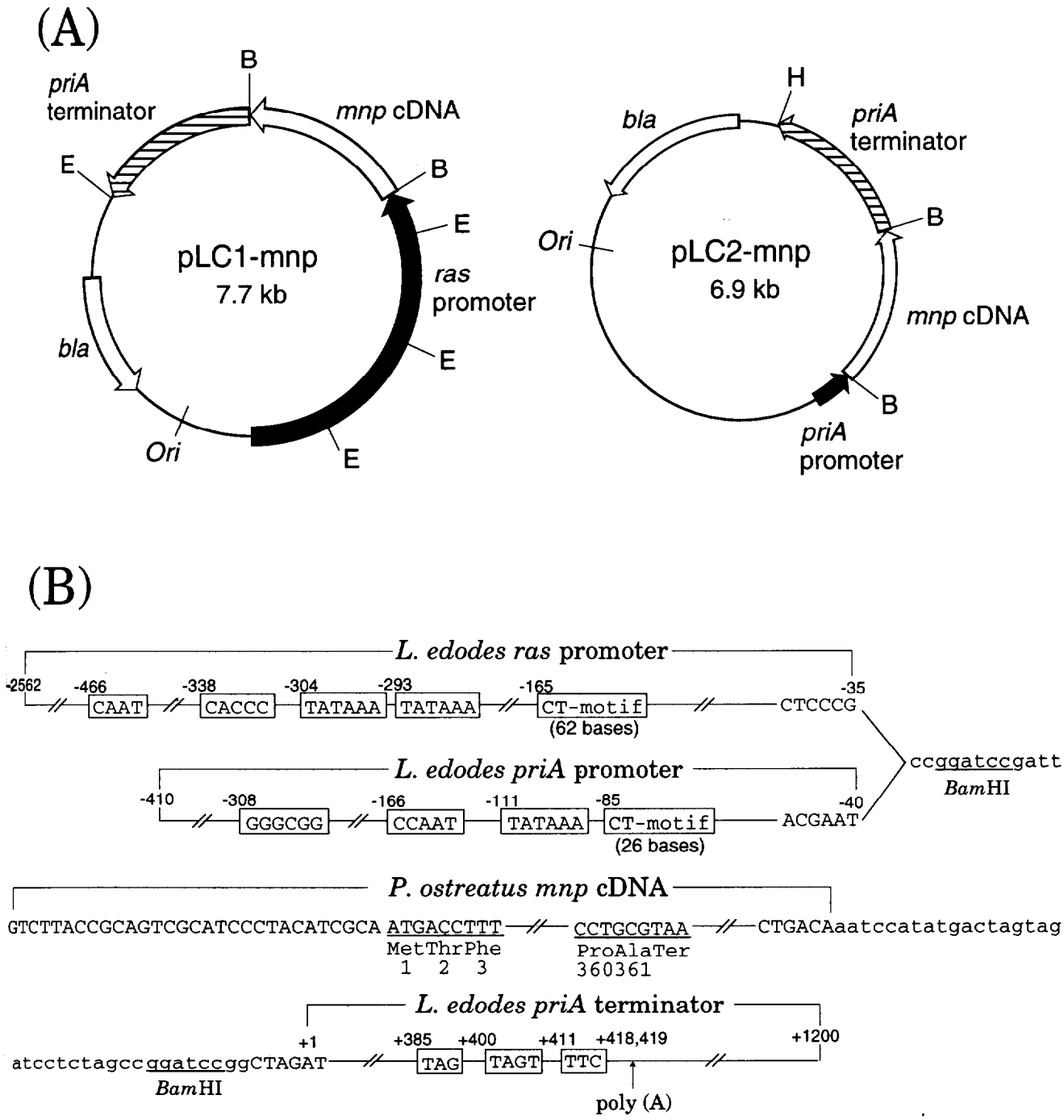

Figure 2.5 Structures of the *P. ostreatus* MnP-expressing recombinant plasmids pLC1-mnp and pLC2-mnp

Structures of pLC1-mnp and pLC2-mnp (A), and the structural features of the *ras* and *priA* promoters and *priA* terminator and the nucleotide sequences at the fusion junction between the promoters, *P. ostreatus mnp* cDNA, and the terminator are shown (B). In (A), thin lines are pUC19 (for pLC1-mnp) or pBR322 (for pLC2-mnp). The abbreviations are; B, *Bam*HI; E, *Eco*RI; H, *Hin*dIII. In (B), the conserved sequences of eukaryotic promoter and terminator and CT-motifs are boxed and shaded, respectively. The numbers in the promoter regions and terminator region refer to the nucleotide positions relative to the first nucleotide (+1) of the start codon and to the nucleotide (+1) next to the termination codon, respectively.

added. The protoplasts were incubated at room temperature for 5 min. To regenerate the protoplasts, 1.0 ml aliquots were mixed with 10 ml of the regeneration medium containing 0.7 % agar (kept molten at 50 ~ 55°C) and poured over a layer of the regeneration medium containing 1.5 % agar in 9 cm plastic plates. The plates were inverted and incubated at 30°C. Colonies were examined after 10 - 14 days.

2.2.4 DNA isolation and Southern-blot analysis

Genomic DNAs of *C. cinereus* and *P. ostreatus* were isolated as described by Zolan and Pukkila (Zolan and Pukkila, 1986). Plasmid DNAs were isolated from *E. coli* by the alkaline lysis method and purified by centrifugation to equilibrium in cesium chloride-ethidium bromide gradients (Sambrook *et al.*, 1989). The undigested and *Bam*HI-digested genomic DNAs (20 μg each) were fractionated on a 0.8 % agarose gel, transferred to a nylon membrane (Hybond-N, Amersham Pharmacia Biotech.) by the method of Southern (Southern, 1975). Probes were labeled with [α-^{32}P]dCTP using a Random Primer DNA Labeling Kit Ver. 2 (Takara Shuzo Co., Japan) according to the manufacturer's instruction. The filter was hybridized under stringent condition according to the method previously described (Hori *et al.*, 1991) and autoradiographed.

2.2.5 Assessment of lignin degradation

Ten ml of MYG medium containing 10 mg of lignin (Tokyo-kasei Kôgyo, Japan) and 2.5 mg of $MnCl_2$ in an L-shaped tube was inoculated with three / (7 x 7x 1 mm) cubes of the MYG agar colonized with *C. cinereus* mycelium and cultivated at 30°C for the indicated periods with shaking. Degradation of lignin was determined by the decrease of the absorbance at 275 nm of the supernatant, which shows the degradation of the aromatic rings. The decrease of the absorbance at 480 nm was measured for decolorization of lignin (brown color). The absorbance of the cultured

medium containing 10 mg / 10 ml lignin was 27.15 at 275 nm and 2.19 at 480 nm, and these values were taken as 100 %.

2.3 Results and discussion

2.3.1 Expression of the MnP gene in *C. cinereus* under control of the *Le.ras* and *priA* promoter

To express the foreign genes in basidiomycetes, two choromosome-integrating vectors, pLC1 (Kajiwara, 1993) and pLC2 were constructed. pLC1 (6.4 kb) is the pUC19-based vector carrying the *Le.ras* promoter (2.5 kb, see Fig. 2.1) and the *priA* terminator (1.2 kb, see Fig. 2.3) consisting of sequence required for both transcriptional termination and polyadenylation (Zaret and Sherman, 1982). pLC2 (5.6 kb) is the pBR322-based vector carrying the *priA* basal promoter (0.37 kb, see Fig. 2.2) and its terminator. Both vectors contains the *Bam*HI-cloning site between the promoter and terminator. Our group has already shown that not only in *L. edodes* but also in heterologous basidiomycetous fungi, *Pleurotus ostreatus*, the *Le.ras* promoter of pLC1 efficiently expresses the *E. coli* transposon Tn903-derived aminoglycoside phosphotransferase type 1 gene (*aph1*) (Kajiwara, 1993), the *E. coli* ß-glucronidase (GUS) gene and the *Streptomyces hygroscopicus* derived phosphinotricin acetyltransferase gene (*bar*).

In this study, pLC1-mnp and pLC2-mnp containing the manganese (II) peroxidase (MnP) cDNA (*mnpc*, see Fig. 2.4) derived from *P. ostreatus* as a reporter gene were constructed (Fig. 2.5). MnP is a key peroxidase in the degradation of lignin in *P. ostreatus* (Asada *et al.*, 1995) and its activities are measured easily. These recombinant plasmids were introduced into the *C. cinereus* LT2-44 (*trp1-1, 1-6*) genome by co-transforming with pCc1001 carrying the *C. cinereus TRP1* gene and selecting for Trp^+ transformants. For each experiment 4 µg each of pCc1001 and pLC1-mnp or pLC2-mnp were presented to 2×10^7 total protoplasts. From

two independent co-transformations a total of about 60 Trp^+ colonies were obtained at a frequency 5 to 10 per μg of transforming pCc1001 DNA in both cases of pLC1-mnp and pLC2-mnp. Thirteen each Trp^+ colonies were selected at random and cultivated on MYG agar plates. To assess the expression of the MnP genes by the *Le.ras* and *priA* promoters, the mycelial colonies grown on the plates were screened for a lignin-decolorization activity in MYG liquid medium containing 0.1 % lignin and 0.025 % $MnCl_2$, obtaining two each Trp^+ transformants which show the clearly higher activities than that of the recipient. The two Trp^+ MnP^+ transformants derived from the introduction of pLC1-mnp were named TF1-2 and TF1-4 and those of pLC2-mnp were TF2-1 and TF2-7.

To ascertain the presence of the introduced DNAs in the transformants, Southern-blot analysis was done using the ^{32}P-labeled 1.3-kb *Bam*HI fragment containing the *P. ostreatus mnpc* as a probe (see Fig. 2.5). In the DNA samples of the four Trp^+ MnP^+ transformants without restriction enzyme digestion, specific hybridization signals were observed at the high-molecular weight DNA region corresponding to the chromosomal DNA region (data not shown). No specific hybridization signal was found in the DNA sample of the Trp^+ transformant obtained by introduction of pCc1001 DNA alone. Similar results were obtained by using the ^{32}P-labeled probe of pUC19 or pBR322.

Next, all the DNA samples were digested with *Bam*HI and subjected to Southern-blot analysis using the aforementioned ^{32}P-labeled 1.3-kb *mnpc* probe. As shown in Fig. 2.6, TF2-1, TF2-7, TF1-2, and TF1-4 all gave one intense hybridization signal at the position corresponding to the size (1.3 kb) of the probe. No hybridization signal was observed in the case of the Trp^+ transformant (lane 5). The *Bam*HI-digest of the DNA of *P. ostreatus* IFO30160, from which the *mnpc* was derived, was also analyzed. It gave a single faint band at the position of 9 kb

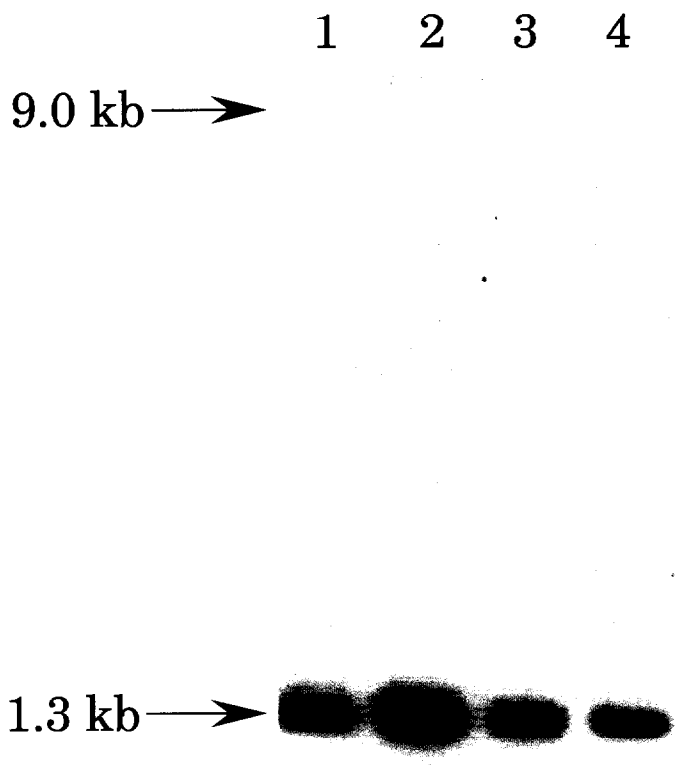

Figure 2.6

Southern-blot analysis of the *Bam*HI-digests of total DNAs prepared from the four Trp^+ MnP^+ transformants of *C. cinereus*.

Lane 1, TF2-1; lane 2, TF2-7; lane 3, TF1-2; lane 4, TF1-4; lane 5, DNA from the control Trp^+ transformant of *C. cinereus* ; lane 6, DNA from *P. ostreatus* IFO30160. The 1.3-kb *Bam*HI fragment containing the *P. ostreatus mnp*c was used as a probe.

(lane 6). These results suggest that the introduced pLC1-mnp and pLC2-mnp DNAs had been integrated into chromosomal DNAs of the four Trp^+ MnP^+ transformants.

Comparison of the radioactivities the sum of both intense (1.3 kb) and faint (2.6 kb) hybridization bands with the activity of the single band of *P. ostreatus* IFO30160 suggests that TF2-1, TF2-7, TF1-2, and TF1-4 carry 6, 10, 6, and 5 copies of the *mnpc* sequence. The same aliquot of DNA as that used in the above experiments was taken out from each of the DNA preparations of the transformants and *P. ostreatus* IFO30160 and all were digested with both *Xho*I and *Sal*I. The digests were subjected to Southern-blot analysis using the probe of ^{32}P-labeled 1.3-kb *Xho*I - *Sal*I genomic fragment containing the *C. cinereus ras* gene (Ishibashi and Shishido, 1993). The four Trp^+ MnP^+ transformants and control Trp^+ transformant all gave one faint signal at the position of around 1.3-kb (data not shown). Their intensities were almost the same and similar to the intensity of the 9-kb signal in the *Bam*HI-digest of *P. ostreatus* IFO30160 (lane 6 of Fig. 2.6). These results suggest the equal loading and transfer of DNA preparations and satisfactory estimates of the copy numbers of *mnpc* sequence for the four transformants.

These results showed that *P. ostreatus* MnPs were produced in *C. cinereus* transformants, suggesting that the *mnpc* sequences introduced into the chromosomes with pLC1 and pLC2 sequences were expressed efficiently under the controls of the *Le.ras* and *priA* promoters.

2.3.2 The assessment of the *Le. ras* and *priA* promoter activities in *C. cinereus* by the measurement of the lignin-decolorization and -degradation

TF2-7 containing the most high copy number of the *mnpc* sequence and the control Trp^+ transformant were cultured in 10 ml of MYG liquid medium containing 0.1% lignin and 0.025% $MnCl_2$ in an L-shaped tube at 30°C with shaking. Triplicated tubes were prepared and used for cultivation. After the indicated periods, 0.3 ml aliquots were taken out from each of the three cultures and mixed, followed by centrifugation. The supernatants were investigated for decolorization of the brown color of lignin by measuring the decrease of the absorbance at 480 nm (Fig. 2.7A) and degradation of the aromatic rings of lignin by measuring the decrease of the absorbance at 275 nm (Fig. 2.7B). Decolorization and degradation of lignin by TF2-7 were completed after 16 days of cultivation, while only 35 - 40% of lignin was decolored and degraded by the control (Fig. 2.8). Similar results were obtained in both MY medium (without glucose) and protoplast regeneration medium without sucrose (see Materials and methods). The ligninolytic activities in the supernatants of the cultures of TF2-7 and the Trp^+ control were determined by rapid and sensitive assay using Remazol Brilliant Blue R dye (RBBR, Ulmer *et al.*, 1984), demonstrating that the activity of TF2-7 is ca. 30 times as high as the control.

The results analogous to TF2-7 were obtained in the experiments using the TF2-1, TF1-2, and TF1-4, though their lignin-decolorization and -degradation activities were slightly lower than those of TF2-7 (data not shown). Several other Trp^+ colonies obtained by the introduction of pCc1001 and the recipient LT2-44 gave the same results as the Trp^+ control used. These results showed that the *Le.ras* and *priA* promoter activities efficiently express at the almost same, easily detectable levels in *C. cinereus*.

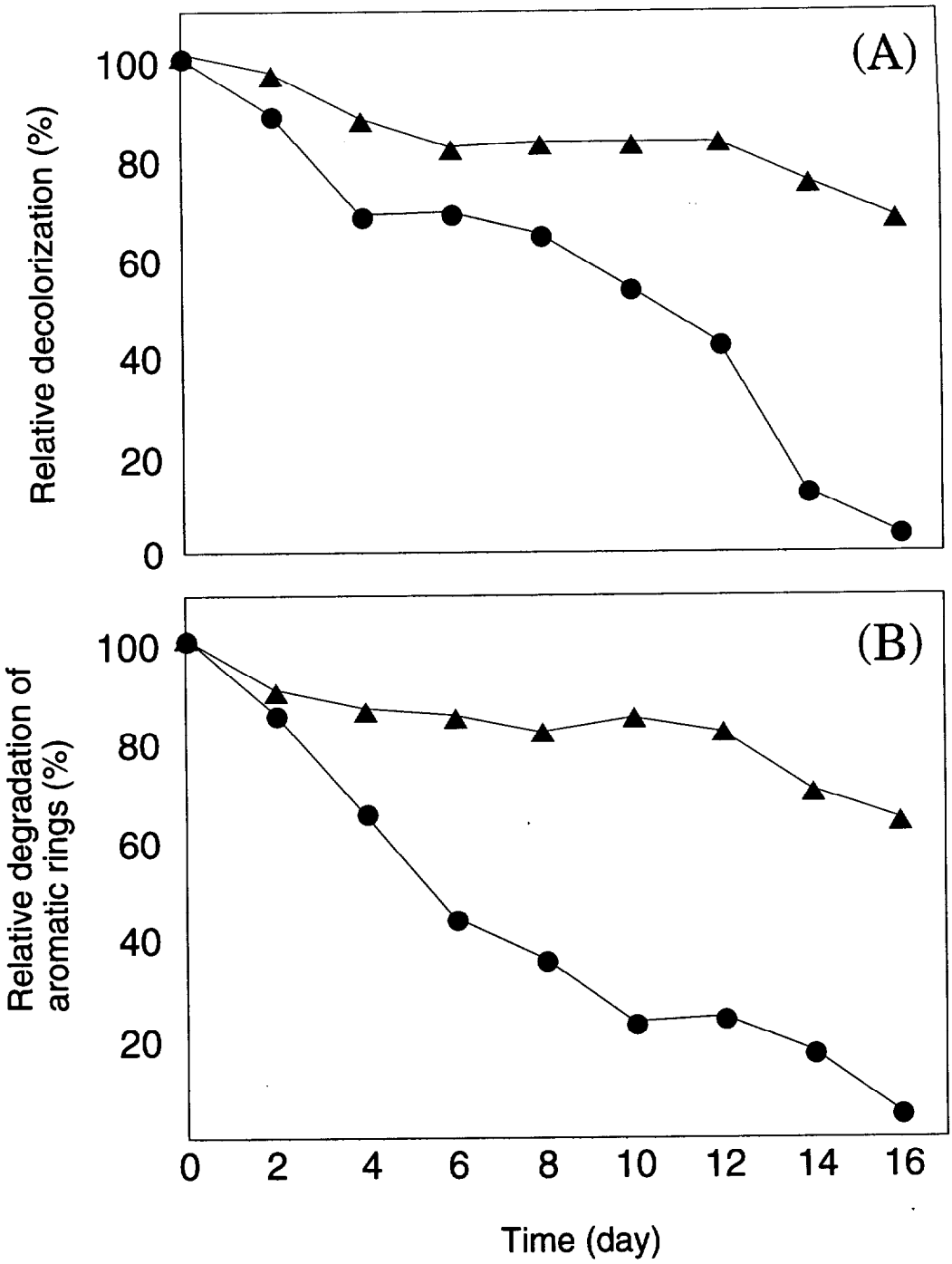

Figure 2.7

Decolorization (**A**) and degradation (**B**) of lignin during the cultivations in the lignin-containing MYG medium

The decolorization and degradation of lignin during the cultivations of the Trp^+ MnP^+ transformant TF2-7 (●) and the control Trp^+ transformant (▲) of *C. cinereus* are shown by the decrease of the absorbance at 480 nm or 27 5 nm, respectively, in which the absorbance at the start time of cultivation is taken as 100%.

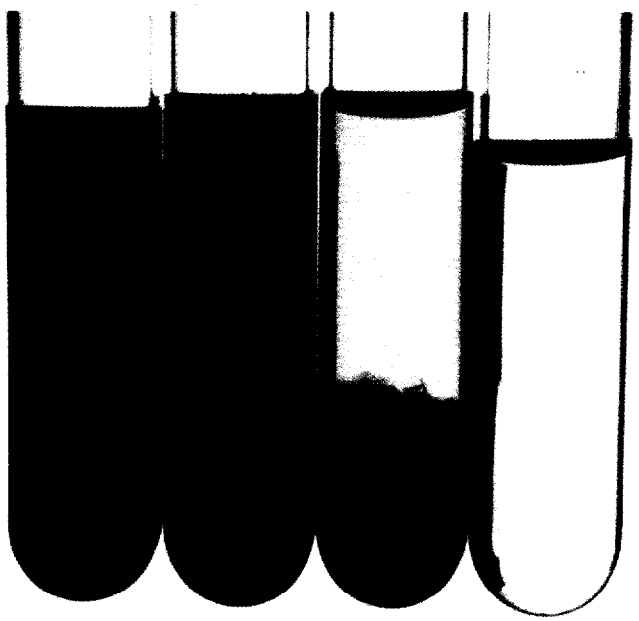

Figure 2.8

Decolorization of lignin by the Trp^+ MnP^+ transformant TF2-7 and the control Trp^+ transformant in the lignin-containing MYG medium

Ten ml of MYG medium containing 10 mg of lignin and 2.5 mg of $MnCl_2$ in an L-shaped tube was inoculated with three / (7 x 7x 1 mm) cubes of the MYG agar colonized with the *C. cinereus* Trp^+ MnP^+ transformant TF2-7 or control Trp^+mycelium and cultivated at 30°C for 16 days with shaking. A, MYG medium + 1 mg/ml lignin; B, A + the control Trp^+ transformant; C, A + the Trp^+ MnP^+ transformant TF2-7; D, MYG medium

In this chapter, the promoters of *ras* and *priA* genes derived from *L. edodes* on the novel heterologous protein expression vectors were shown to be useful for expression of the *P. ostreatus* manganese (II) peroxidase in *C. cinereus*. This is the first report on the efficient expression of foreign gene in *C. cinereus*.

Chapter 3

Structure and function in *Escherichia coli* of plasmids containing pyrimidine/purine-biased sequence originated from the 5'-promoter region of the basidiomycete *ras* gene

3.1 Introduction

Our group has recently found that the basidiomycete *L. edodes ras* gene (Hori *et al.*, 1991; Kajiwara and Shishido, 1992) possesses a CT-motif which contains the transcription initiation site and a short (7 bases) mirror repeat (see Fig. 2.1). The *ras* CT-motif extended over 62 nucleotides (55 are pyrimidines). As mentioned in Chapter 1, similar CT-rich sequences have also been found in the 5' promoter regions of various fungal genes (Gurr *et al.*, 1988, see Table 1.1). The CT-motifs in the 5'-promoter region of genes as well as other core promoter elements (such as CAAT box, GC box and TATA box) have been postulated to play an important role in regulation of gene expression. However, structure-biological function relationships have not been well studied for these sequences.

In this chapter, we investigated whether the *ras* CT/AG-biased sequence forms an unusual structure in pBR322 isolated from *E. coli* strains DM800 (*ΔtopA gyrB225*) (Sternglanz *et al.*, 1981; DiNardo *et al.*, 1982) and JM109 (*topA*$^+$ *gyrA96*) (Yanisch-Perron *et al.*, 1985) using S1 nuclease (Shishido and Ando, 1982). It has been known that pBR322 DNA isolated from DM800 carrying a deletion of the topoisomerase I gene is extremely heterogeneous in linking number and highly negatively supercoiled when compared with that from JM109 (Pruss, 1985) and formation of non-B, unusual DNA structures in naturally occurring sequences usually depends on negative supercoiling (Wells *et al.*, 1988). On the basis of these fact, the topological structures of pBR322 DNAs with the CT/AG-biased sequence

and its deletion derivatives isolated from *E. coli* were analyzed.

3.2 Materials and methods

3.2.1 Construction of pBR322 derivatives carrying the CT/AG-biased sequence of the *L. edodes ras* gene

The 129-bp *Eco*RI-*Rsa*I DNA fragment containing the *ras* CT/AG sequence (see Fig. 2.1) was inserted between the *Eco*RI and *Hin*cII sites on pUC19. The *Hin*dIII-linearized recombinant pUC19 was blunt-ended and ligated to the *Eco*RI adaptor (5'-GGAATTCC). The 155-bp *Eco*RI fragment with the *ras* CT/AG sequence was inserted into the *Eco*RI site of pBR322. Based on the orientation of insertion of the CT/AG sequence, two pBR322 derivatives with a single CT/AG-sequence were obtained and designated pBR322-CT[ras] and pBR-invCT[ras] (Fig. 3.1). In the pBR-CT[ras] the pyrimidine-rich sequence was on the pBR322 *tet*-coding strand and in the pBR-invCT[ras] the purine-rich sequence was on this strand. The plasmid DNAs carrying small deletions within the CT/AG sequence were constructed as follows. The pBR-CT[ras] DNA was partially digested with S1 to convert 50 % of the DNA to a linear form. The S1-linearized DNA separated by agarose gel electrophoresis was blunt-ended by T4 DNA polymerase and recircularized by self-ligation. Two pBR-CT[ras] derivatives lacking the nucleotides from 33 to 45 and 33 to 51 were obtained and named pBR-CT[ras]Δ13 and pBR-CT[ras]Δ19, respectively (see Fig. 3.4). The following pBR322 derivatives were also constructed as a control for the experiments. The *Bgl*I-fragment containing the *lacZ* sequence of pUC19, which contains no CT/AG-biased sequence, was blunt-ended and ligated to the *Eco*RI adaptor. This 154-bp *Eco*RI fragment was inserted into the *Eco*RI site of pBR322 and the resulting recombinant plasmids were named pBR-gal' or pBR-invgal'. In the former, the *lacZ*-coding sequence was on the *tet*-coding strand. DNAs of the pBR322 derivatives were used to transform *E. coli*

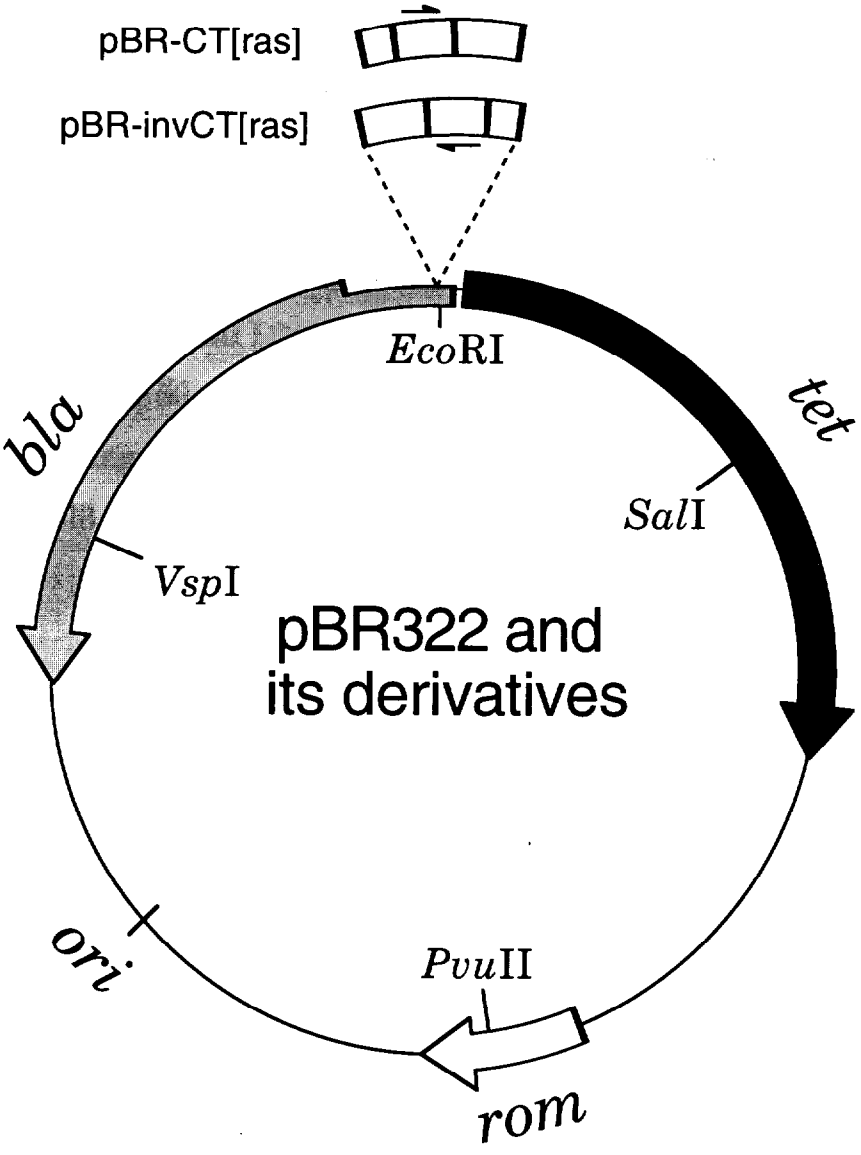

Figure 3.1 Structures of pBR322 and its derivatives carrying the CT/AG-biased sequence of the *ras* gene

The *ras* CT/AG-biased sequence is shown in Fig. 3.4. In pBR-CT[ras] the pyrimidine-rich sequence was on the pBR322 *tet*-coding strand and in pBR-invCT[ras] the purine-rich sequence was on this strand. Location and direction of transcription of the *tet* gene (initiated at nucleotide 45 (Brosius et al., 1982)), the *bla* gene (initiated at nucleotides 36 and 4187 (Brosius et al., 1982)) and the *rom* gene (Watson, 1988), location of the origin (*ori*) of replication, and restriction sites of *Eco*RI (4359), *Sal*I (651), *Pvu*II (2064) and *Vsp*I (3537) on the pBR322 genome (Watson, 1988) are indicated. The *ras* CT/AG-biased sequence (shaded)-containing fragments (open arc bars) inserted into the *Eco*RI site are shown, in which the direction of the arrow marks that of the CT strand.

DM800 (*ΔtopA gyrB225*) (Sternglanz *et al.*, 1981; DiNardo *et al.*, 1982) and JM109 (*topA*$^+$ *gyrA96*) (Yanisch-Perron *et al.*, 1985). Restriction endonucleases, DNA modifying enzymes, and the *Eco*RI adaptor were purchased from Takara Shuzo and/or Nippon Gene and used according to the supplier's instructions.

3.2.2 Preparation of plasmid DNAs

LB medium containing 50 μg of ampicillin per ml was used to grow all the *E. coli* transformants carrying the plasmid. Cells from an overnight (stationary) culture were diluted 100-fold into 300 ml of fresh growth medium, grown at 37 °C with aeration to late exponential phase ($A_{600} \approx 0.7$), quickly chilled and centrifuged. Plasmid DNAs were extracted by an alkaline extraction procedure and purified by treatment with RNase A and proteinase K as described previously (Shishido *et al.*, 1987).

3.2.3 S1 nuclease digestion

S1 nuclease provided by Sankyo Chem. Co. was further purified as reported previously (Shishido, 1979). Three μg aliquots of plasmid DNAs were incubated with 3 units of S1 at 37 °C for 60 min in the reaction buffer (200 μl) containing 45 mM sodium acetate (pH 4.5), 1.5 mM $ZnSO_4$, 1.5 mM $MnCl_2$ and 150 mM NaCl. The reactions were stopped by addition of Tris-HCl (pH 8.5) and EDTA to give final concentrations of 100 mM and 25 mM, respectively. One unit of S1 activity is defined as the amount of the enzyme that converts 50 % of 3 μg of single-stranded pBR322 DNA to acid-soluble form under the above conditions.

3.2.4 Gel electrophoresis

Agarose gel electrophoresis was carried out as described previously (Shishido *et al.*, 1987). Chloroquine-agarose gel electrophoresis was performed according to the method reported by Pruss (Pruss, 1985).

3.2.5 Primer extension analysis

Restriction fragments (20 ng each) were incubated with 1 pmol of end-labeled synthetic primer at 95 °C for 5 min and then at 65 °C for 30 min in T7 DNA polymerase buffer (40 mM Tris-HCl buffer (pH 7.5), 20 mM $MgCl_2$ and 50 mM NaCl). To the incubation mixture, T7 DNA polymerase (0.5 unit of Sequenase™, United States Biochemicals), dithiothreitol (final conc. 5 mM) and deoxynucleoside triphosphates (final conc. 1 mM each) were added and further incubated at 37 °C for 10 min. After ethanol precipitation the reactions were electrophoresed on 8 % polyacrylamide gels containing 7 M urea, followed by autoradiography. The sizes of the primer extension products were determined from the sequence ladders (ACGT) which were derived from the CT/AG-biased sequence of pBR-CT[ras] by the dideoxy chain-termination method of Sanger *et al.* (1977).

3.2.6 Tetracycline resistance

Plasmid-harboring *E. coli* cells precultured in LB medium with 1 μg of tetracycline (Tc) per ml were transferred to fresh LB medium with 20 μg of Tc per ml and incubated at 37 °C. At the indicated period, absorbance at 600 nm was measured. Late-exponential phase ($A_{600} \approx 0.7$) cultures were diluted 100-fold and spotted on LB agar plates containing increasing concentrations of Tc. The plates were observed for the presence or absence of growth.

3.2.7 Measurement of ß-lactamase activity

Periplasmic ß-lactamase fractions were prepared as follows. Late-exponential phase ($A_{600} \approx 0.7$) cultures of plasmid-harboring *E. coli* cells in 10 ml of LB medium with ampicillin (50 μg/ml) were harvested by centrifugation and washed with ice-cold 50 mM Na-phosphate buffer (pH 6.8), then resuspended in 2 ml of the Na-phosphate buffer containing 20 % glycerol. The cells were disrupted by sonication and centrifuged at 16,000 rpm in a microcentrifuge at 4 °C, and the supernatants were used as the periplasmic ß-lactamase fractions. Protein

concentration was determined by Coomassie dye-binding assay (Bradford assay) (Bradford, 1976) with bovine serum albumin as a standard protein. The ß-lactamase activity was assayed by measuring the degradation of pyridinium-2-azo-*p*-dimethylaniline chromophore (PADAC) (Kato and Shimizu, 1992; Kuriki, 1987). Hydrolysis of PADAC (Calbiochem) was carried out in 1.4 ml of reaction mixture containing 50 mM Na-phosphate (pH 6.8) and 5 µM PADAC. The protein extract (2 µg) was added to the reaction mixture, and the decrease of absorbance at 570 nm was measured at 25°C. The amount of hydrolyzed PADAC was calculated using the molar absorption coefficient (45,000) of PADAC.

3.3 Results

3.3.1 Analysis of S1-cleavability of pBR322 and its derivatives

To investigate whether the *ras* CT/AG-biased sequence forms S1-cleavable, nonbase-paired sites, DNAs of pBR322 and its derivatives isolated from *E. coli* topoisomerase I deletion mutant DM800 (*ΔtopA gyrB225*) (Sternglanz *et al.*, 1981; DiNardo *et al.*, 1982) were digested with S1 nuclease at pH 4.5. The full-length S1-linearized DNAs were further digested with restriction endonucleases which have a single unique cleavage site on the DNAs (see Fig. 3.1). Fig. 3.2 shows the agarose gel electrophoretic patterns obtained for pBR322, pBR-CT[ras] and pBR-invCT[ras]. *Pvu*II-, *Sal*I- and *Vsp*I-digests of the S1-linearized pBR322 (containing ~50% open circular DNA) yielded a number of discrete DNA bands (lanes 1, 4, 7, respectively). These indicate that pBR322 possesses multiple S1-sites, although S1 cleaves the DNA once at each of these sites. There was diversity in the intensity of the DNA bands on the gels. The sizes corresponding to the two intense DNA bands observed in the digest by *Pvu*II (3.36 and 1.00 kb), *Sal*I (2.41 and 1.95 kb) or *Vsp*I (3.89 and 0.47 kb) summed up to the full length size (4361bp) of pBR322 (Watson, 1988). The results show that pBR322 possesses one site

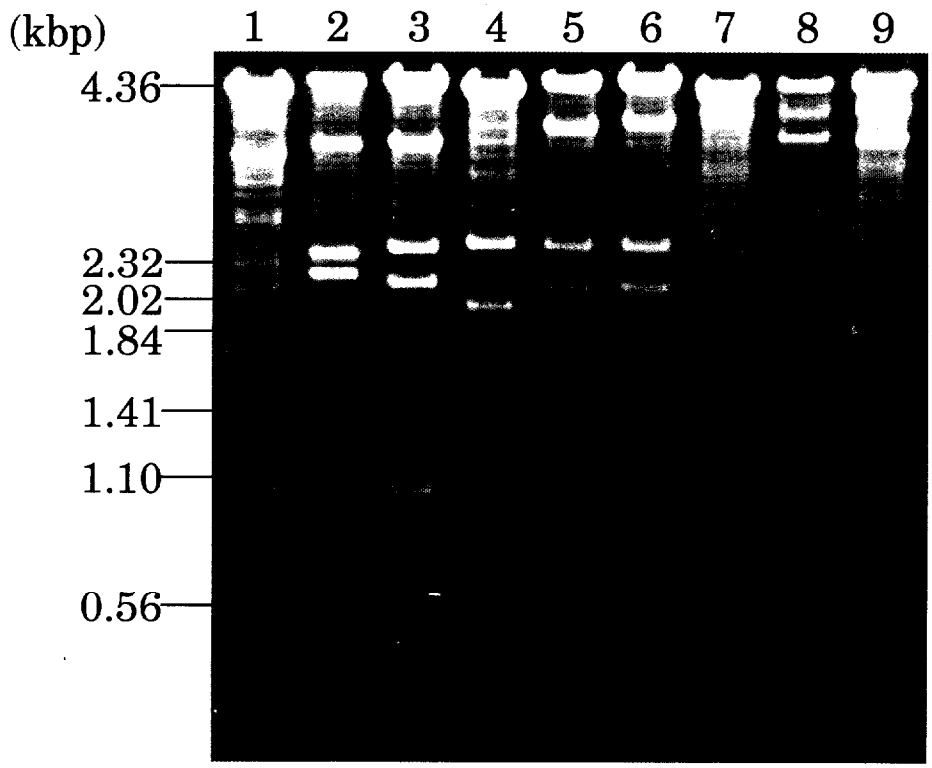

Figure 3.2

DNA fragments produced after digestion of the S1-generated unit-length linear pBR322 and its derivatives (containing ~50% open circular DNA) with restriction endonucleases

The S1-digested DNAs were then digested with *Pvu*II (lanes 1-3), *Sal*I (lanes 4-6) and *Vsp*I (lanes 7-9). Electrophoresis was done in a 1 % agarose slab gel under the conditions described previously (Shishido *et al.* 1987). Lanes 1, 4 and 7, pBR322; lanes 2, 5 and 8, pBR-CT[ras]; lanes 3, 6 and 9, pBR-invCT[ras]. The *Hin*dIII-digest of phage λ DNA and *Hin*cII- and *Pvu*II-digests of pBR322 DNA were used as molecular size markers. Sizes (kb) are indicated to the left in the panel.

(nucleotide ~3100) of highly preferential cleavage, supporting the previous observations by other investigators (Lilley, 1980; Panayotatos and Wells, 1981). In all the cases of *Pvu*II-, *Sal*I-, and *Vsp*I-digests of the S1 linearized pBR-CT[ras] (lanes 2, 5 and 8) and pBR-invCT[ras] (lanes 3, 6 and 9), two additional intense DNA bands were observed at 2.35 and 2.16 kb, 3.76 and 0.75 kb, 3.64 and 0.87 kb, respectively, for the former and at 2.40 and 2.11 kb, 3.81 and 0.70 kb, 3.59 and 0.92 kb, respectively, for the latter. The sizes of the two fragments summed up to the nearly full-length size (4512 bp) of the plasmid DNAs, showing the generation of another strong cleavage site (region) on both pBR-CT[ras] and pBR-invCT[ras]. This site (region) was found to fall into the CT/AG-biased sequence of both plasmid DNAs. DNAs of pBR-CT[ras] and pBR-invCT[ras] isolated from JM109 (*topA*$^+$ *gyrA96*) (Yanisch-Perron *et al.*, 1985), on the other hand, were not preferentially cleaved by S1 within the CT/AG sequence, generating the corresponding two faint DNA bands in each of the cases of *Pvu*II-, *Sal*I-, and *Vsp*I-digestion (data not shown). It has been known that pBR322 DNA isolated from DM800 is extremely heterogeneous in linking number and highly negatively supercoiled when compared with that from JM109 (Pruss, 1985) and formation of non-B DNA structures in naturally occurring sequences usually depends on negative supercoiling (Wells *et al.*, 1988). Therefore the CT/AG-biased sequence of the *ras* gene requires higher levels of negative supercoiling for formation of the preferentially S1-cleavable (stable), nonbase-paired structure. As a control for the experiments, the following four pBR322 derivatives were used: pBR-gal' and pBR-invgal' were constructed by insertion of the *E. coli lacZ* sequence (containing no CT/AG-biased sequence) into the *Eco*RI site of pBR322 in both orientations, and pBR-CT[ras]Δ13 and pBR-CT[ras]Δ19 were pBR-CT[ras] derivatives lacking a part of the mirror repeat sequence (the nucleotides from 33 to 45 and 33 to 51, respectively, see Fig. 3.4 and Materials and methods). In the cases of these plasmids, a preferentially S1-cleavable structure was not formed within/around the inserted sequence even if

they were isolated from DM800 (data not shown).

3.3.2 Mapping of the S1-cleavage sites within the CT/AG-biased sequence of pBR322 derivative pBR-CT[ras]

The S1-cleavage sites were analyzed by the primer extension method using the following two primers; primer R, 5'-GTATCACGAGGCCCTT identical with the sequence from 4335 to 4350 of pBR322 and primer H, 5'-GCAATTTAACTGTGAT complementary to the sequence from 64 to 49 of pBR322 (see Fig. 3.1). In the *Pvu*II-digests of the S1-linearized pBR-CT[ras] (lane 2 of Fig. 3.2), DNA fragments at/around the two intense bands (2.35 and 2.16 kb) were subjected to analysis. In the extension of the CT-rich strand (the larger fragment and primer R), three intense and five faint bands were observed at nucleotides 45 (C), 46 (C) and 48 (T) and nucleotides 32 (T), 37 (C), 38 (C), 42 (T) and 55 (T), respectively, on the CT-rich strand (panel A of Fig. 3.3), indicating that the template (AG-rich) strand ended at the positions marked by arrows in Fig. 3.4, *i.e.*, S1 cleavages occurred at the arrow positions. In the case of the AG-rich strand (the smaller fragment and primer H), three intense bands were observed at nucleotides 60 (A), 57 (A) and 56 (A) (panel B of Fig. 3.3). The ends of the CT-rich template strand (the sites of S1 cleavage) are marked by arrows in Fig. 3.4. These results demonstrate that the *ras* CT/AG-biased sequence forms an extended open structure sensitive to S1 cleavage.

3.3.3 Tc^r levels of *E. coli* carrying pBR322 and its derivatives

Although maximum Tc concentration permitting growth of DM800 (JM109) carrying pBR322 was 16 (125) μg per ml, DM800 (JM109) cells carrying pBR-CT[ras] could grow on agar plates at Tc concentrations up to 20 (175) μg per ml. DM800 (JM109) carrying pBR-CT[ras]Δ13 and pBR-CT[ras]Δ19, however, could not grow at the same Tc concentration as pBR-CT[ras] though they were

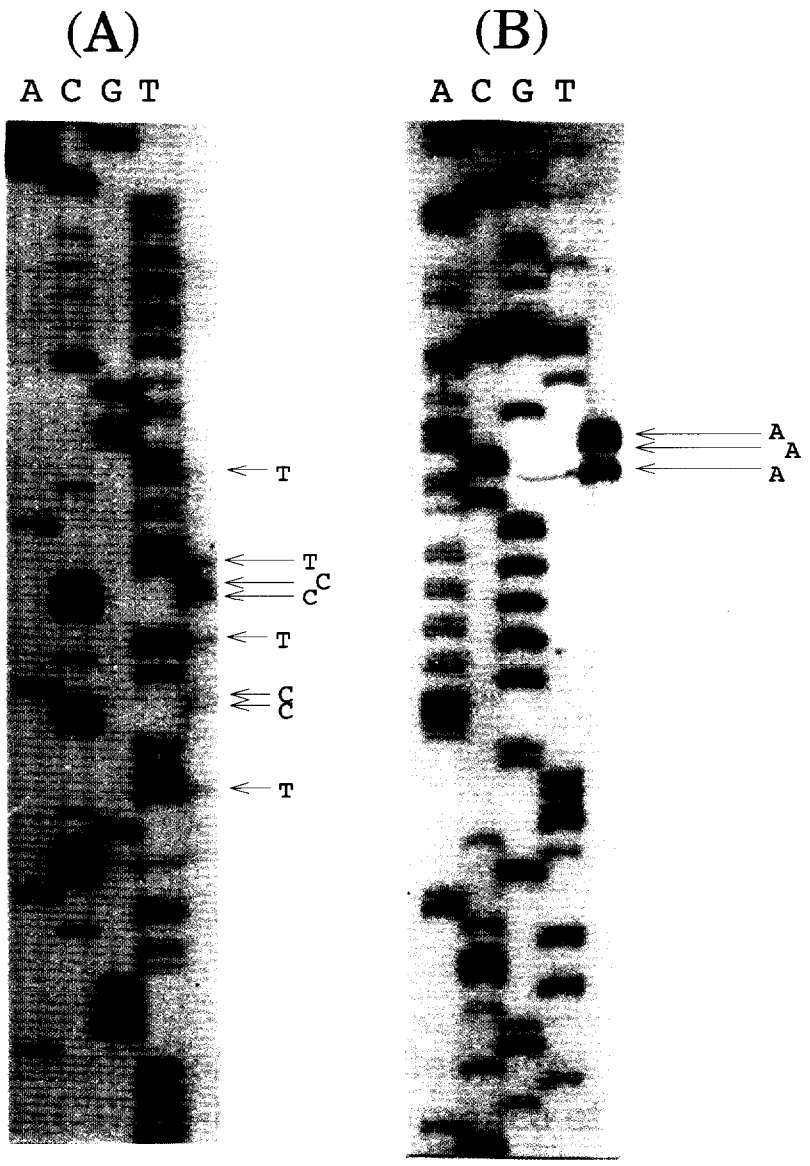

Figure 3.3

Determination of the S1-cleavage sites within the CT/AG-biased sequence of pBR322 derivative pBR-CT[ras] by the primer extension method

The extensions of the CT-rich strand with primer R (panel A) and the AG-rich strand with primer H (panel B) were carried out using the larger or smaller fragment of the *Pvu*II-digests of pBR-CT[ras]. The nucleotides corresponding to the ends of extension products (marked by arrows) were determined from the sequence ladders (ACGT) which were derived from pBR-CT[ras] with primers R and H by the dideoxy chain-termination method of Sanger *et al.* (1977).

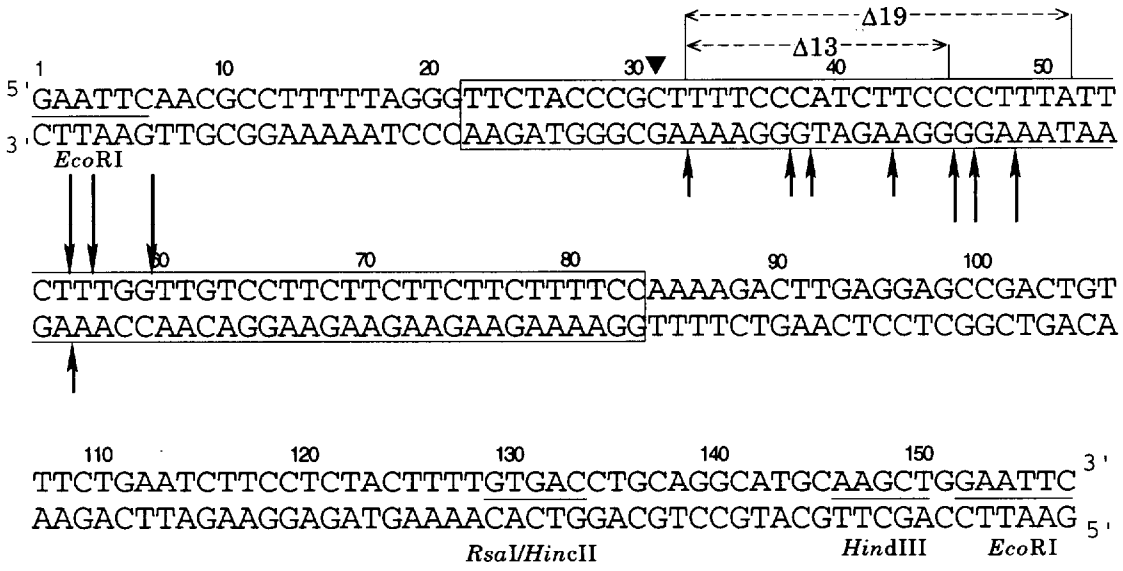

Figure 3.4 Summary of the S1-cleavage sites within the CT/AG-biased sequence of the *ras* gene

The nucleotide sequence of the CT/AG-biased sequence (boxed)-containing region of the *ras* gene is shown. Mirror repeat sequences involved in the formation of the putative intramolecular triplex structure are shaded on the pyrimidine strand (see Chapter 6). Closed arrowhead is the transcriptional initiation site determined for the *ras* transcription in *L. edodes* in a previous paper (Kajiwara *et al.* 1992) . The S1-cleavage sites on the template strand in the extensions of the CT and AG strands are shown by vertical arrows. Their lengths correspond to the frequencies of S1 cleavages judged from the results of Fig. 3.3, with the most preferential sites marked by long arrows. Restriction sites used for the construction of recombinant plasmids are also shown. Two broken lines with arrowheads above the sequence indicate the regions of deletion in pBR-CT[ras]Δ13 and pBR-CT[ras]Δ19. In pBR-CT[ras]Δ19 one end of the deletion does not match the position of the arrow of the S1-cleavage. This must be due to the occurrence of a second S1 cut on the opposite strand near to (not at) the site nicked first, yielding a 3'-protruding end.

resistant to 18 (140) μg of Tc per ml. DM800 (JM109) carrying pBR-invCT[ras] could not grow in the presence of 13 (100) μg of Tc per ml, but it was resistant to 11 (75) μg of Tc per ml. DM800 (JM109) carrying the *E. coli lacZ* sequence (adopting usual B structure)-containing plasmids pBR-gal' and pBR-invgal' showed the same level of Tc^r as that carrying pBR322. The copy numbers of pBR322 and its six derivatives in DM800 (JM109) were almost the same, suggesting that the CT/AG sequence does not affect the regulation of replication of the plasmid DNAs. The results show that pBR-CT[ras] (pBR-invCT[ras]) confers higher (lower) levels of Tc^r on DM800 and JM109 than pBR322 does. pBR-CT[ras]Δ13 and pBR-CT[ras]Δ19 confer pBR322-like Tc^r on both strains. The plasmid-carrying DM800 cells, however, are highly sensitive to Tc when compared with the plasmid-carrying JM109 cells.

The growth of DM800 carrying pBR322 and its derivatives was examined in liquid medium. DM800 cells carrying pBR-CT[ras] showed almost no growth in the presence of 7 μg of Tc per ml and the difference in growth rate in the presence of 5 μg of Tc per ml between the DM800 cells carrying each of the plasmids was not clear. JM109 cells carrying each of the plasmids, on the other hand, grew well in liquid medium containing 20 μg of Tc per ml. So we examined the JM109 cells at this concentration of Tc. As shown in Fig. 3.5, the growth rate of JM109 carrying pBR-CT[ras] was clearly higher than that carrying pBR322 or either of the pBR-CT[ras] deletion derivatives. JM109 carrying pBR-invCT[ras] grew at the most reduced rate. Thus, the plasmids were ordered with respect to the expression of Tc^r in JM109 (DM800) as follows: pBR-CT[ras]>pBR-CT[ras]Δ13≥pBR-CT[ras]Δ19≥pBR322>pBR-invCT[ras].

3.3.4 ß-Lactamase activity in *E. coli* carrying pBR322 and its derivatives

The ß-lactamase activity expressed in DM800 (JM109) carrying pBR-CT[ras]

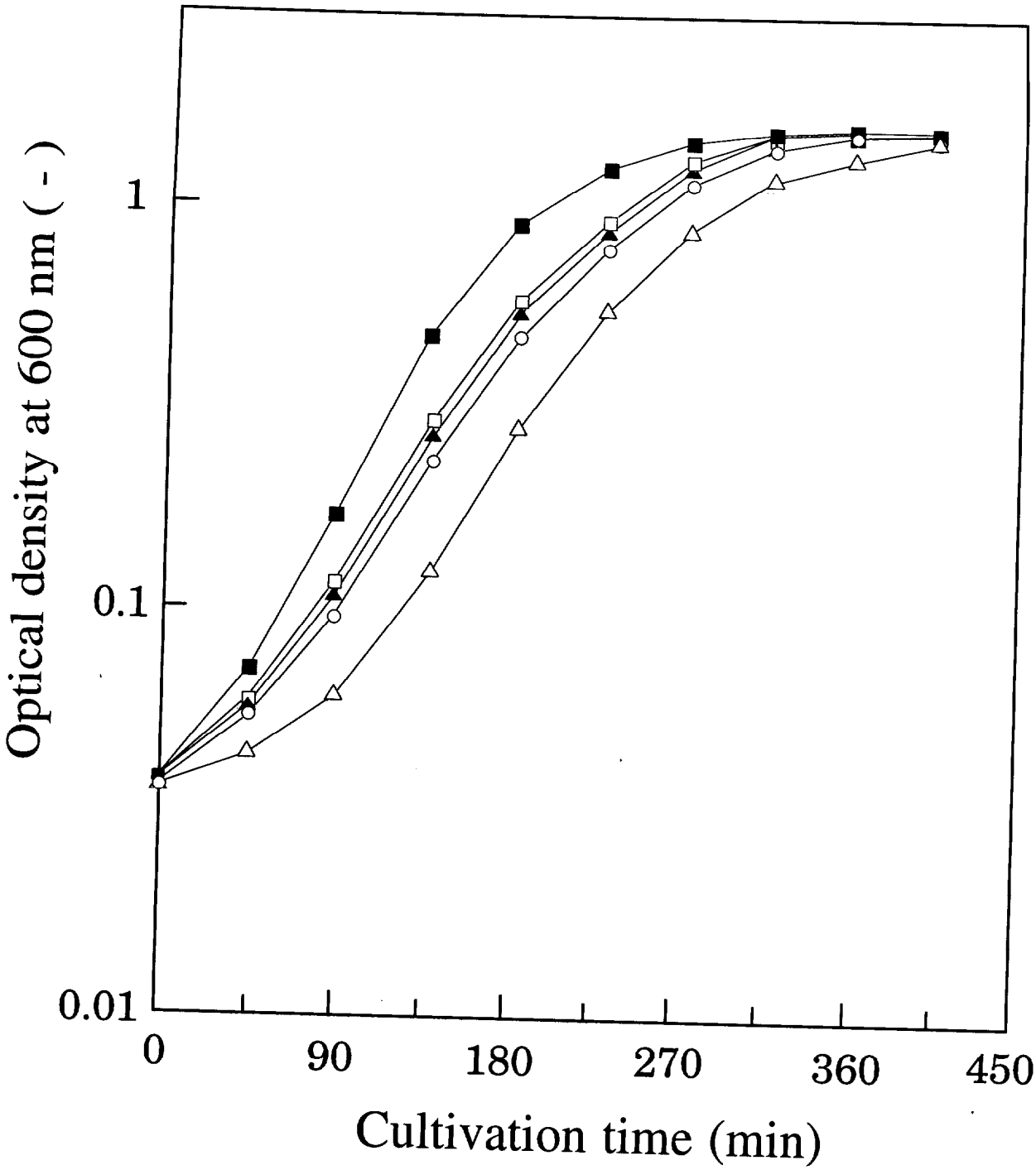

Figure 3.5 Growth curves of the JM109 cells carrying pBR322 and its derivatives

Plasmid-harboring *E. coli* cells were cultured in LB medium containing 20 μg of Tc per ml at 37°C. At the indicated period, absorbance at 600 nm was measured. The plasmids carried were as follows: pBR322 (○), pBR-CT[ras] (■), pBR-invCT[ras] (△), pBR-CT[ras]Δ13 (□), pBR-CT[ras]Δ19(▲). Absorbance values are the average of 3 independent experiments.

was similar to that carrying pBR-invCT[ras]. These activities were clearly lower than that carrying pBR322 (Fig. 3.6). DM800 transformants carrying pBR-CT[ras] or pBR-invCT[ras] showed lower levels of the activity than JM109 transformants carrying either of them. DM800 (JM109) carrying pBR-CT[ras]Δ13 or pBR-CT[ras]Δ19 showed clearly higher activities than that carrying pBR-CT[ras]. pBR-gal' and pBR-invgal' conferred very similar activities of ß-lactamase to that of pBR-CT[ras]Δ19 on DM800 and JM109 (data not shown).

3.3.5 Negative superhelicity of pBR322 and its derivatives propagated in DM800

To understand the experimental results described above, the topological structures of the plasmid DNAs were analyzed. In the negative supercoiling distribution of pBR322 DNA isolated from DM800 (lanes 1 and 8 of Fig. 3.7A), the bottom band contains the most negatively supercoiled DNA, intermediate bands contain DNA with fewer supercoils (the topoisomers migrate more slowly with less supercoiling), and the top band contains nicked circular DNA (Pruss, 1985). The two derivatives pBR-CT[ras] (lane 2) and pBR-invCT[ras] (lane 3) displayed supercoiling distributions wherein a smaller amount of highly negatively supercoiled DNA species remained, while the control four derivatives pBR-gal' (lane 4), pBR-invgal' (lane 5), pBR-CT[ras]Δ19 (lane 6) and pBR-CT[ras]Δ13 (lane 7) exhibited pBR322-like high levels of negative supercoiling. pBR-CT[ras] seems to contain a slightly more highly negatively supercoiled DNA species than pBR-invCT[ras]. To obtain more detailed information about the difference in negative superhelical density between pBR-CT[ras] and pBR-invCT[ras], two-dimensional chloroquine-agarose gel electrophoresis was done (panels B1, 2 and 3 of Fig. 3.7). Compared with pBR-CT[ras] (B2), pBR-invCT[ras] (B3) contained a larger amount of positively supercoiled DNA molecules (in the upper arc) which were derived from less negatively supercoiled DNA species propagated in DM800, confirming that the negatively superhelical density of pBR-invCT[ras] is lower

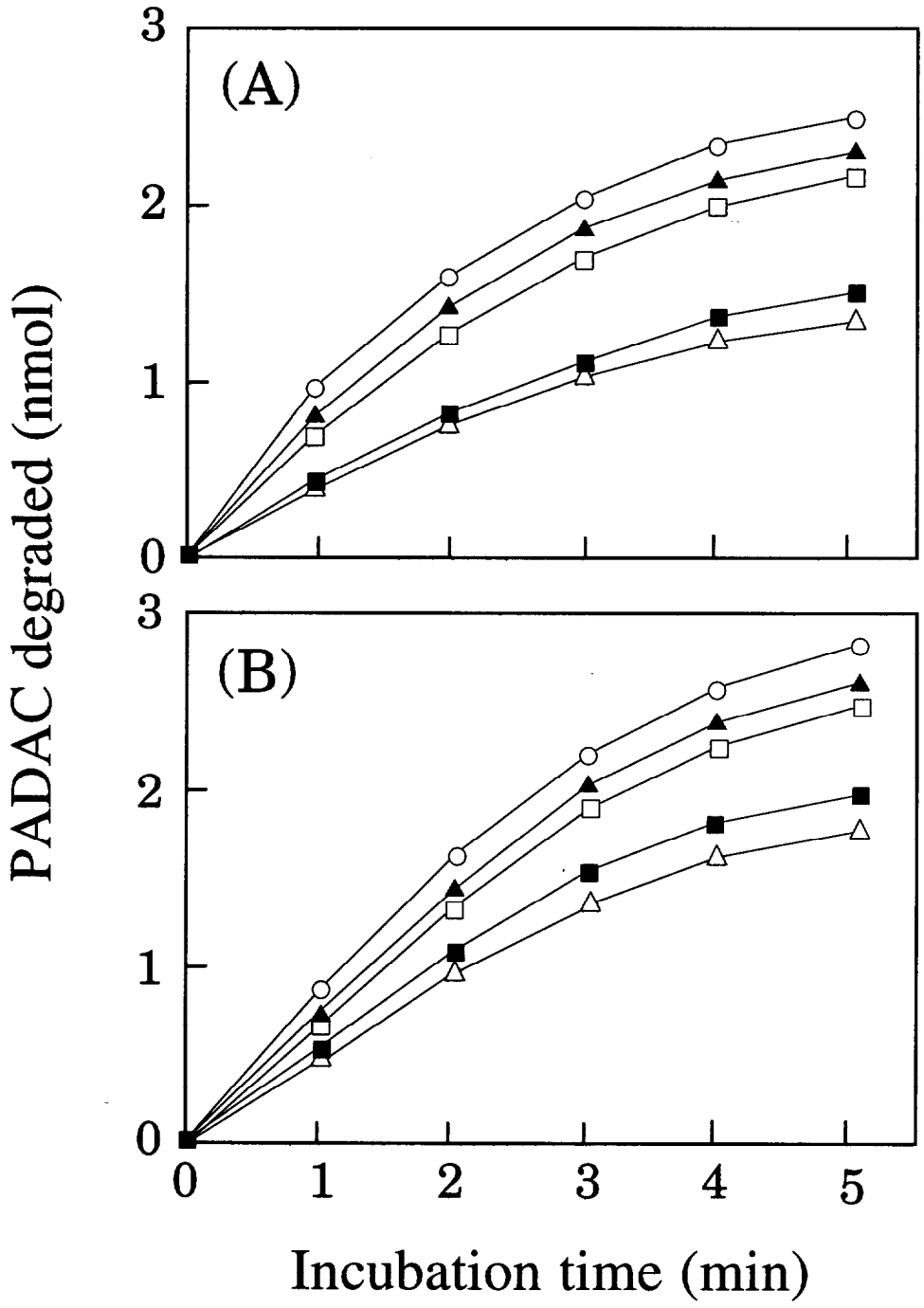

Figure 3.6 The periplasmic ß-lactamase activities of DM800 (A) and JM109 (B) carrying pBR322 and its derivatives determined by measuring the degradation of PADAC

The reaction was performed in 50 mM Na-phosphate buffer (pH 6.8) containing 5 μM PADAC at 25 °C. The decrease of absorbance at 570 nm was measured at the indicated period and the amount of hydrolyzed PADAC was calculated. The plasmids carried were as follows: pBR322 (○), pBR-CT[ras] (■), pBR-invCT[ras] (△), pBR-CT[ras]Δ13 (□), pBR-CT[ras]Δ19(▲). Absorbance values are the average of 3 independent experiments.

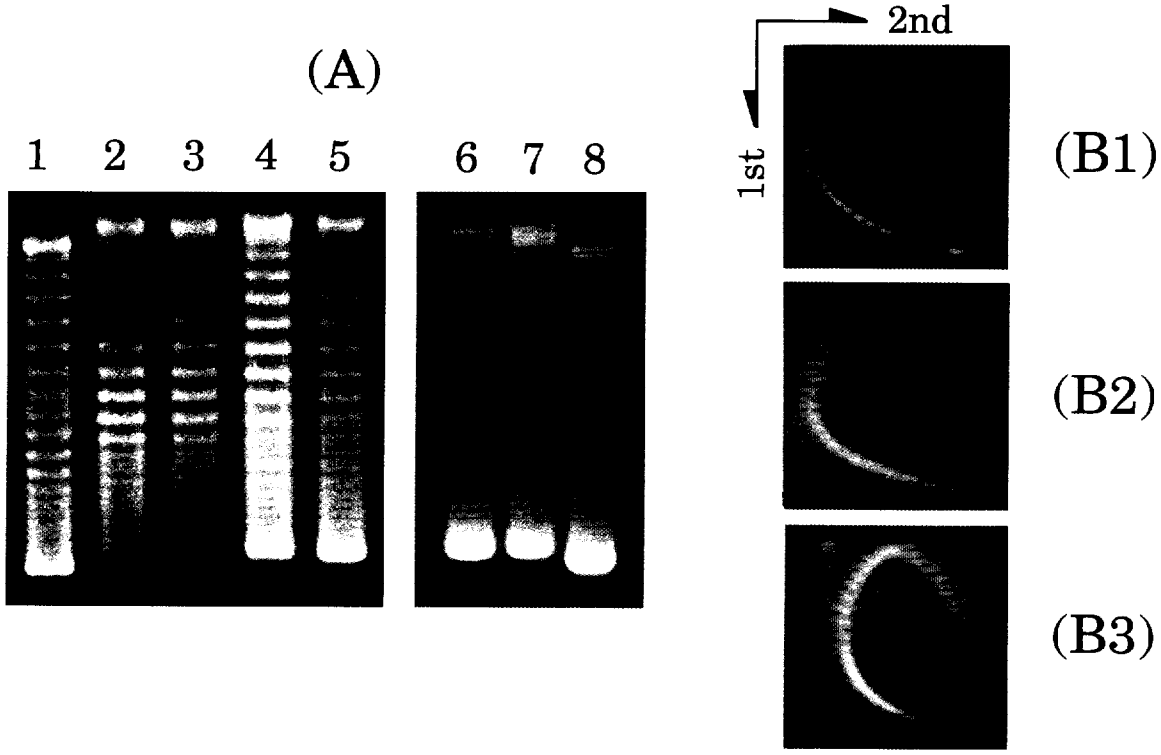

Figure 3.7

Chloroquine-agarose gel electrophoretic analysis of the degree of negative supercoiling of the plasmid DNAs isolated from DM800

(A) One-dimensional electrophoretic patterns. Samples (2 μg each) of pBR322 (lanes 1 and 8), pBR-CT[ras] (lane 2), pBR-invCT[ras] (lane 3), pBR-gal' (lane 4), pBR-invgal' (lane 5), pBR-CT[ras]Δ19 (lane 6) and pBR-CT[ras]Δ13 (lane 7) were electrophoresed in a 1 % agarose horizontal slab gel containing chloroquine (100 μg/ml) according to the method of Pruss (1985). (B1~B3) Two-dimensional electrophoretic patterns. Samples (2 μg each) of pBR322 (B1), pBR-CT[ras] (B2) and pBR-invCT[ras] (B3) were loaded on gel. Chloroquine was present at 48 μg/ml in the first (vertical) dimension and at 1 96 μg/ml in the second (horizontal) dimension. During electrophoresis in the first dimension, topoisomers in the lower arcs of the three distributions were negatively supercoiled, while those in the upper arcs were positively supercoiled, causing the two arcs of each distribution to be superimposed. Electrophoresis in the second dimension resolved the superimposed topoisomers.

than that of pBR-CT[ras]. Negative superhelical densities of DNAs of pBR322, pBR-CT[ras] and pBR-invCT[ras] isolated from JM109 were also analyzed. However, no clear difference in the densities could be detected between the three plasmid DNAs.

3.4 Discussion

In this chapter, it has been shown above that the CT/AG-biased sequence with a short (7 bases) mirror repeat from the basidiomycete *L. edodes ras* gene forms an extended S1-cleavable open structure in pBR322 DNA and affects the expressions of the plasmid-coding *tet* and *bla* genes in *E. coli*.

The *ras* CT/AG-biased sequence forms an extended open, non-base paired structure preferentially sensitive to S1 cleavage under higher levels of negative supercoiling. The S1-cleavage sites determined by the extension of the CT-rich strand did not coincide with those of the AG-rich strand except for the cleavage between nucleotides 55 and 56 (see Fig. 3.4). This suggests that S1 cleavages occurred simultaneously at site(s) on the CT-strand and site(s) on the AG-strand, and then second S1 cuts occurred on the opposite strand at or near the sites nicked first to yield linear DNA molecules slightly smaller than full length size.

Compared with those carrying pBR322, DM800 and JM109 carrying pBR-CT[ras] showed much higher levels of tetracycline resistance (Tc^r), while both strains carrying pBR-invCT[ras] showed clearly lower levels of Tc^r. pBR-CT[ras] and pBR-invCT[ras], however, conferred reduced activity of ß-lactamase on DM800 and JM109. The CT/AG sequence of the *ras* gene is probably also widely single-stranded in supercoiled plasmids in *E. coli* cells; DNAs of pBR322, pBR-CT[ras] and pBR-invCT[ras] isolated from DM800 were found to be cleaved by single-strand-specific Bal31 nuclease (Shishido and Ando, 1982) at neutral pH and under physiological conditions within regions similar to those cleaved by S1 (data

not shown), although the restriction DNA bands were relatively diffused on gels because Bal31 possesses a higher quasi-processive exonuclease activity that simultaneously degraded both 3'- and 5'-termini of duplex DNA (Shishido and Ando, 1982). So the upstream sequences of the pBR322-*tet* promoter region (nucleotides 10-45) (see Fig. 3.1) are expected to be easily unwound in the DNA of pBR-CT[ras], resulting in an efficient initiation of transcription of the *tet* gene. Even though in the DNA of pBR-invCT[ras] the unwound upstream region must be much closer to the pBR322-*tet* promoter, the plasmid confers lower levels of Tc^r on *E. coli* cells. Probably the CT/AG sequence does not adopt a canonical unwound structure in supercoiled plasmid in *E. coli*; it presumably forms an intramolecular triplex structure transiently via the mirror repeat. The sequence between the putative triplex portion and pBR322-*tet* promoter may be tightly double helical. This state is probably unfavorable for the initiation of transcription of the *tet* gene.

On the other hand, transcription of the *bla* gene is initiated at nucleotides 36 and 4187 and proceeds in the direction opposite to that of the *tet* gene (Brosius *et al.*, 1982) (see Fig. 3.1). The results, therefore, suggest that the *ras* CT/AG sequence-containing fragment inserted into the *Eco*RI site may inhibit the *bla* transcription started at nucleotide 36 in spite of the orientation of insertion of the fragment [RNA polymerase may stall at the unusual structure (intramolecular triplex?) formed in the CT/AG sequence], but it has almost no effect on the *bla* transcription initiated at nucleotide 4187, which is distant from the *Eco*RI site.

The chloroquine-agarose gel electrophoresis demonstrated that compared with pBR-CT[ras], pBR-invCT[ras] contained a larger amount of positively supercoiled DNA molecules which were derived from less negatively supercoiled DNA species propagated in DM800, confirming that the negatively superhelical density of pBR-invCT[ras] is lower than that of pBR-CT[ras]. The high levels of negative supercoiling of pBR322 in DM800 are known to be attributed to the generation of twin supercoiled domains during transcription of the *tet* gene: in the absence of the

topoisomerase I, the positively supercoiled domain is effectively relaxed by gyrase, resulting in a net accumulation of negative supercoils (Wu *et al.*, 1988; Tsao *et al.*, 1989). The presence of the *bla* gene is considered not to be required for high levels of negative plasmid supercoiling; the pBR322 deletion plasmid lacking the *bla* gene showed a pBR322-like high level of negative supercoiling (Pruss and Drlika, 1986; Shishido *et al.*, 1989). As transcription proceeds, DNA in front of the transcription complex becomes positively supercoiled, and DNA behind the complex becomes negatively supercoiled (Tsao *et al.*, 1989). The inserted CT/AG-biased sequence-containing region present in the negative domain (*Eco*RI site) of the two pBR322 derivatives may form an altered structure, presumably such that introduction of negative turns into the derivatives is insufficient when compared with pBR322 DNA and/or some gyrase molecules do remove negative turns in the derivatives. The level of Tc^r of *E. coli* carrying pBR-CT[ras] is clearly higher than that carrying pBR-invCT[ras], showing more efficient initiation of the transcription of the *tet* gene in pBR-CT[ras]. This causes more frequent formation of twin supercoiled domains in pBR-CT[ras] than in pBR-invCT[ras], resulting in the increase of negative superhelical density of the plasmid.

The CT/AG-biased sequence with mirror repeat symmetry has been reported to form an intramolecular triplex structure (Mirkin *et al.*, 1987) under conditions of negative supercoiling and either low pH (Lyamichev *et al.*, 1985) or neutral pH in the presence of divalent cations (Kohwi and Kohwi-Shigematsu, 1988). So we constructed pBR-CT[ras]Δ13 and pBR-CT[ras]Δ19, which are the pBR-CT[ras] plasmids lacking the counterpart of the mirror repeat of the CT/AG sequence (see Fig. 3.4). The S1-digestion analysis of the two DNAs isolated from DM800 revealed that an S1-cleavable structure was not formed within the shortened CT/AG sequence (data not shown), showing that the mirror repeat is involved in the formation of S1-cleavage sites and presumably in that of the H-y3 isomer of an intramolecular triplex structure (the 3' half of the mirror repeat of the pyrimidine

strand is the third strand, see Fig, 1.3) at pH 4.5. Concerning the possibility of formation of the intramolecular triplex structure of the *ras* CT/AG-biased sequence, I will discuss in Chapter 6.

Chapter 4

Structure and function of pyrimidine/purine-biased sequence originated from the 5'-promoter region of the basidiomycete *Lentinus edodes priA* gene

4.1 Introduction

Our group has recently found that the developmentally regulated *priA* gene (Kajiwara *et al.*, 1992), as like the *Le.ras* gene, possesses a CT-motif with a short mirror repeat (6 bases) in and immediately upstream of which its transcriptional initiation sites are present. The *priA* CT-motif extended over 26 nucleotides (25 are pyrimidines). In Chapter 3, the topological structure of the *L. edodes ras* CT/AG-biased sequences was analyzed. The experimental results showed that stable S1-sensitive nonbase-paired site is formed within the *Le. ras* CT/AG-biased sequence only under high levels of negative supercoiling generated in *E. coli* DM800 (*ΔtopA gyrB225*) (Sternglanz *et al.*, 1981; DiNardo *et al.*, 1982). Deletion analysis revealed that the mirror repeat is involved in the formation of S1-cleavage sites. So it has been shown that the mirror repeat sequence seems to be involved in formation of non-B, unusual DNA structure. In this chapter, topological structure of the *priA* CT/AG-biased sequence was analyzed by the methods using for the *ras* CT/AG-biased sequence. The biological function of the *priA* CT/AG-biased sequence in the basidiomycete *C. cinereus* was also studied, revealing that the mirror repeat plays an important role for expression of the *priA* promoter activity toward a transgene.

4.2 Materials and methods

4.2.1 Construction of pBR322 derivatives carrying the CT/AG-biased sequence of the *priA* gene

The 109-bp *Rsa*I - *Hin*fI fragment containing the *priA* CT/AG-biased sequence (see Fig. 4.4) was blunt-ended and ligated to the *Eco*RI adaptor (5'-CGAATTCG). The 121-bp *Eco*RI fragment with the *priA* CT/AG-biased sequence was inserted into the *Eco*RI site of pBR322 (Watson, 1988). Based on the orientation of insertion of the CT/AG-biased sequence, two pBR322 derivatives with a single CT/AG-biased sequence were obtained and designated pBR-CT[priA] and pBR-invCT[priA] (Fig. 4.1). In pBR-CT[priA] the pyrimidine-rich sequence was on the pBR322 *tet*-coding strand and in pBR-invCT[priA] the purine-rich sequence was on this strand. The pBR-CT[priA] and pBR-invCT[priA] derivatives containing the two point mutations (the replacement of two dTMP residues by dGMP residues (see Fig. 4.4)) in the counterpart of the mirror repeat of the CT/AG-biased sequence were constructed as follows. The 116-bp *Rsa*I - *Bam*HI fragment containing the point-mutated CT/AG-biased sequence was excised from pLC2mutCT-bar (described below), blunt-ended and ligated to the *Eco*RI adaptor. This 128-bp *Eco*RI fragment was inserted into the *Eco*RI site of pBR322 in both orientations and the resulting derivatives were named pBR-mutCT[priA] and pBR-inv.mutCT[priA]. DNAs of the pBR322 derivatives were used to transform *E. coli* JM109 (*topA*$^+$ *gyrA96*) (Yanisch-Perron *et al.*, 1985) and DM800 (*ΔtopA gyrB225*) (Sternglanz *et al.*, 1981; DiNardo *et al.*, 1982). Restriction endonucleases, DNA modifying enzymes and the *Eco*RI adaptors were purchased from Takara Shuzo Co., Japan or Nippon Gene Co., Japan and used according to the suppliers' instructions.

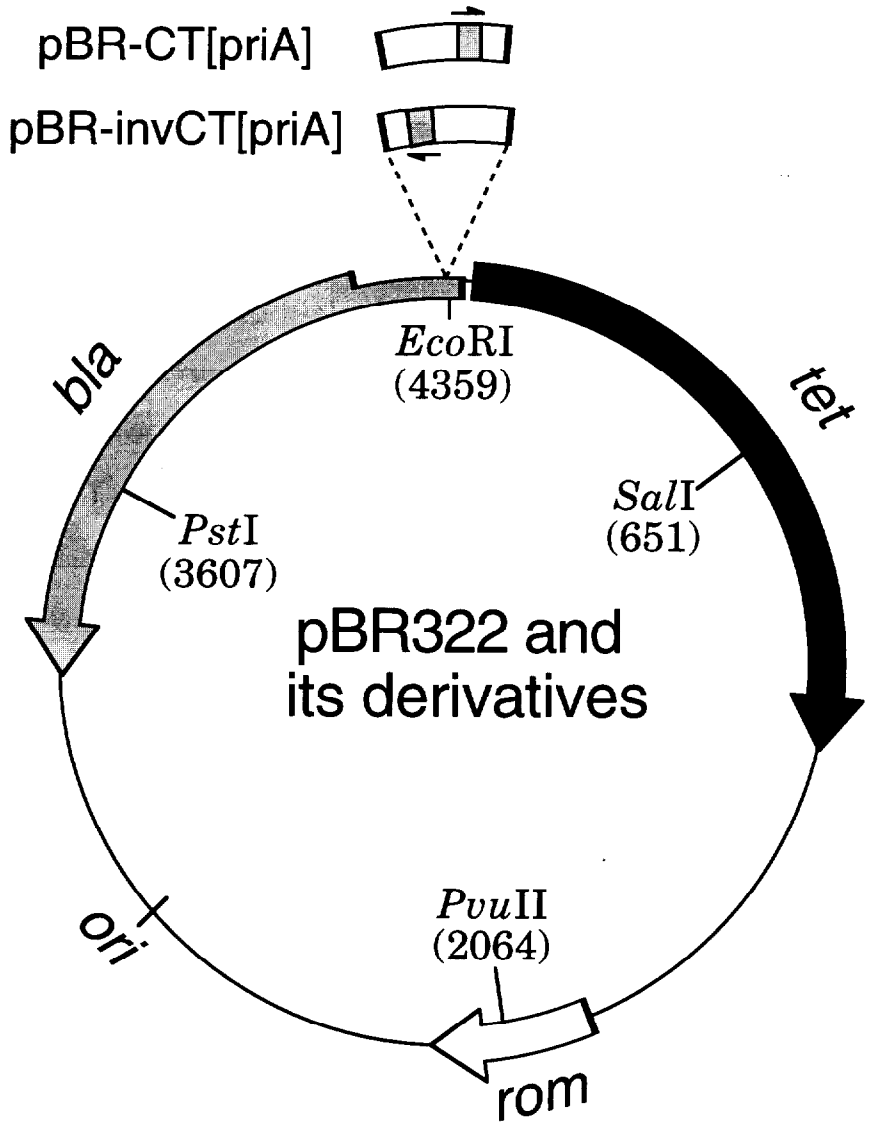

Figure 4.1

Structures of pBR322 and its derivatives carrying the CT/AG-biased sequence of the *priA* gene

The nucleotide sequences of the *priA* CT/AG sequence-containing fragment are shown in Fig. 4.4. Location and direction of transcription of the *tet* gene (initiated at nucleotide 45 (Brosius *et al.* 1982)), the ß-lactamase gene (*bla*) (initiated at nucleotides 36 and 4189 (Brosius et al. 1982)) and the *rom* gene (Watson 1988), location of the origin of replication (*ori*), and restriction sites of *Eco*RI (4359), *Sal*I (651), *Pvu*II (2064) and *Pst*I (3607) on the pBR322 genome (Watson 1988) are indicated. The *priA* CT/AG-biased sequence (shaded)-containing fragments (open arc bars) inserted into the *Eco*RI site are shown, in which the direction of the arrow marks that of the CT strand.

4.2.2 Construction of pLC2-bar and its derivative carrying the point-mutated CT/AG-biased sequence of *priA*

pLC2 (5.6 kb) is the pBR322-based chromosome-integrating vector carrying the *priA* basal promoter (0.37 kb) and its terminator (1.2 kb) and has the *Bam*HI-cloning site, which is useful for foreign protein expression (see Chapter 2). Plasmid pLC-bar, containing the 0.56-kb bialaphos-resistance gene (*bar*) derived from *Streptomyces hygroscopicus* was digested with *Bam*HI. The resulting 0.56-kb *Bam*HI fragment with *bar* gene was inserted into the *Bam*HI site of pLC2, yielding pLC2-bar (see Fig. 4.5). pLC2-bar derivative containing the two point mutations in the counterpart of the mirror repeat of the CT/AG-biased sequence was constructed as follows. The 0.74-kb *Hinc*II fragment containing the *priA* promoter (see Fig. 2.2, Kajiwara *et al.*, 1992) was inserted into the blunt-ended *Cla*I site (position 23) on pBR322 and the resulting recombinant plasmid was used as a template for PCR (polymerase chain reaction) -mediated site-directed mutagenesis. Four primers (H, R, U and Y) were used. Primer R, 5'-GTATCACGAGGCCCTT is identical with the sequence from 4335 to 4350 of pBR322 and primer H, 5'-GCAATTTAACTGTGAT is complementary to the sequence from 64 to 49 of pBR322. Primer Y, 5'-CCCTCTCCGCGCTTGCACCA and primer U, 5'-CGGACTGGTGCAAGCGCGGAGAGGGAGAGA are the complementary sequences designed to conversion of two dTMP residues to the dGMP residues (see Fig. 4.4). The first half and last half of the two point-mutated CT/AG-biased sequence amplified individually using the primers R and U and the primers Y and H, respectively, were mixed to generate long single-stranded DNAs hybridized at their 3'-terminal short sequences (containing the mutation points), and then, repair DNA synthesis was done to generate the entirely double-stranded DNA (0.83 kb). The 0.83-kb PCR product was entirely sequenced to confirm the presence of the desired mutations and the absence of additional mutations. The 0.58-kb *Bam*HI - *Sph*I fragment containing the *priA* point-mutated promoter was excised from the 0.83-kb PCR product. The corresponding 0.58-kb *Bam*HI - *Sph*I

fragment containing the *priA* wild-type promoter was excised from pLC2-bar (see Fig. 4.5) and it was replaced by the same restriction fragment containing the *priA* mutant promoter, yielding the recombinant plasmid pLC2mutCT-bar.

4.2.3 Preparation of plasmid DNAs

Plasmid DNAs were prepared as described in Materials and methods of Chapter 3 (section 3.2.2).

4.2.4 S1 Nuclease digestion and gel electrophoresis

These were done as described in Materials and methods of Chapter 3 (section 3.2.3).

4.2.5 Primer extension analysis of S1-cleavage sites

Using restriction fragments (20 ng each), PCR was carried out in the reaction buffer (5 µl) containing 50 fmols of the IRD41-labeled synthetic primer (Aloca Co., Japan), deoxynucleoside triphosphates (final conc. 2.5 mM each), 1 × KOD DNA polymerase buffer (120 mM Tris-HCl buffer (pH 7.5), 6 mM $(NH_4)_2SO_4$, 10 mM KCl, 0.1 % Triton X-100, 0.001 % BSA and 2.5 mM $MgCl_2$) and 0.5 unit of KOD DNA polymerase (TOYOBO Biochemicals Co., Japan). The thermal cycle was 30 s at 95°C, 30 s at 50°C and 30 s at 74°C for 30 cycles. The reactions were electrophoresed on 4 % polyacrylamide gels containing 7 M urea in a LI-COR model 4000L automated DNA sequencer and the image created during electrophoresis was analyzed using the Base ImagIR™ image analysis program. The sizes of the primer extension products were determined from sequence ladders (ACGT) by the dideoxy chain-termination method of Sanger *et al.* (1977).

4.2.6 *C. cinereus* strains and media

These were described in Materials and methods of Chapter 2 (section 2.2.1).

4.2.7 Transformation of *C. cinereus*

This was done as described in Materials and methods of Chapter 2 (section 2.2.3).

4.2.8 DNA isolation of *C. cinereus* and Southern-blot analysis

These were done as described in Materials and methods of Chapter 2 (section 2.2.4).

4.2.9 RNA isolation of *C. cinereus* and Northern-blot analysis

Total cellular RNA was isolated from *C. cinereus* transformants as follows. The mycelial cells were quick frozen in liquid nitrogen and powdered by a homogenizer. This powder (about 500 mg) was transferred to a 15 ml plastic tube and 4 ml each of LETS buffer (10 mM Tris-HCl (pH 7.4), 10 mM EDTA, 100 mM LiCl, 0.2 % SDS, 0.1 % Diethyl pyrocarbonate) and LETS-saturated phenol were added in the tube. The suspension was mixed, vortexed vigorously and incubated at 65°C for 30 min with brief vortexing at 10 min intervals. The tube was centrifugated and the aqueous phase was transferred to a fresh tube and extracted twice with phenol:chloroform:isoamyl alcohol (25:24:1). After ethanol precipitation RNA samples were electrophoresed in 2.2 M formaldehyde - 1.2 % agarose gel. Subsequent procedures of Northern-blot analysis were as in Southern-blot analysis.

4.2.10 Mapping of the transcriptional initiation sites by the primer extension analysis

Poly $(A)^+$ RNA (5 µg each) prepared from the total cellular RNA of *C. cinereus* transformants using Oligotex™-dT30<Super> (Takara Shuzo Co., Japan) was incubated with 30 pmol of the ^{32}P-labeled synthetic oligonucleotide (5'-CTGCGGCTCGGTACGGAAGTTGACCGTGCT) complementary to the

nucleotides +123 to +94 of the *bar*-coding sequence at 65°C for 10 min in reverse transcription buffer (50 mM Tris-HCl (pH 8.3), 75 mM KCl, 3 mM $MgCl_2$) containing 2 mM each deoxynucleoside triphosphates, followed by a slow cooling down to 42°C. To the incubation mixture, dithiothreitol (final conc. 10 mM) and reverse transcriptase (200 units of SuperScript™II RNase H^- type, GIBCO-BRL) were added and further incubated at 37°C for 30 min. After ethanol precipitation the reactions were electrophoresed on 8 % polyacrylamide gels containing 7 M urea, followed by autoradiography. The sizes of the primer extension products were determined from sequence ladders (TGCA) by the dideoxy chain-termination method of Sanger *et al.* (1977).

4.3 Results

4.3.1 Analysis of S1-cleavability of pBR322 and its derivatives

To investigate whether the *priA* CT/AG-biased sequence forms S1-cleavable nonbase-paired sites, DNAs of pBR322 and its derivatives isolated from *E. coli* topoisomerase I deletion mutant DM800 (*ΔtopA gyrB225*) (Sternglanz *et al.*, 1981; DiNardo *et al.*, 1982) and *E. coli* JM109 (*topA*$^+$*gyrA96*) (Yanisch-Perron *et al.*, 1985) were analyzed by the methods using for the *ras* CT/AG-biased sequence (see section 3.3.1). DNAs were digested with S1 at pH 4.5 and the full-length S1-linearized DNAs were further digested with restriction endonucleases which have a single unique cleavage site on the DNAs (see Fig. 4.1). Figure 4.2 shows the agarose gel electrophoretic patterns obtained for pBR322, pBR-CT[priA] and pBR-invCT[priA] isolated from DM800. *Pvu*II-, *Sal*I- and *Pst*I-digests of the S1-linearized pBR322 (containing ~ 50 % open-circular DNA) yielded a number of discrete and two intense DNA bands on the gels (lanes 1, 6 and 11, respectively, see section 3.3.1). In all the cases of *Pvu*II-, *Sal*I-, and *Pst*I-digests of the S1-linearized pBR-CT[priA] (lanes 2, 7, and 12) and pBR-invCT[priA] (lanes 3, 8, and

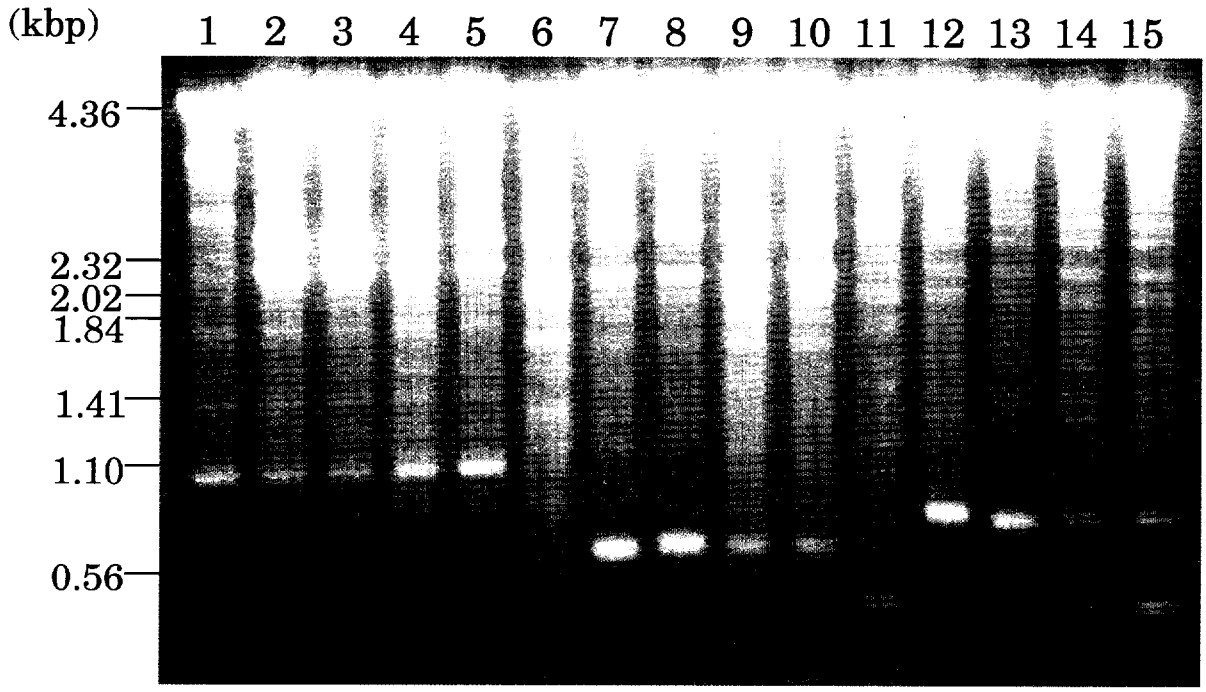

Figure 4.2

DNA fragments produced after digestion of the S1-generated unit-length linear pBR322 and its derivatives (containing ~50% open circular DNA) with restriction endonucleases

The S1-digested DNAs were then digested with *Pvu*II (lanes 1-5), *Sal*I (lanes 6-10) and *Pst*I (lanes 11-15). Lanes 1, 6 and 11, pBR322; lanes 2, 7 and 12, pBR-CT[priA]; lanes 3, 8 and 13, pBR-invCT[priA]; lanes 4, 9 and 1 4, pBR-mutCT[priA]; lanes 5, 10 and 15, pBR-inv.mutCT[priA]. The *Hin*dIII-digest of phage λ DNA and *Hin*cII- and *Pvu*II-digests of pBR322 DNA were used as molecular size markers. Sizes (kb) are indicated to the left in the panel.

13), two additional intense DNA bands were observed at 2.4 and 2.1 kb, 3.8 and 0.7 kb, 3.6 and 0.9 kb, respectively, for the former, and at 2.3 and 2.2 kb, 3.8 and 0.7 kb, 3.7 and 0.8 kb, for the latter. The sizes of the two fragments summed up to the nearly full-length size (4478 bp) of the plasmid DNAs, showing the generation of another strong cleavage site (region) on both pBR-CT[priA] and pBR-invCT[priA]. This site (region) was found to fall into around the CT/AG-biased sequence of both plasmids. The same result was obtained for DNAs pBR-CT[priA] and pBR-invCT[priA] isolated from JM109 (*topA*$^{+}$*gyrA96*) (data not shown). Differently from the CT/AG-biased sequence of the *ras* gene (see Chapter 3), the CT/AG-biased sequence of the *priA* gene does not require higher levels of negative superhelical density for formation of the stable S1-cleavable nonbase-paired structure.

4.3.2 Mapping of the S1-cleavage sites around the CT/AG-biased sequence of pBR322 derivative pBR-CT[priA]

The S1-cleavage sites were analyzed by the primer extension method using primer H and primer R (see Materials and methods of Chapter 4, section 4.2.2) in Fig. 4.3. In the *Pvu*II-digests of the S1-linearized pBR-CT[priA] (lane 2 of Fig. 4.2), DNA fragments at/around the two intense bands (2.4 and 2.1 kb) were subjected to analysis. In the extension of the AG-rich strand (the smaller fragment and primer H), one strong and one weaker bands were observed at the positions of nucleotides 102 (T) and nucleotides 101 (G), respectively, on the AG-rich strand (panel A of Fig. 4.3), indicating that the template (CT-rich) strand ended at the positions marked by arrows in Fig. 4.4, i. e., S1-cleavages occurred at the arrow positions. These S1-cleavage sites agreed with those estimated in the experiments of Fig. 4.2. In the case of the CT-rich strand (the larger fragment and primer R), two strong and one weaker bands were observed at the positions of nucleotides 82 (T) and 83 (C) and nucleotide 84 (C), respectively, on the CT-rich strand (panel B of Fig. 4.3).

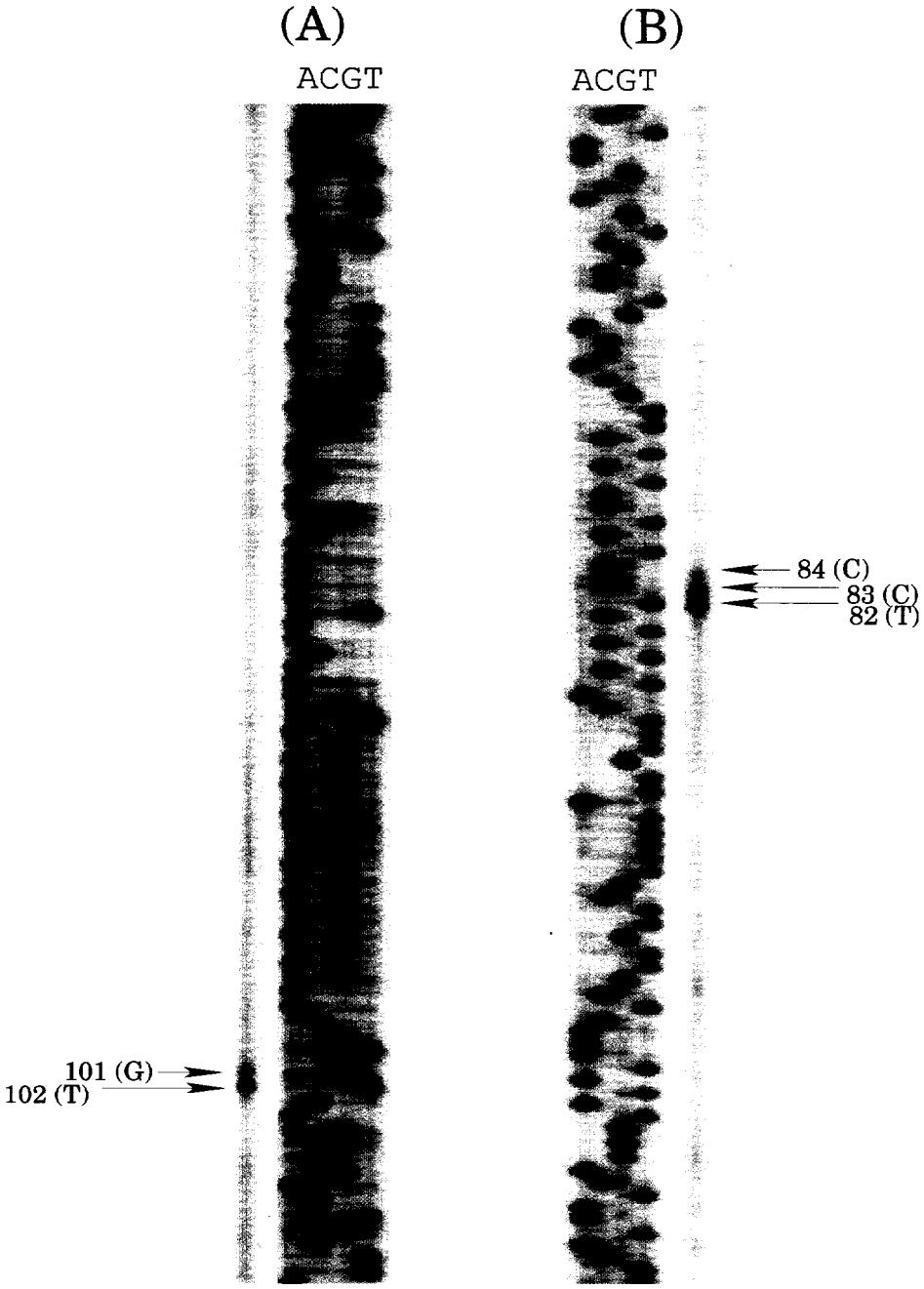

Figure 4.3

Determination of the S1-cleavage sites within the CT/AG-biased sequence of pBR322 derivative pBR-CT[priA] by the primer extension method

The extensions of the AG-rich strand with primer H (A) and the CT-rich strand with primer R (B) were carried out using the smaller or larger fragment of the *Pvu*II-digests of pBR-CT[priA]. The nucleotides corresponding to the ends of extension products (marked by arrows) were determined from the sequence ladders (ACGT) which were derived from pBR-CT[priA] with primers H and R.

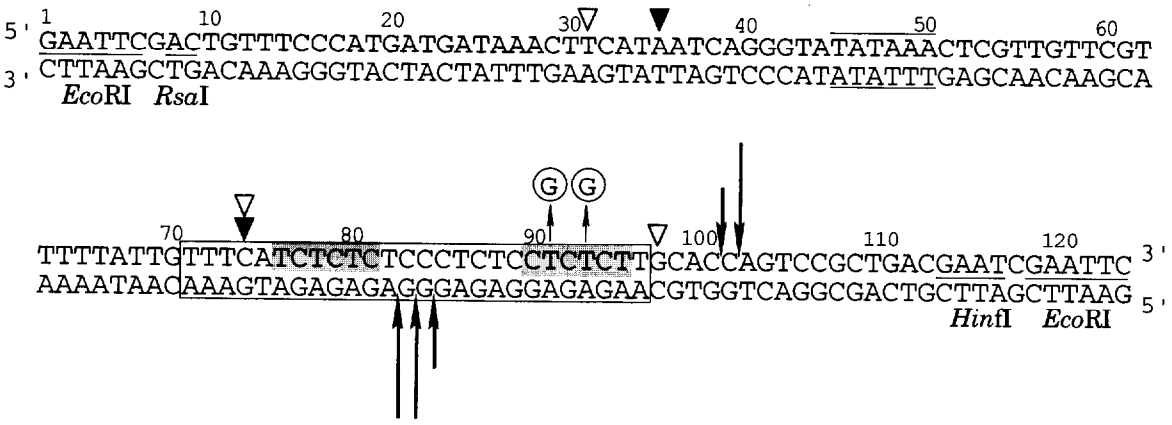

Figure 4.4 Summary of the S1-cleavage sites within/around the CT/AG-biased sequence of the *priA* gene

The nucleotide sequence of the CT/AG-biased sequence (boxed) -containing region of the *priA* gene is shown. Mirror repeat sequences involved in the formation of the putative intramolecular triplex structure are shaded on the pyrimidine strand (see Chapter 6). Closed arrowheads and open arrowheads are transcriptional initiation sites determined for the *priA* transcription in *L. edodes* in a previous paper (Kajiwara *et al.* 1992) and those determined for the *bar* transcription in *C. cinereus*, respectively. The S1-cleavage sites on the template strand in the extensions of the CT and AG strands are shown by arrows. Their lengths correspond to the frequencies of S1 cleavages judged from the results of Fig. 4.3, with the most preferential sites marked by long arrows. The putative TATAAA box is marked by over- and underline. Restriction sites used for the construction of recombinant plasmids are also shown. The two dGMP residues (circled) substituted for the two dTMP residues in the counterpart of the mirror repeat are shown above the sequence.

The ends of the AG-rich template strand (the sites of S1 cleavage) are marked by arrows in Fig. 4.4. These data demonstrate that the S1-cleavage sites fall within the CT/AG-biased sequence and the region just downstream of it; the CT/AG-biased sequence induces the formation of the extended open structure sensitive to S1 cleavage. The S1-cleavage sites determined by the extension of the AG-rich strand did not coincide with those of the CT-rich strand. This suggests that S1 cleavages occurred simultaneously at site(s) on the AG-strand and site(s) on the CT-strand, and then second S1 cuts occurred on the opposite strand at or near the sites nicked first to yield linear DNA molecules slightly smaller than full length size.

To assess the role of the mirror repeat in the CT/AG-biased sequence for the formation of S1-cleavable structure, we constructed pBR-mutCT[priA] and pBR-inv.mutCT[priA], which contain the two point mutations in the mirror repeat of the *priA* CT-motif. The two dTMP residues (nucleotides 91 and 93) were replaced by dGMP residues (Fig. 4.4). These plasmid DNAs were propagated in DM800 and subjected to S1 analysis. In all the cases of *Pvu*II-, *Sal*I-, and *Pst*I-digests of the S1-linearized pBR-mutCT[priA] (lanes 4, 9 and 14) and pBR-inv.mutCT[priA] (lanes 5, 10 and 15), two additional DNA bands were observed at 2.4 and 2.1 kb, 3.9 and 0.6 kb, 3.6 and 0.9 kb, respectively, for both the former and the latter. They were relatively faint when compared with those derived from pBR-CT[priA] and pBR-invCT[priA]. These suggest that an S1-cleavable structure was not formed within the *priA* sequence containing the mutated CT/AG-biased sequence and instead preferential S1-cleavage sites were located around the *tet* promoter region of pBR322.

4.3.3 Responsibility of the mirror repeat in the CT/AG-biased sequence for an expression of the promoter activity in *C. cinereus* of the *priA* gene

The recombinant plasmids pLC2-bar and pLC2mutCT-bar were used for the experiments (Fig. 4.5). The former possesses the *priA* promoter containing the

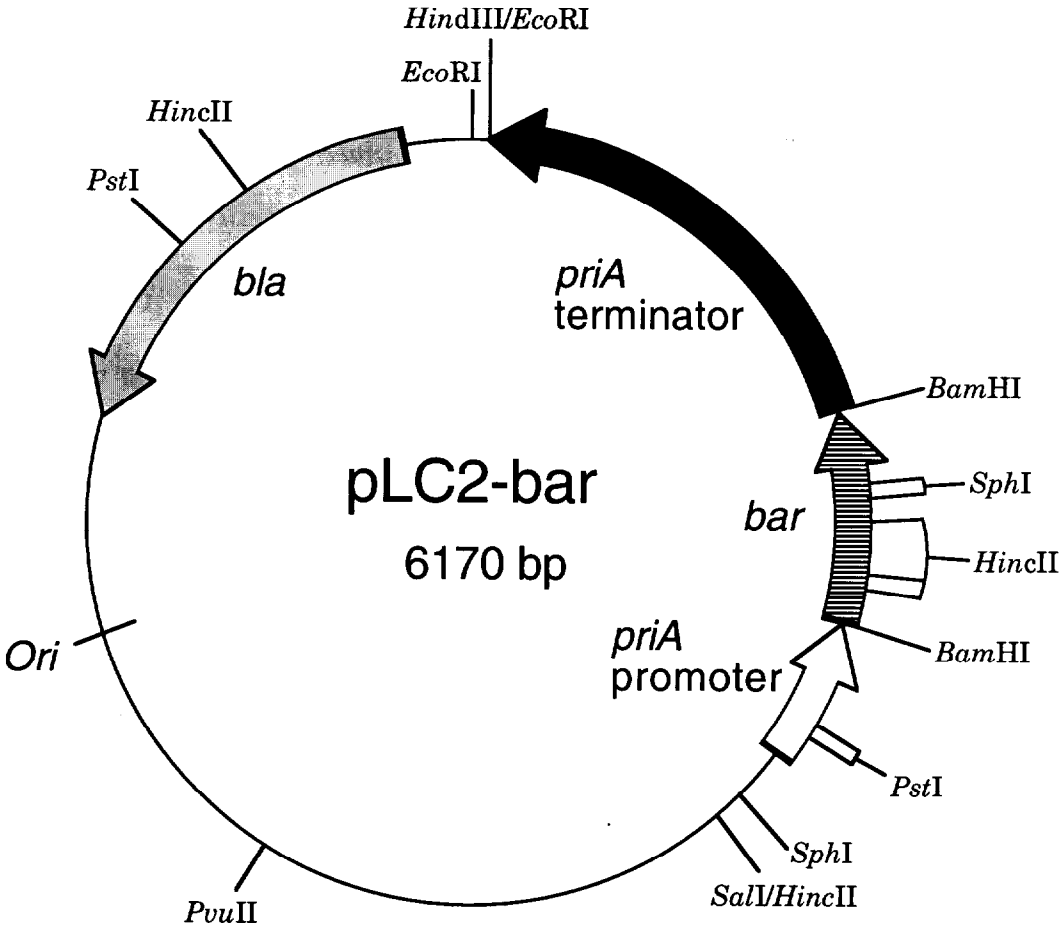

Figure 4.5 Structure of the *Streptomyces*-derived bialaphos-resistance gene product expressing recombinant plasmid pLC2-bar

pLC2mutCT-bar, not shown in the figure, was also constructed. It contains two point mutations in the counterpart of the mirror repeat of the CT/AG-biased sequence so that the two dTMP residues are replaced by the dGMP residues (see Fig. 4.4). Thin lines are pBR322 sequences. The *bla* gene and the origin (*ori*) of replication are shown. Restriction sites of *Bam*HI, *Eco*RI, *Hinc*II, *Hin*dIII, *Pst*I, *Pvu*II, *Sal*I and *Sph*I on the recombinant plasmid are indicated. Arrows show the directions of the transcription of the genes.

naturally occurring CT/AG-biased sequence and the latter has that carrying the mutated CT/AG-biased sequence. They have the *S. hygroscopicus bar* gene as a reporter. pLC2-bar and pLC2mutCT-bar were introduced into the genome of *C. cinereus* LT2-44 (*trp1-1, 1-6*), in which a transformation system is well established, by co-transformation with pCc1001 carrying the *C. cinereus TRP1* gene (Binninger *et al.*, 1987), and selecting for Trp^+ transformants. For each experiment 4 μg each of pCc1001 and pLC2-bar or pLC2mutCT-bar was presented to approx. 2×10^7 protoplasts. From two independent co-transformations a total of 24 and 17 Trp^+ colonies were obtained through introduction of pCc1001 and pLC2-bar or pCc1001 and pLC2mutCT-bar, respectively. All the Trp^+ colonies were cultivated on MYG agar plates. The mycelial colonies grown on the plates were screened for a bialaphos resistance in MYG agar plates containing 100 μg bialaphos per ml. Seven out of 24 Trp^+ colonies obtained by the introduction of pLC2-bar were resistant to bialaphos and these transformants were named WB-1, WB-2, WB-3, WB-4, WB-5, WB-6 and WB-7. On the other hand, four out of 17 Trp^+ colonies obtained by the introduction of pLC2mutCT-bar showed a bialaphos resistance. However, three colonies except for only one were found to be abortive transformants. They grew slightly on the bialaphos-containing plates and they lost the bialaphos resistance during cultivation in MYG medium without bialaphos for six weeks. We attempted several times to isolate stable bialaphos-resistance transformant(s) by the introduction of pLC2mutCT-bar, but our efforts resulted in a failure. So the aforementioned one bialaphos-resistant transformant, named WB-m1 was used for the following experiments.

To ascertain the presence of the introduced DNA in the bialaphos-resistant Trp^+ transformants, Southern-blot analysis was done using the ^{32}P-labeled 0.56-kb *Bam*HI fragment containing the *bar* gene as a probe. In the DNA samples of WB-

1, WB-3, WB-7 and WB-m1 without restriction enzyme digestion, specific hybridization signals were observed at the high-molecular-mass DNA region corresponding to the chromosomal DNA (data not shown). No specific hybridization signal was found in the DNA sample of the Trp^+ transformant, named W-1, obtained by the introduction of pCc1001 alone.

Next all the DNA samples (20 μg each) were digested with both *Pst*I and *EcoR*I (see Fig. 4.6A) and subjected to Southern-blot analysis using the probe of the aforementioned ^{32}P-labeled 0.56-kb *Bam*HI fragment. As shown in the upper picture of Fig. 4.6B, WB-m1 (lane 1), WB-1 (lane 2), WB-3 (lane 3) and WB-7 (lane 4) all gave one intense hybridization signal at the position corresponding to the size (2.0 kb) of the chromosomal DNA fragments produced by digestion with both *Pst*I and *Eco*RI (see Fig. 4.6A). No hybridization signal was observed in the case of W-1 (lane 5). These results suggest that the introduced pLC2-bar and pLC2mutCT-bar DNAs had been integrated into chromosomal DNA of the transformants. Detection of the hybridization band at 2.0-kb position is considered to show that almost the entire expression cassette is integrated, which consists of the majority of *priA* promoter (containing CCAAT box, TATA box and CT-motif), *bar* gene and *priA* terminator. To ensure equal loading of the DNA preparations and estimate the copy numbers of the *bar* sequence on the chromosomes of WB-m1, WB-1, WB-3 and WB-7, the samples (20 μg each) used in the above experiment were digested with both *Xho*I and *Sal*I, and then subjected to Southern-blot analysis using the probe of ^{32}P-labeled 1.3-kb *Xho*I - *Sal*I genomic fragment containing the *C. cinereus ras* gene that exists as one copy on the chromosome (Ishibashi and Shishido, 1993). The specific ^{32}P-activity of the *ras* probe was almost the same as that of the *bar* probe. All the transformants gave one faint signal at the position of around 1.3 kb (Fig. 4.6B, lower picture). Their intensities were almost the same each other and very similar to the intensity of the 2.0-kb signal of WB-1. The *bar*

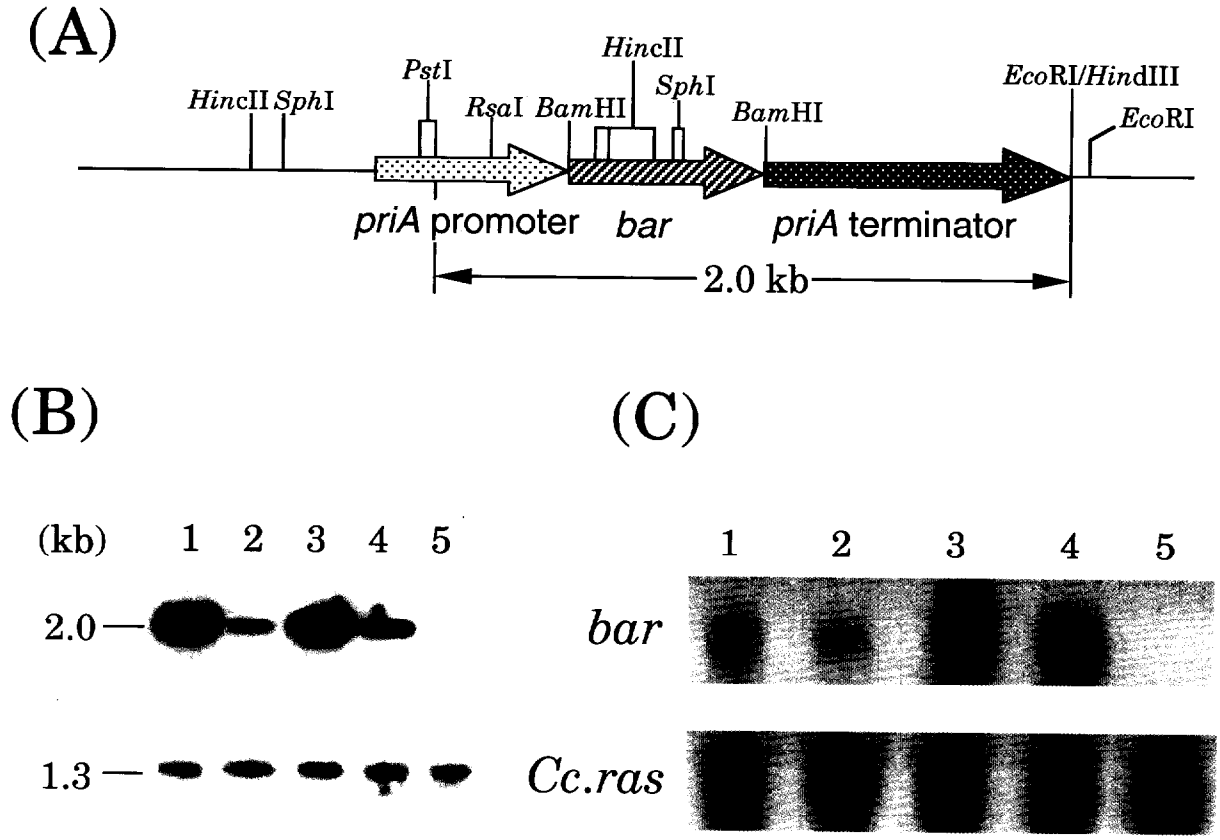

Figure 4.6

Analyses of total cellular DNA and RNA of various bialaphos-resistance transformants of *C. cinereus*

(A) Restriction map of pLC2-bar. The 2.0-kb *Pst*I - *Eco*RI fragment is indicated by arrow. (B) Southern-blot analyses of the [*Pst*I+*Eco*RI] (upper picture) and the [*Xho*I+*Sal*I] (lower picture) -digests of total cellular DNA prepared from WB-m1 (lane 1), WB-1 (lane 2), WB-3 (lane 3), WB-7 (lane 4) and W-1 (lane 5) using the 32P-labeled probes of the 0.56-kb *Bam*HI fragment carrying the *bar* gene (upper picture) and the 1.3-kb *C. cinereus Xho*I - *Sal*I genomic fragment carrying the *ras* gene (lower picture) (Ishibashi and Shishido 1993), respectively. (C) Northern-blot analysis of total cellular RNA isolated from the five transformants identical to those in panel B. The aforementioned 32P-labeled DNA fragments were used as probes.

and *ras* hybridization bands were cut out from the membranes, and their radioactivities were counted. The data suggests that WB-m1, WB-1, WB-3 and WB-7 carry about 9, 1, 8 and 3 copies of the *bar* sequence (inserted between *priA* wild-type or mutant promoter and *priA* terminator), respectively, on their chromosomes.

To ascertain the presence of the *bar* transcript in the transformants, Northern-blot analysis was done for total cellular RNA isolated from the transformants using the ^{32}P-labeled 0.56-kb *Bam*HI fragment containing the *bar* gene as a probe (Fig. 4.6C). No specific hybridization signal was found in the RNA blot of W-1 (lane 5). As was expected, a very intense signal of 1.1 kb (*bar* band) was detected in the RNA blot of WB-3 (lane 3). The RNA blot of WB-7 (lane 4) gave a relatively intense signal, but that of WB-1 (lane 2) gave a faint signal. The intensities of these signals seemed to coincide with the copy numbers of the *bar* sequence. The RNA blot of WB-m1 (lane 1), on the other hand, gave clearly weaker signal than that of WB-7 as well as WB-3. To ensure equal loading and transfer of the RNA preparations in this experiment, the Northern-blots hybridized with the *bar* probe were put into a boiling 0.1 % SDS and kept in it until a room temperature. After confirming a perfect removal of the *bar* probe by autoradiography, the resulting Northern-blots were rehybridized with ^{32}P-labeled probe of the *C. cinereus ras* gene (Ishibashi and Shishido, 1993). All the transformants gave one intense signal at the position of around 1.2 kb and their intensities were similar (Fig. 4.6C). The negatives of the autoradiographic patterns pictured in Fig. 4.6C yielded a densitometric measurement of the intensities of *bar* and *ras* bands. WB-m1, WB-3 and WB-7 were estimated to contain the *bar* transcript about 1.5, 7 and 3 times as much as WB-1. These data show that the *bar* gene is efficiently transcribed under the control of *priA* wild-type promoter, but a clearly lower steady state level of the *bar* transcript is observed under the control of *priA* mutant promoter.

The growth of WB-m1, WB-1, WB-3 and WB-7 were examined in MYG agar

plates containing 100 μg or 300 μg bialaphos per ml (Fig. 4.7). As was expected, WB-3 and WB-7 grew well on bialaphos-containing plates, while WB-m1 and WB-1 displayed a significantly slow growth.

4.3.4 Mapping of the transcriptional initiation sites of the *bar* gene integrated in the chromosomes of the *C. cinereus* transformants

Transcriptional initiation sites of the *bar* gene integrated in the chromosomes of WB-3 and WB-m1 were analyzed by the primer extension method (Fig. 4.8). Previous our paper (Kajiwara *et al.*, 1992) has reported that the transcription in *L. edodes* of *priA* gene starts from the two sites, i. e., 121 and 82 nucleotides upstream from the *priA* start codon (these are shown by closed arrowheads in Fig. 4.4). The primer extension of the *bar* transcript isolated from WB-3 (lane 1) gave three bands at the positions corresponding to nucleotides 31, 74 and 97 in the region containing the CT/AG-biased sequence (shown by open arrowheads in Fig. 4.4), while the *bar* transcript isolated from WB-m1 (lane 2) gave a single band at the position corresponding to nucleotide 97. The upstream two initiation sites out of the three determined for *bar* transcription in WB-3 (*C. cinereus*) matched the two sites determined for *priA* transcription in *L. edodes* (Kajiwara *et al.*, 1992) and the remainder was the site found only in *C. cinereus*. A single initiation site found in WB-m1 was the site determined only in *C. cinereus*. These data indicate that the inefficient transcription of *bar* gene in WB-m1 (as shown in Fig. 4.6C) is due to a decrease in the number of the transcriptional initiation sites.

4.4 Discussion

In this chapter, we described that the *priA* CT/AG-biased sequence can form a preferentially S1-cleavable nonbase-paired structure in *E. coli* supercoiled plasmid DNA. Formation of the open structure was shown to be induced by the mirror repeat present in the CT/AG-biased sequence, implying the formation of an

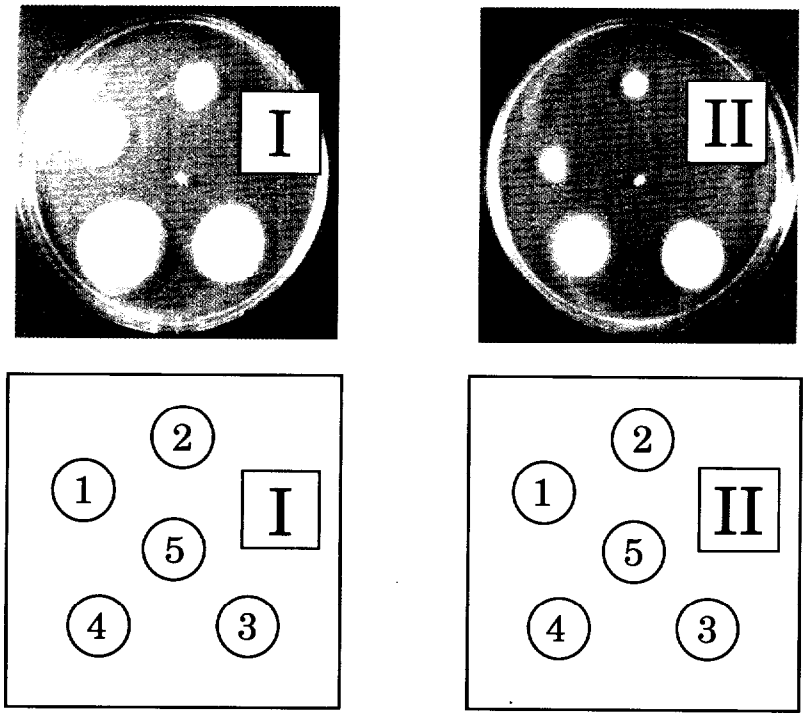

Figure 4.7

The growth of the five transformants were examined in the MYG medium containing 100 μg (I) or 300 μg (II) bialaphos per ml.

The numbers (1 ~ 5) indicated are identical to the numbers of lanes in panels B and C of Fig. 4.6: 1, WB-m1; 2, WB-1; 3, WB-3; 4, WB-7; 5, W-1.

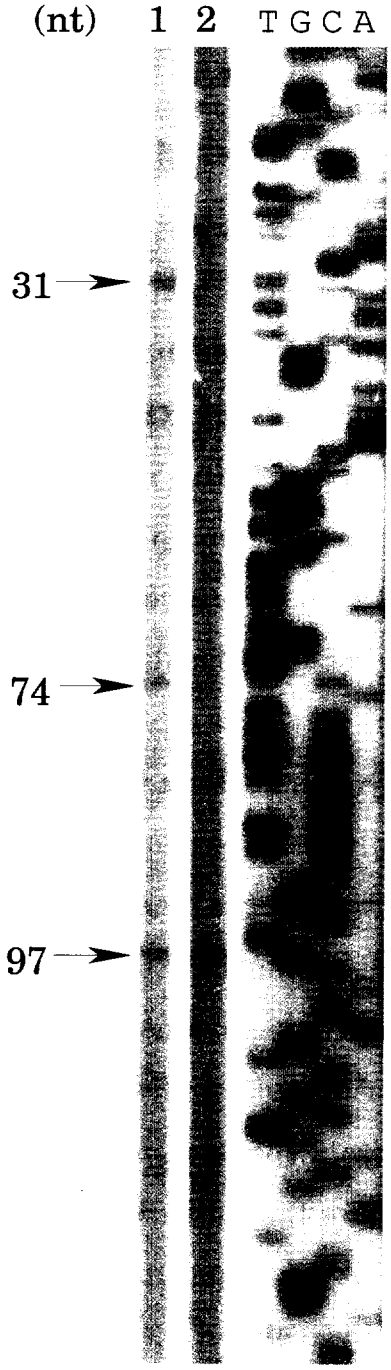

Figure 4.8

Determination of the transcriptional initiation sites in *C. cinereus* of the *bar* gene by primer extension

Poly(A)$^+$ RNA prepared from mycelia of WB-3 (lane 1) and WB-m1 (lane 2) were subjected to the analysis. The nucleotides corresponding to the ends of extension products (marked by arrows) were determined from the sequence ladders (TCGA) which were derived from the pLC2mutCT-bar. The numbers (nucleotides 31, 74 and 97 for WB-3 (lane 1) and nucleotide 97 for WB-m1 (lane 2) shown in the figure corresponds to the numbers of the nucleotides indicated by open arrowheads in Fig. 4.4.

intramolecular triplex in the CT/AG-biased sequence.

The experimental results suggest that differently from the CT/AG-biased sequence of *Le.ras* gene (see Chapter 3), the CT/AG-biased sequence of the *priA* gene does not require higher levels of negative superhelical density for formation of the stable S1-cleavable nonbase-paired structure and an S1-cleavable structure was not formed within the *priA* sequence containing the mutated CT/AG-biased sequence and instead preferential S1-cleavage sites were located around the *tet* promoter region of pBR322. Primer extension analysis revealed that these S1-sites are in the nucleotides 15 ~ 18 (around -35 region of *tet* promoter) of pBR322, which are contained in an inverted repeat sequence (data not shown). As described earlier, pBR322 possesses multiple sites infrequently cleaved by S1 (see lanes 1, 6, 11 in Fig. 4.2). One of them coincides with this inverted repeat sequence. The results, taken together, indicate that the mirror repeat is responsible for the formation of S1-cleavable unbase-paired sites within/around the CT/AG-biased sequence. Insertion of the CT/AG-biased sequence with the mutations of the mirror repeat into the *Eco*RI site of pBR322 somehow increases the frequency of S1-cleavage at the inverted repeat sequence originally present in the plasmid.

It was shown that the *bar* gene is efficiently transcribed under the control of *priA* wild-type promoter, but a clearly lower steady state level of the *bar* transcript is observed under the control of the *priA* mutant promoter. So the mirror repeat in the CT-motif is considered to play an important role for an efficient expression of the promoter activity of *priA* gene. The clearly low promoter activity of *priA* mutant promoter with the mutated mirror repeat may be the main reason why it was not easy to isolate bialaphos-resistant transformants by introduction of pLC2mutCT-bar, as described in section 4.3.3.

The unusual structure formed involving the *priA* CT/AG-biased sequence, presumably the intramolecular triplex structure, appears to be responsible for an efficient expression of the *priA* promoter activity in *C. cinereus*. Concerning the problem why the two point-mutations in the mirror repeat of the *priA* CT/AG-

biased sequence resulted in a loss of the two transcriptional initiation sites upstream of the mirror repeat, but they not in a loss of the downstream site, the simplest interpretation may be as follows. A physical force to form the unusual open structure within and just downstream of the CT/AG-biased sequence induces local removal of histone octamers from chromosome and generation of local naked DNA region. RNA polymerase (possibly together with the protein(s) essential to initiation of transcription) binds to the naked DNA region. Some molecules of RNA polymerase start transcription at the downstream site but other molecules slide up to the upstream sites and start transcription there. The initiation of transcription at the downstream site, however, also occurs in the absence of the unusual open structure.

Chapter 5

A promoter activity in *Saccharomyces cerevisiae* of the 3'-regulatory region of the basidiomycete *Lentinus edodes priB* gene

5.1 Introduction

In most eukaryotic gene expression systems accompanied with RNA polymerase II, core promoter elements of 5'-promoter regions of genes (such as GC box, CAAT box and TATA box) act as signals determining the transcriptional initiation site(s) and frequency of transcription (Maniatis *et al.*, 1987). When transcription initiates, transcription factors bind to these promoter elements in various combinations to guide RNA polymerase to the appropriate initiation site (Johnson and McKnight, 1989). However, these elements are not necessarily required for initiation of transcription because the 5'-promoter regions of genes do not always contain these core promoter elements (Smale and Baltimore, 1989). The region around the transcriptional initiation site(s) often contains CT-motif(s) as well as other core promoter elements and CT-motifs have been postulated to play a role in regulation of gene expression. As described in Chapters 3 and 4, it was shown that the CT/AG-biased sequences originated from the 5'-promoter region of the *L. edodes* genes form a preferentially S1-cleavable nonbase-paired structure (presumably an intramolecular triplex structure) induced by the mirror repeat sequence and the unusual structure formed involving the *priA* CT/AG-biased sequence appears to be responsible for an efficient expression of the *priA* promoter activity in *C. cinereus*

We have isolated a novel gene, the *priB* gene which encodes a 565 amino-acids protein with a 'Zn(II)2Cys6 zinc cluster' DNA binding motif and is actively transcribed in an early stage of fruiting-body formation of *L. edodes* (Endo *et al.*, 1994). The PRIB protein (64 kD) produced in *E. coli* was shown to bind both the 5'-

and 3'-regulatory regions of the *priB* gene *in vitro* (Endo *et al.*, 1994; Miyazaki, 1998). Random binding-site selection analysis revealed the 16-bp consensus sequence (5'-GGGGGGGACAGGANCC-3') for PRIB binding. The 5'- and 3'-regulatory region of the *priB* gene contained four and one sequences similar to this consensus sequence, respectively (Miyazaki *et al.*, 1997; Miyazaki, 1998; Kaneko *et al.*, 1998). These imply the possibility that the PRIB protein is involved in regulation of the transcription of the *priB* gene.

During the analyses of the *priB* 5'- and 3'-regulatory regions, we have found that the 5'-promoter region contains two CAAT box and a CT/AG-biased sequence extended over 20 nucleotides (19 are pyrimidines) and, more interestingly, the 3'-regulatory region also contains several promoter-like motifs, i. e., a GC box-like sequence, two CAAT boxes and two TATA box-like sequences, and two CT-motifs both extended over 26 nucleotides (23 are pyrimidines) and the aforementioned 16-bp sequence similar to the consensus sequence of the PRIB binding site. The 3'-regulatory region contained a short (61 bp) intron (Fig. 5.1). These led us to attempt to examine whether the *priB* 3'-regulatory region displays promoter activity in *S. cerevisiae* in which autonomously replicating plasmid vectors are available. In basidiomycetous fungi the only chromosome-integrating vectors are available, so a precise analysis of promoter activity may be not so easy. The experimental results revealed that the *priB* 3'-regulatory region actually possesses the promoter activity in *S. cerevisiae* and the 61-bp intron showed an inhibitory effect on the activity.

5.2 Materials and methods

5.2.1 Strains

E. coli JM109 (*topA*$^+$ *gyrA96*) (Yanisch-Perron *et al.*, 1985) and DM800 (*ΔtopA gyrB225*) (Sternglanz *et al.*, 1981; DiNardo *et al.*, 1982) were used for *E. coli*

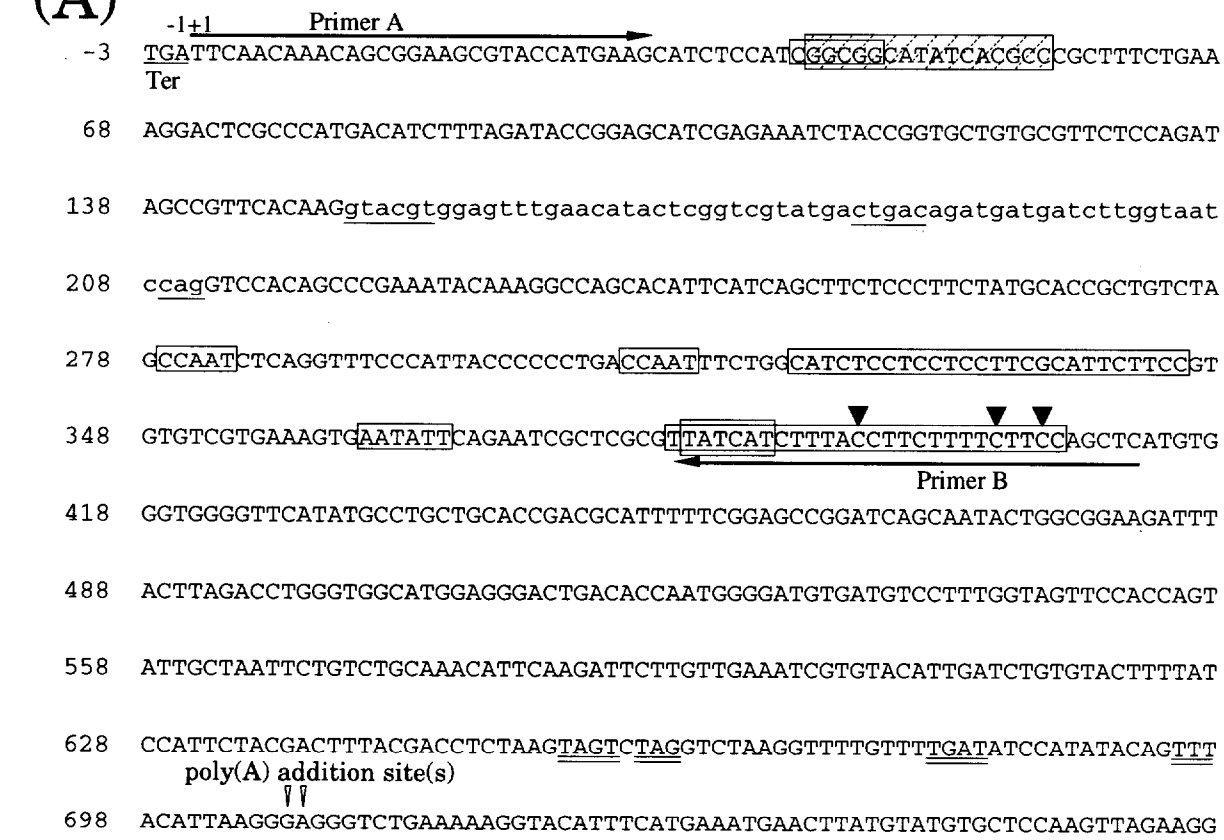

Figure 5.1

The nucleotide sequence (A) and the schematic diagram (B) of the 3'-noncoding region of the *priB* gene

(A) Two CT/AG-biased sequences are boxed and shaded. One GC box-like sequence, two CAAT boxes, two TATA box-like sequences are boxed. The 16-bp sequence similar to the consensus sequence of PRIB-binding site is boxed and striped. The termination codon (Ter) of the *priB* gene and the 61-bp intron are shown in italics and lower-case letters, respectively. Consensus sequences for splicing are underlined. Putative signals for transcription termination and poly (A) addition are double-underlined. Poly (A) addition site(s) is also shown. The nucleotide sequence coordinates are presented on the left-hand side. The nucleotide next to the termination codon of *priB* is assigned the +1 coordinate. Two primers (A and B) used for PCR are indicated by horizontal long arrows. Closed arrowheads are transcriptional initiation sites determined in Fig. 5.7 for the modified *lacZ* gene in *S. cerevisiae*. The sequence data reported in this paper will appear in the DDBJ/EMBL/GenBank nucleotide sequence databases under accession No. D14489. (B) The first nucleotide each of the 16-bp sequence, 61-bp intron, core promoter elements and CT/AG-biased sequences are indicated. Poly (A) addition site(s) and restriction sites of *Bam*HI, *Eco*RI and *Pst*I are shown by indicating their first nucleotide positions.

transformations and plasmid amplifications. *S. cerevisiae* YPH499 (*Mat a, ura3-52, lys2-801, ade2-101, trp1-Δ63, his3-Δ200, leu2-Δ1*) (Sikorski and Hieter, 1989) was transformed with the chromosome-integrating vector YIp32 carrying yeast ß-isopropylmalate dehydrogenase (*LEU2*) gene (Botstein *et al.*, 1979). The Leu^+ prototrophic YPH499 strain (described as YPH499(Leu^+)) was used for yeast transformations.

5.2.2 Construction of plasmids

pBR322 derivatives carrying the promoter consensus-like sequences and CT/AG-biased sequences of the 3'-regulatory region of the *priB* gene were constructed as follows (Fig. 5.2). The 0.41-kb and 0.35-kb fragments containing the promoter-like sequences of the *priB* 3'-regulatory region were obtained by PCR using the cloned 1.2-kb *Pst*I - *Bam*HI genomic DNA fragment (see Fig. 5.1B) and the 2.7-kb *priB* cDNA fragment, respectively, as templates. Two primers (primer 3'-F, 5'-TTCAACAAACAGCGGAAGCGTACCATGAAG and primer 3'-R, 5'-GAGCTGGAAGAAAAGAAGGTAAAGATGATA) (see Fig. 5.1A) were used for the experiments. The 0.41-kb and 0.35-kb fragments were ligated to the *Bam*HI adaptor (5'-CCGGATCCGG) and inserted into the *Bam*HI site of pUC19 after digestion with *Bam*HI, yielding pUC-3'NCR and pUC-3'UTR, respectively (NCR denotes noncoding region of genomic DNA and UTR is untranslated region of cDNA). The 3'NCR and 3'UTR are the identical sequence only except that the former contains an intron (61 bp). In pUC-3'NCR and pUC-3'UTR the purine-rich sequence is on the *lacZ*-coding strand of pUC19. The two recombinant plasmids were digested with *Eco*RI and *Pst*I and the resulting 0.45-kb and 0.39-kb *Eco*RI - *Pst*I fragments containing the 3'NCR and 3'UTR were inserted between the *Eco*RI and *Pst*I sites of pBR322, yielding pBR-3'NCR and pBR-3'UTR. In these plasmids the purine-rich sequence is on the tetracycline-resistance gene (*tet*)-coding strand of pBR322.

Plasmids used for transformation of *S. cerevisiae*, which contain the modified *lacZ* gene as a reporter, were constructed as follows (see Fig. 5.2 and 5.3). The 0.54-kb fragment containing the promoter region of *S. cerevisiae LEU2* gene and *Eco*RI and *Bam*HI restriction sites of each end was obtained by PCR using plasmid YIp32 as a template and two oligonucleotides (primer E, 5'-GGGAATTCGGCTTCCTTGTTC ATGTGTGTT and primer B, 5'-CCGGATCCTAGAATGGTATATCCTTGAAAT) as primers. This 0.54-kb fragment was digested with *Eco*RI and *Bam*HI and inserted between the *Eco*RI and *Bam*HI sites of pUC19, yielding pUC-LEU2pro. Plasmid pLC1-gen (Kajiwara, 1993), containing the aminoglycoside 3'-phosphotransferase gene (*aph1*) derived from transposon Tn903 (Oka *et al.*, 1981; Lang-Hinrichs *et al.*, 1989) was digested with *Bam*HI. The 1.2-kb *Bam*HI fragment containing the *aph1* sequence with a translational initiation site was fused after the 3'NCR on pUC-3'NCR, the 3'UTR on pUC-3'UTR, and the *LEU2* promoter on pUC-LEU2pro by using *Bam*HI site. These three recombinant plasmids were partially (or completely) digested with *Bam*HI to convert the DNA to a linear form and recircularized by self-ligation after the ends had been filled-up. By these treatments, the junctions between the DNA fragments to be analyzed and *aph1* sequence converted to be *Bam*HI-uncleavable sequence. These modified plasmids were digested with *Nru*I, ligated to the *Eco*RI adaptor (5'-CGGATCCG) and digested with *Bam*HI and *Eco*RI (or *Eco*RI alone). The 0.47-kb and 0.41-kb *Bam*HI - *Eco*RI fragments containing the 3'NCR plus 36 bp *aph1* sequence and the 3'UTR plus 36-bp *aph1* sequence, respectively, and the 0.60-kb *Eco*RI fragment containing the *LEU2* promoter sequence plus 36-bp *aph1* sequence were inserted between the *Bam*HI and *Eco*RI sites or into the *Eco*RI site of the yeast autonomously replicating plasmid vector YEp356R carrying the *lacZ'* sequence lacking the promoter and 5'-terminal sequence encoding the N-terminal 8 amino acids of ß-galactosidase, yielding YEp3'NCR-lacZ, YEp3'UTR-lacZ and YEpLEU2pro-lacZ, respectively (see Fig. 5.3). As a promoterless control, plasmid YEp-lacZ was also constructed as follows. pUC-3'NCR.aph1 (see Fig. 5.2) was

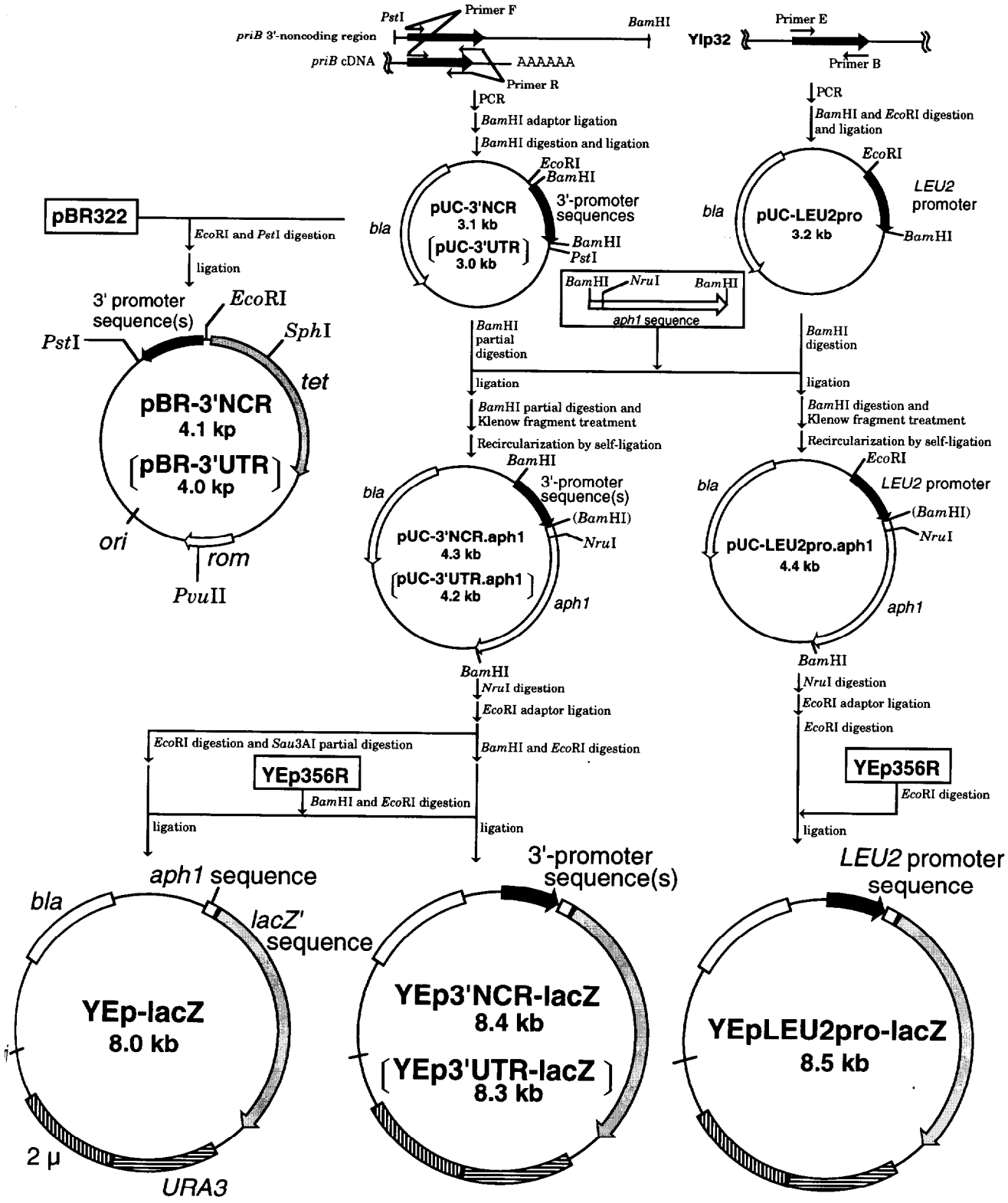

Figure 5.2

Construction of plasmids pBR-3'NCR (4.1 kb), pBR-3'UTR (4.0 kb), YEp3'NCR-lacZ (8.4 kb), YEp3'UTR-lacZ (8.3 kb), YEp-lacZ (8.0 kb) and YEpLEU2pro-lacZ (8.5 kb)

In pBR-3'NCR and pBR-3'UTR the purine-rich sequence was on the pBR322 *tet*-coding strand. Locations and directions of transcription of the *tet* gene (Brosius et al., 1982) and the *rom* gene (Watson, 1988) location of the origin of replication (*ori*), and restriction sites of *Eco*RI (4069), *Sph*I (562), *Pvu*II (2064) and *Pst*I (3607) on the pBR322 genome (Watson, 1988) are indicated. In YEp-lacZ, the *aph1* sequence, *lacZ'* gene, ß-lactamase gene (*bla*), *S. cerevisiae URA3* gene, the origin (*ori*) of replication in *E. coli* and the sequence (2 μ) derived from 2 μm plasmid containing the origin of replication in *S. cerevisiae* are shown. The names of these sequences are omitted in YEp3'NCR-lacZ, YEp3'UTR-lacZ and YEpLEU2pro-lacZ. Restriction sites of *Bam*HI, *Eco*RI, *Nru*I and *Pst*I are shown and the modified, uncleavable *Bam*HI sites are shown in parentheses.

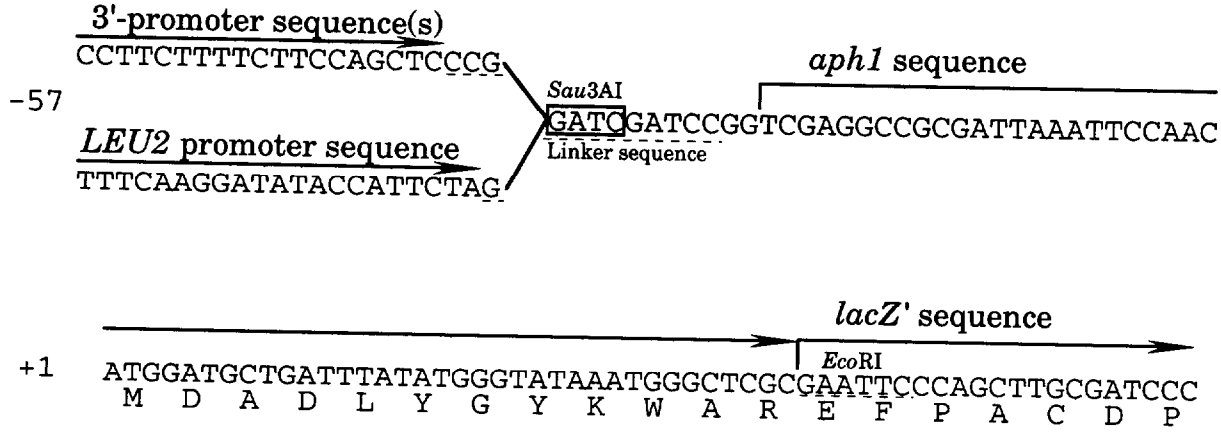

Figure 5.3 The nucleotide sequence of the 5'-flanking region of the modified *lacZ* gene

The nucleotide and deduced amino acid sequences of YEp3'NCR-lacZ, YEp3' UTR-lacZ and YEpLEU2pro-lacZ at the fusion junction between the end of promoter sequences, *aph1* sequence containing 12 amino-acids translation initiation site and *LacZ'* gene. The nucleotide sequence coordinates are presented on the left-hand side. The start codon of the fusion protein (APH1 and LacZ) is assigned the +1 coordinate.

digested with *Nru*I and ligated to the *Eco*RI adaptor (5'-CGGATCCG). The 72-bp *Eco*RI - *Sau*3AI fragment containing 36-bp *aph1* sequence was inserted between the *Bam*HI and *Eco*RI sites of YEp356R.

5.2.3 Preparation of plasmid DNAs

LB medium containing 4 µg and 40 µg of tetracycline per ml was used to grow the *E. coli* DM800 and JM109 transformants, respectively, carrying pBR322, pBR-3'NCR and pBR-3'UTR. LB medium containing 50 µg of ampicillin per ml was used to grow all the JM109 transformants carrying the pUC-based recombinant plasmids. Cells were grown at 37°C with aeration to late exponential phase ($A_{600} \approx$ 0.7), quickly chilled and centrifuged. Plasmid DNAs were extracted and purified according to the method described previously (Shishido *et al.*, 1987).

5.2.4 S1 Nuclease digestion and gel electrophoresis

These were done as described in Materials and methods of Chapter 3 (section 3.2.3).

5.2.5 Primer extension analysis for determination of S1-cleavage sites

This was done as described in Materials and methods of Chapter 3 (section 3.2.5).

5.2.6 Yeast transformation

S. cerevisiae transformation was performed by the lithium-acetate method according to Ito *et al.* (1983). For the selection of Ura^+ transformants, cells were spreaded on SD medium-agar plates (0.7 % yeast nitrogen base, 2% dextrose, 2% agar) containing 40 µg/ml of adenine, 20 µg/ml of L-histidine, 30 µg/ml L-lysine and 40 µg/ml L-tryptophane. The plates were incubated at 30°C for 3 days. When required, L-leucine and L-threonine were added to the medium to give a final

concentration of 60 µg/ml or 200 µg/ml, respectively.

5.2.7 Assay of ß-galactosidase activity

The ß-galactosidase activity was assayed by measuring the degradation of *o*-nitrophenyl-ß-D-galactoside (ONPG) (Miller, 1972; Guarente, 1983). Permeabilized cells of plasmid-harboring *S. cerevisiae* were prepared according to the method reported by Guarente (Guarente, 1983). The cells (1×10^7) were suspended to 1 ml of Z buffer (Per liter, 16.1 g of $Na_2HPO_4 \cdot 7H_2O$, 5.5 g of $NaH_2PO_4 \cdot H_2O$, 0.75 g of KCl, 0.246 g of $MgSO_4 \cdot 7H_2O$, 2.7 ml of 2-mercaptoethanol; pH 7.0). Three drops of chloroform and two drops of 0.1 % SDS were added and vortexed at top speed for 10 seconds. The mixture was preincubated in water bath at 28°C for 5 minutes and then, briefly, 0.2 ml of a 4 mg/ml ONPG stock solution was added to the mixture. The reaction was stopped by adding 0.5 ml of 1 M Na_2CO_3. The optical density at 420 nm was measured. Assays are normalized to the OD_{600} of the culture and to the assay time and the specific activity (units) of ß-galactosidase was calculated according to the following formula: $1000 \times OD_{420}$ / time of the reaction (min) × volume of culture used in assay (in ml) × OD_{600} (Miller, 1972; Guarente, 1983).

5.2.8 Mapping of the transcriptional initiation sites by the primer extension analysis

This was done as described in Materials and methods of Chapter 4 (section 4.2.10).

5.3 Results

5.3.1 Analysis of S1-cleavability of pBR322 and its derivatives

To investigate whether the CT/AG-biased sequences of the 3'-regulatory region of the *priB* gene form S1-cleavable, nonbase-paired sites, DNAs of pBR322 and its derivatives isolated from *E. coli* topoisomerase I deletion mutant DM800 (*ΔtopA gyrB225*) (Sternglanz *et al.*, 1981; DiNardo *et al.*, 1982) were analyzed by the methods using for the *ras* and *priA* CT/AG-biased sequences (see sections 3.3.1 and 4.3.1.). DNAs were digested with S1 at pH 4.5 and the full-length S1-linearized DNAs were further digested with restriction endonucleases which have a single unique cleavage site on the DNAs (see Fig. 5.2). Figure 5.4 shows the agarose gel electrophoretic patterns obtained for pBR322, pBR-3'UTR and pBR-3'NCR isolated from DM800. pBR-3'NCR (pBR-3'UTR) is pBR322 derivative containing the *priB* 3'-noncoding region (the *priB* 3'-noncoding region lacking the 61-bp intron). *Pvu*II- and *Sph*I-digests of the S1-linearized pBR322 (containing ~ 50 % open-circular DNA) yielded a number of discrete and two intense DNA bands on the gels (lanes 1 and 4, respectively, see sections 3.3.1 and 4.3.1). In both cases of *Pvu*II- and *Sph*I-digests of the S1-linearized pBR-3'UTR (lanes 2 and 5) and pBR-3'NCR (lanes 3 and 6), two additional relatively intense DNA bands were observed at 2.4 and 1.6 kb, 3.1 and 0.9 kb, respectively, for the former, and at 2.5 and 1.6 kb, 3.1 and 1.0 kb, respectively, for the latter. The sizes of the two fragments summed up to the nearly full-length size (4011 bp and 4072 bp) of the plasmid DNAs, showing the generation of another preferential cleavage site (region) on both pBR-3'UTR and pBR-3'NCR. This site (region) was found to fall around the CT/AG-biased sequences of both plasmids. On the other hand, DNAs of pBR-3'UTR and pBR-3'NCR isolated from JM109 (*topA*$^+$ *gyrA96*) (Yanisch-Perron *et al.*, 1985), as well as these of pBR-CT[ras] and pBR-invCT[ras] (see Chapter 3), were not preferentially cleaved by S1 around the CT/AG-sequences, generating the

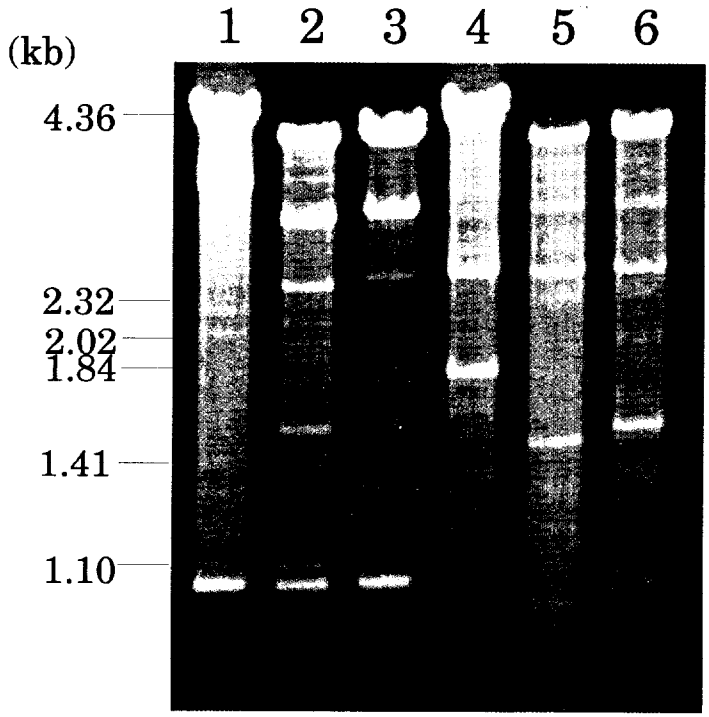

Figure 5.4

DNA fragments produced after digestion of the S1-generated unit-length linear pBR322, pBR-3'NCR and pBR-3'UTR (each containing ~50 % open circular DNA) with restriction endonucleases

The S1-digested DNAs were then digested with *Pvu*II (lanes 1-3) and *Sph*I (lanes 4-6) (see Fig. 5.2). Lanes 1 and 4, pBR322; lanes 2 and 5, pBR-3'UTR; lanes 3 and 6, pBR-3'NCR. The *Hin*dIII-digest of phage λ DNA and *Hinc*II- and *Pvu*II-digests of pBR322 DNA were used as molecular size markers. Sizes (kb) are indicated to the left in the panel.

corresponding two faint DNA bands in each of the cases of *Pvu*II- and *Sph*I-digestion (data not shown).

5.3.2 Mapping of the S1-cleavage sites around the CT/AG-biased sequences of pBR322 derivative pBR-3'NCR

The S1-cleavage sites were analyzed by the primer extension method using the following two primers; primer H, 5'-GCAATTTAACTGTGAT complementary to the sequence from 64 to 49 of pBR322, primer P, 5'-GCTAGAGTAAGTAGTT identical with the sequence from 3557 to 3571 of pBR322 (see Fig. 5.2). In the *Pvu*II-digests of the S1-linearized pBR-3'NCR (lane 3 of Fig. 5.4), DNA fragments at/around the two relatively intense bands (2.5 and 1.6 kb) were subjected to analysis. In the extension of the CT-rich strand (the larger fragment and primer H), one intense and three faint bands were observed at the positions of the nucleotide 382 (T) and the nucleotides 308 (A) 333 (T) and 366 (T), respectively, on the CT-rich strand (panel A of Fig. 5.5), indicating that the template (AG-rich) strand ended at the positions marked by arrows in Fig. 5.6, i. e., S1-cleavages occurred at the arrow positions. In the case of the AG-rich strand (the smaller fragment and primer P), sixteen bands were observed at the positions of nucleotides 380 (G), 386 (G), 388 (A) ~ 390 (A), 392 (A) ~ 399 (A), 403 (G) 406 (G) and 408 (T) on the AG-rich strand (panel B of Fig. 5.5). The ends of the CT-rich template strand (the sites of S1 cleavage) are marked by arrows in Fig. 5.6. These data demonstrate that the majority of S1-cleavage sites fall within and around the downstream CT/AG-biased sequence, showing the downstream CT/AG-biased sequence forms the extended open structure sensitive to S1 cleavage.

5.3.3 Expression of the modified *lacZ* gene in *S. cerevisiae* under control of the *priB* 3'-regulatory region

To examine whether the *priB* 3'-regulatory region containing the promoter-like sequences and CT-motifs exhibit actually promoter activity in *S. cerevisiae*, the

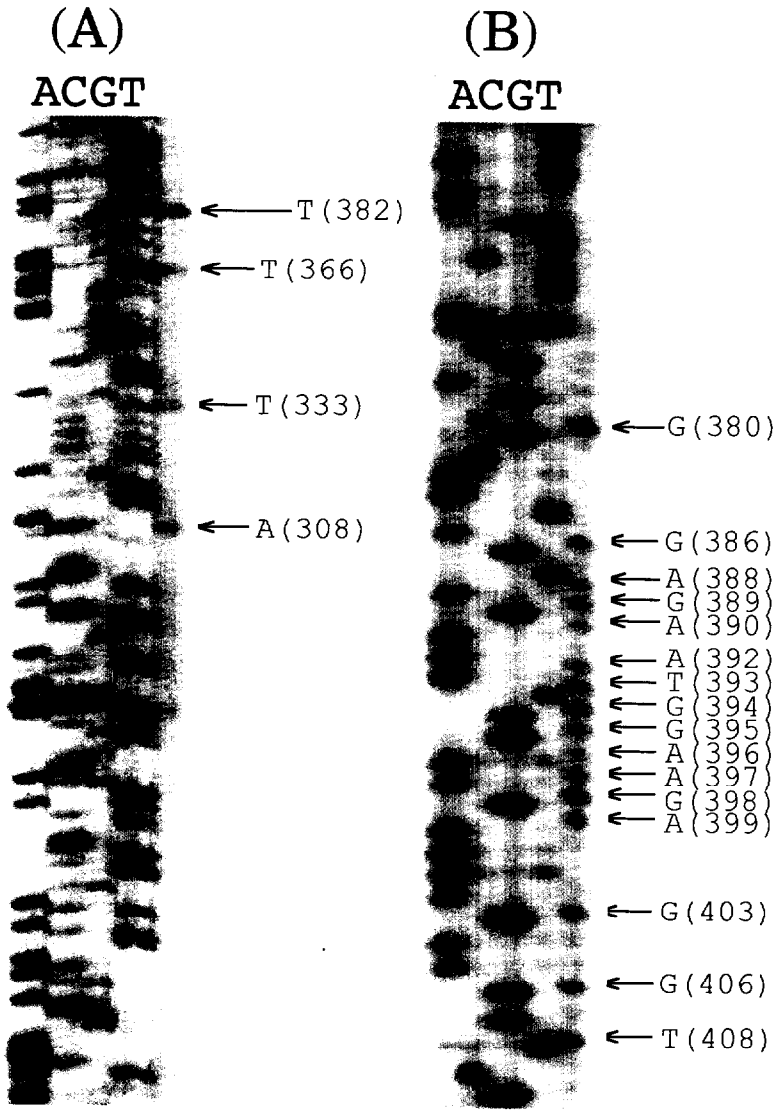

Figure 5.5

Determination of the S1-cleavage sites within/around the CT/AG-biased sequences of pBR-3'NCR by the primer extension method

The extensions of the CT-rich strand with primer H (A) and the AG-rich strand with primer P (B) were carried out using the larger or smaller fragment of the *Pvu*II-digests of pBR-3'NCR (see Fig. 5.4). The nucleotides corresponding to the ends of extension products (marked by arrows) were determined from the sequence ladders (ACGT) which were derived from pBR-3'NCR with primers H and P. The numbers in the parentheses are the nucleotide positions derived from the coordinates of Fig. 5.1.

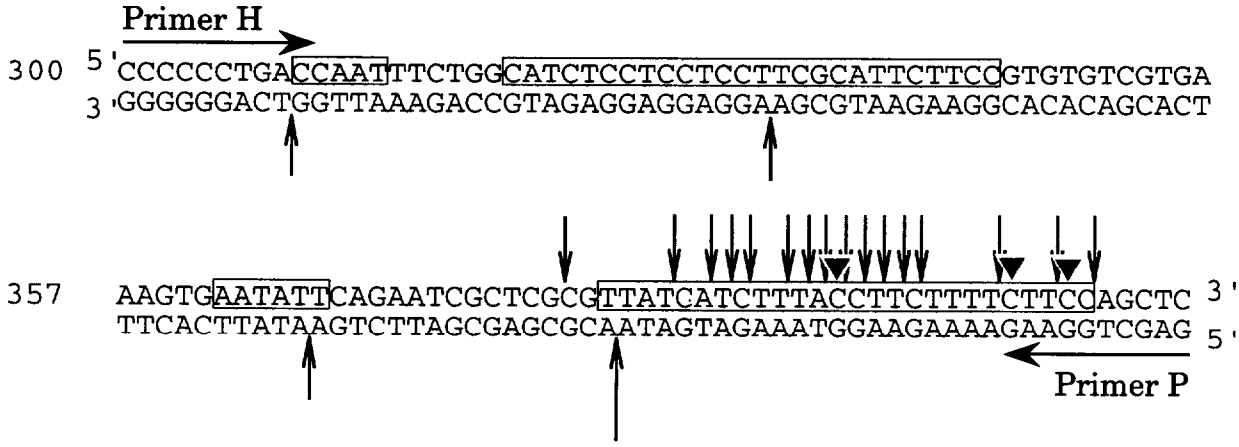

Figure 5.6

Summary of the S1-cleavage sites within/around the CT/AG-biased sequences of the 3'-regulatory region of the *priB* gene

The two 26-bp CT/AG-biased sequences, CCAAT box and TATA box-like sequence are boxed. The S1-cleavage sites on the template strand in the extensions of the CT and AG strands are shown by vertical arrows. Their lengths correspond to the frequencies of S1 cleavages judged from the results of panels A and B of Fig. 5.5, with the more preferential sites marked by long arrows. In the figure, three transcriptional initiation sites determined for the modified *lacZ* gene in *S. cerevisiae* in Fig. 5.7 are shown by arrowheads.

autonomously replicating YEp356R (Myers *et al.*, 1986a; Rose and Botstein, 1983) -based plasmids YEp3'NCR-lacZ and YEp3'UTR-lacZ were constructed (Fig 5.2A). By using these plasmids, the promoter activity can be measured quantitatively as a ß-galactosidase activity. YEpLEU2pro-lacZ and YEp-lacZ were also constructed. The former contains *S. cerevisiae LEU2* promoter and the latter contains no promoter (see Fig. 5.2 and 5.3). These plasmids were introduced into *S. cerevisiae* cells and the transformants with the plasmid were selected. The activity of ß-galactosidase was measured for these transformants grown in SD medium supplemented with leucine and threonine. Table 5.1 shows the ß-galactosidase activities of the *S. cerevisiae* transformants carrying the aforementioned plasmids. When the ß-galactosidase activity conferred by YEpLEU2pro-lacZ was taken as 100, the activities conferred by YEp3'NCR-lacZ and YEp3'UTR-lacZ were 55.5 % and 107.0 %, respectively. The activity conferred by YEp-lacZ was nearly zero. When transformants carrying YEpLEU2pro-lacZ was grown in the absence of leucine and threonine, about 11-fold increase of the ß-galactosidase activity was observed (Table 5.1). These results strongly suggest that the *priB* 3'-regulatory region actually function as a promoter in *S. cerevisiae.* This activity is similar to the activity of the *S. cerevisiae LEU2* promoter expressed under the repressed condition (in the presence of leucine and threonine). The intron present in the 3'-promoter region is considered to have an inhibitory effect on the promoter activity because YEp3'UTR-lacZ conferred higher ß-galactosidase activity than YEp3'NCR-lacZ.

5.3.4 Mapping of the transcriptional initiation sites of the modified *lacZ* gene on YEp3'NCR-lacZ and YEp3'UTR-lacZ

Transcriptional initiation sites of the 36-bp *aph1* sequence - *lacZ* fusion gene on YEp3'NCR-lacZ and YEp3'UTR-lacZ were analyzed by the primer extension method. The 17-base M13 Primer (5'-GTTTTCCCAGTCACGAC) was used as a primer. As shown in Fig. 5.7, the primer extension of the modified *lacZ* transcripts

Table 5.1 ß-galactosidase activity in *S. cerevisiae* strain YPH499(Leu$^+$)

Plasmids	Specific enzyme activity (units) [a]	Relative activity (%) [b]
YEp3'NCR-lacZ	11.1	55.5
YEp3'UTR-lacZ	21.4	107.7
YEpLEU2pro-lacZ [c]	20.0	100.0
YEpLEU2pro-lacZ [d]	226.7	1133.5
YEp-lacZ	< 0.1	< 0.1

[a] ß-galactosidase units were calculated as described in Materials and methods. Units shown are the average of 3 independent experiments.

[b,c] The activity of the transformant carrying YEpLEU2pro-lacZ grown in SD medium supplemented with leucine and threonine at concentrations of 60 µg/ml and 200 µg/ml, respectively, was taken as 100.

[d] The transformant carrying YEpLEU2pro-lacZ was grown in SD minimal medium without leucine and threonine.

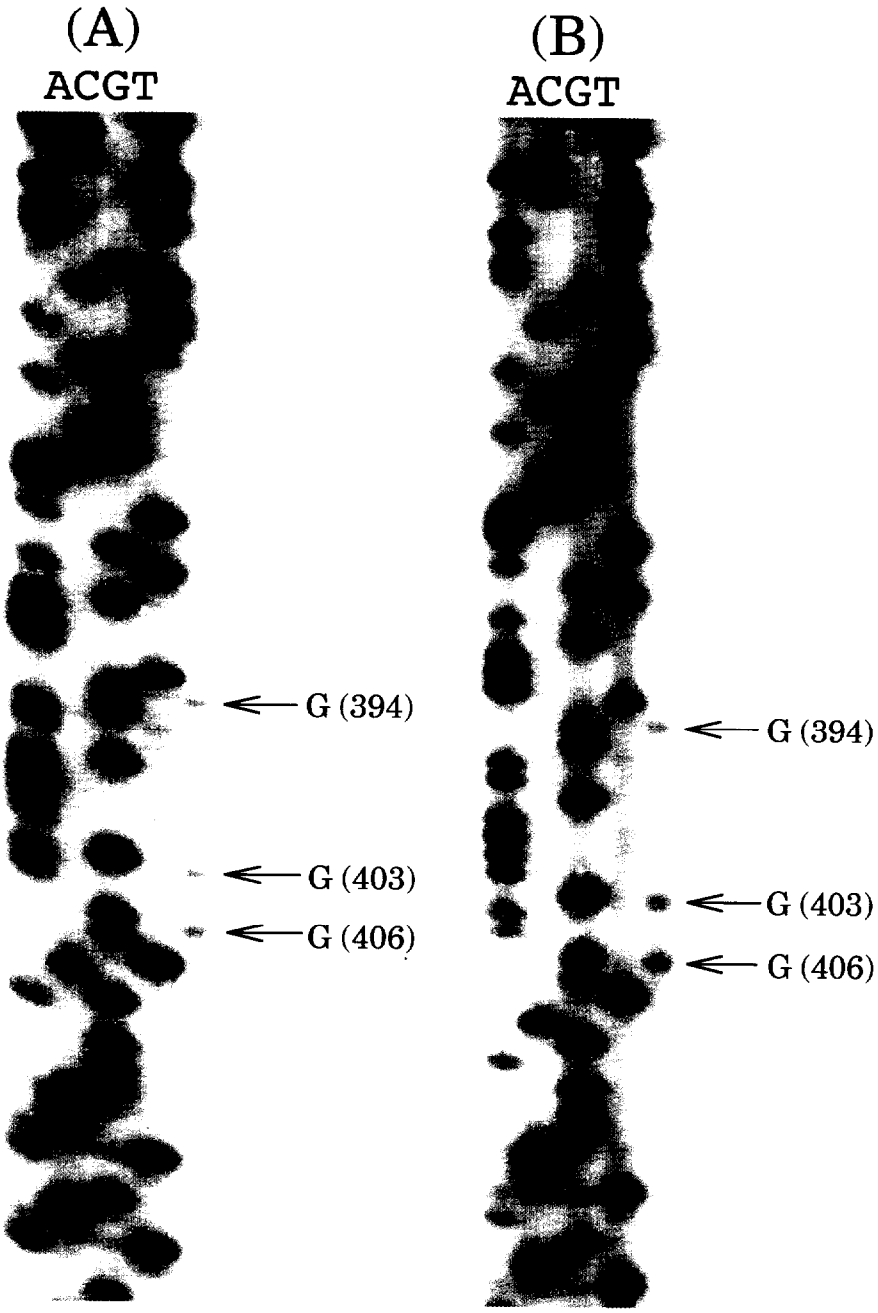

Figure 5.7

Determination of the transcriptional initiation sites in *S. cerevisiae* of the modified *lacZ* gene on YEp3'NCR-lacZ and YEp3'UTR-lacZ by the primer extension method

Poly $(A)^+$ RNA prepared from the *S. cerevisiae* transformants carrying plasmids YEp3'NCR-lacZ (A) and YEp3'UTR-lacZ (B) were subjected to the analysis. The sizes of the primer extension products were determined from the sequencing ladders (ACGT) which were derived from YEp3'NCR-lacZ and YEp3'UTR-lacZ using the 17-base M13 primer M4 (see Materials and methods) as the sequencing primer. The numbers (nt 394, 403 and 406) shown in the figure corresponds to the numbers of the nucleotide indicated by closed arrowheads in Fig. 5.1A and Fig. 5.6.

isolated from the yeast transformant carrying YEp3'NCR-lacZ (A) or YEp3'UTR-lacZ (B) gave three bands at the positions corresponding to the nucleotides 394, 403 and 406 on the 3'-regulatory region of the *priB* gene. These three transcriptional initiation sites all fall within the downstream CT-motif (see the closed arrowheads in Fig. 5.1A and Fig. 5.6). These results show the downstream CT-motif is essential for initiation of the transcription of the modified *lacZ* in *S. cerevisiae.*

5.4 Discussion

In this chapter, we described a promoter activity in *S. cerevisiae* of the 3'-regulatory region of the *priB* gene. This is the first report showing a promoter activity of the 3'-regulatory region of the gene.

S1 nuclease analysis of plasmid pBR322 DNA containing the 3'-regulatory region of the *priB* gene isolated from *E. coli* DM800 revealed that this region forms an unusual, extended open structure within/around the downstream CT/AG-biased sequence. As like the CT/AG-biased sequence of the *Le.ras* promoter region, the CT/AG-biased sequence of the *priB* 3'-regulatory region also require higher levels of negative supercoiling for formation of the preferentially S1-cleavable (stable), nonbase-paired structure.

The majority of S1-cleavage sites fallen within and around the downstream CT/AG-biased sequence, showing the downstream CT/AG-biased sequence forms the extended open structure sensitive to S1 cleavage. It is interesting to note that the mirror repeat responsible for an intramolecular triplex structure is found only in the downstream CT/AG-biased sequence. The S1-cleavage sites determined by the extension of the AG-rich strand did not coincide with those of the CT-rich strand. This suggests that S1 cleavages occurred simultaneously at site(s) on the AG-strand and on the CT-strand, and then second S1 cuts occurred on the opposite strand at or near the sites nicked first to yield linear DNA molecules slightly

smaller than full length size.

The three transcriptional initiation sites determined by primer extension method in *S. cerevisiae* all fell within the downstream CT-motif (see the closed arrowheads in Fig. 5.1A and Fig. 5.6). This result shows the downstream CT-motif is essential for initiation of the transcription of the modified *lacZ* in *S. cerevisiae*. As described above, the downstream CT/AG-biased sequence of the *priB* 3'-regulatory region in negatively supercoiled pBR322 DNA forms S1-cleavable, nonbase-paired sites. This unusual structure (presumably triplex structure) may be formed also in the YEp-plasmids in *S. cerevisiae* and function in it. Other eukaryotic promoter consensus (-like) elements of the *priB* 3'-region also may be involved in an expression of promoter activity because, as already described above, the intron present between the GC box-like element and CCAAT boxes does affect the promoter activity.

Concerning the biological function of the 3'-regulatory region of the *priB* gene in the basidiomycete *L. edodes*, the followings are considered. The 5'-upstream region of the *priB* gene contains the four binding sequences of the *priB* gene product (PRIB protein) (Miyazaki, 1998). Similar PRIB-binding sequence is present in the *priB* 3'-regulatory region (see Fig. 5.1). So there is the possibility that the *priB* gene is regulated by the PRIB protein through its binding to 5'- and 3'-region of the *priB* gene; the 3'-regulatory region may play as a sort of "enhancer" element for the transcription of the *priB* gene. The other possibility is that the usual 5'-promoter of some gene was inserted between the end of coding region and the transcriptional termination signal plus poly (A) addition site(s) of the *priB* gene. To verify whether the former thought is correct, an *in vitro* analysis may be also required.

Chapter 6

Conclusions

The experimental results obtained in this study showed that the CT/AG-biased sequences having a mirror repeat sequence originated from the 5'-promoter regions of the *Le. ras* and *priA* genes and the 3'-regulatory region of the *priB* gene form an extended S1-cleavable open structure in supercoiled pBR322 DNA.

Putative intramolecular triplex structures (H-y3 isomers) induced by the *ras* and *priA* CT/AG-biased sequences, which are inferred from the distributions of the S1-cleavage site were depicted in Fig. 6.1A and B, respectively. To investigate that these triplex structures were actually formed *in vitro*, two-dimensional chloroquine-agarose gel electrophoretic analysis of the pBR322 derivatives containing the CT/AG-biased sequence was performed under the following conditions. The DNAs were electrophoresed in low pH (≤6.0) buffer containing no chloroquine in the first dimension and in neutral pH buffer containing chloroquine in the second dimension. If the CT/AG-biased sequences form the stable intramolecular triplex structure, one would expect the detection of a break or irregular pulse in the topoisomer arc under these conditions (Shimizu *et al.*, 1990). Unfortunately, a positive indication of the presence of intramolecular triplex structure was not obtained in the experiments (data not shown). Probably, the CT/AG-biased sequences could not form the intramolecular triplex structure very stably under the conditions of the electrophoresis. They may form the triplex structure under more restricted conditions *in vitro*. Alternatively, since the pBR322 derivatives containing these CT/AG-biased sequences is large DNA molecules, a large number of topoisomers were generated by interaction of chloroquine, resulting in failure of detection of a break or irregular pulse during electrophoresis.

It is very interesting that the *priA* promoter containing the only two point

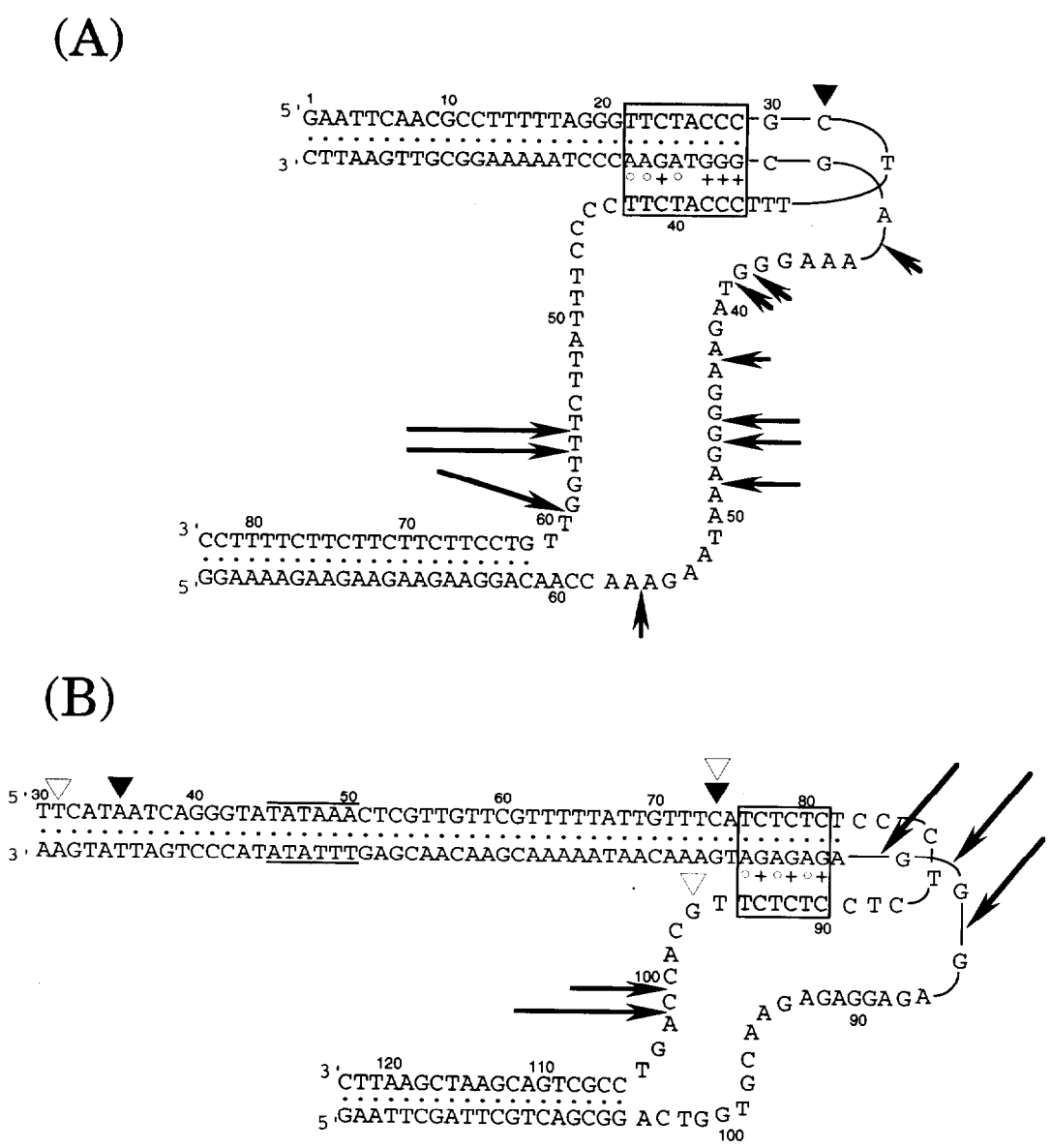

Figure 6.1

Putative intramolecular triplex structures formed in the CT/AG-biased sequences of the *ras* (A) and *priA* (B) genes

Putative intramolecular triplex structures (H-y3 isomers) induced by the *ras* and *priA* CT/AG-biased sequences, which are inferred from the distributions of the S1-cleavage site were depicted. The S1-cleavage sites on the template strand in the extensions of the CT and AG strands are shown by arrows. Their lengths correspond to the frequencies of S1 cleavages judged from the results of Fig. 3.3 and 4.3, with the most preferential sites marked by long arrows. Mirror repeat sequences involved in forming intramolecular triplex structures are shaded and the triplehelix DNA regions are boxed. The canonical Watson-Crick base pairing (•), Hoogsteen base pairing (AoT and C+G) are shown. Closed and open arrowheads show transcriptional initiation sites in *L. edodes* and *C. cinereus*, respectively.

mutations (the replacement of two dTMP residues by dGMP residues) in the counterpart of the mirror repeat of the CT/AG-biased sequence resulted in a loss of the two transcriptional initiation sites upstream of the mirror repeat in *C. cinereus*. An S1-cleavable structure was not formed within the mutated CT/AG-biased sequence of the *priA* gene. The importance of the mirror repeat sequence strongly suggests that the mirror repeat sequence of the *priA* CT/AG-biased sequence is involved in the formation of the non-B, unusual DNA structure formation, presumably an intramolecular triplex structure formation. In this study, the non-B, unusual DNA structure formed in the CT/AG-biased sequence was shown to play an important role for expression of the *priA* promoter activity toward a transgene in basidiomycetes.

DNA is not a conformationally homogeneous molecule. In other words, DNA has the capability of adopting several types of conformations as dictated by its sequences. In higher eukaryotic cells, chromosomal DNA conformation may be varied alternately when transcription, replication and recombination initiates, or possibly, the non-B DNA conformations may not be especially unusual. I am afraid the experimental data shown in this study are not sufficient to reveal the function of the non-B, unusual DNA structures formed in the CT/AG-biased sequences originated from *L. edodes* genes in basidiomycetes. However, I hope this study to give valuable and novel informations for understanding the regulation mechanism of gene expression in basidiomycetes.

References

Asada, Y., Watanabe , A., Irie, T., Nakayama, T. and Kuwahara, M. (1995) Structures of genomic and complementary DNAs coding for *Pleurotus ostreatus* manganese (II) peroxidase. *Biochim. Biophys. Acta*, **1251**, 205-209.

Baran, N., Lapidot, A. and Manor, H. (1991) Formation of DNA triplexes accounts for arrests of DNA synthesis at d(TC)n and d(GA)n tracts. *Proc. Natl. Acad. Sci. USA*, **88**, 507-511.

Binninger, D.M., Skrzynia, C., Pukkila, P.J. and Casselton, L.A. (1987) DNA-mediated transformation of the basidiomycete *Coprinus cinereus*. *EMBO Journal*, **6**, 835-840.

Botstein, D., Falco, S.C., Stewart, S.E., Brennan, M., Scherer, S., Stinchcomb, D.T., Struhl, K. and Davis, R.W. (1979) Sterile host yeasts (SHY): a eukaryotic system of biological containment for recombinant DNA experiments. *Gene*, **8**, 17-24.

Bradford, M.M. (1976) A rapid and sensitive method for quantitation of microgram quantities of protein utilizing the principle of protein-dye binding. *Anal. Biochem.*, **72**, 248-254.

Breathnach, R. and Chambon, P. (1981) Organization and expression of eucaryotic split genes coding for proteins. *Annu. Rev. Biochem.*, 349-383.

Brinton, B.T., Caddle, M.S. and Heintz, N.H. (1991) Position and orientation-dependent effects of a eukaryotic Z-triplex DNA motif on episomal DNA replication in COS-7 cells. *J. Biol. Chem.*, **266**, 5153-5161.

Brosius, J., Cate, R.L. and Perlmutter, A.P. (1982) Precise location of two promoters for the beta-lactamase gene of pBR322. S1 mapping of ribonucleic acid isolated from *Escherichia coli* or synthesized *in vitro*. *J. Biol. Chem.*, **257**, 9205-9210.

DiNardo, S., Voelkel, K.A., Sternglanz, R., Reynolds, A.E. and Wright, A. (1982)

Escherichia coli DNA topoisomerase I mutants have compensatory mutations in DNA gyrase genes. *Cell*, **31**, 43-51.

Endo, H., Kajiwara, S., Tsunoka, O. and Shishido, K. (1994) A novel cDNA, *priBc*, encoding a protein with a Zn(II)2Cys6 zinc cluster DNA-binding motif, derived from the basidiomycete *Lentinus edodes*. *Gene*, **139**, 117-121.

Guarente, L. (1983) Yeast promoters and *LacZ* fusions designed to study expression of cloned genes in yeast. *Methods Enzymol.*, **101**, 181-191.

Gurr, S.J., Uncles, S.E. and Kinghorn, J.R. (1988) The structure and organization of nuclear genes in filamentous fungi. In *Gene Structure in Eukaryotic Microbes*. (Kinghorn, J.R. ed.) IRL Press, Oxford, pp. 93-139.

Hanvey, J.C., Shimizu, M. and Wells, R.D. (1988) Intramolecular DNA triplexes in supercoiled plasmids. *Proc. Natl. Acad. Sci. USA*, **85**, 6292-6296.

Hori, K., Kajiwara, S., Saito, T., Miyazawa, H., Katayose, Y. and Shishido, K. (1991) Cloning, sequence analysis and transcriptional expression of a *ras* gene of the edible basidiomycete *Lentinus edodes*. *Gene*, **105**, 91-96.

Ishibashi, O. and Shishido, K. (1993) Nucleotide sequence of a *ras* gene from the basidiomycete *Coprinus cinereus*. *Gene*, **125**, 233-234.

Ito, H., Fukuda, Y., Murata, K. and Kimura, A. (1983) Transformation of intact yeast cells treated with alkali cations. *J. Bacteriol.*, **153**, 163-168.

Johnson, P.F. and McKnight, S.L. (1989) Eukaryotic transcriptional regulatory proteins. *Annu. Rev. Biochem.*, **58**, 799-839.

Kadonaga, J.T., Jones, K.A. and Tjian, R. (1986) Promoter-specific activation of RNA polymerase II transcription by Sp1. *Trends Biochem. Sci.*, **11**, 20-23.

Kajiwara, S. (1993) Molecular Genetical Studies on *ras* Gene and Fruiting Genes of Eubasidiomycetes. Ph. D thesis, Tokyo Institute of Technology.

Kajiwara, S. and Shishido, K. (1992) Characterization of the promoter region of the basidiomycete *Lentinus edodes Le.ras* gene. *FEMS Lett.*, **92**, 147-150.

Kajiwara, S., Yamaoka, K., Hori, K., Miyazawa, H., Saito, T., Kanno, T. and Shishido, K. (1992) Isolation and sequence of a developmentally regulated

putative novel gene, *priA*, from the basidiomycete *Lentinus edodes*. *Gene*, **114**, 173-178.

Kaneko, S., Miyazaki, Y., Yasuda, T. and Shishido, K. (1998) Cloning, sequence analysis and expression of the basidiomycete *Lentinus edodes* gene *uck1*, encoding UMP-CMP kinase, the homologue of *Saccharomyces cerevisae URA6* gene. *Gene*, **211**, 259-266.

Kang, S.M., Wohlrab, F. and Wells, R.D. (1992) Metal ions cause the isomerization of certain intramolecular triplexes. *J. Biol. Chem.*, **267**, 1259-1264.

Kato, M. and Shimizu, N. (1992) Effect of the potential triplex DNA region on the *in vitro* expression of bacterial ß-lactamase gene in superhelical recombinant plasmids. *J. Biochem.*, **112**, 492-494.

Kersten, M.A., Muller, Y., Baars, J.J., Op den Camp, H.J., van der Drift, C., Van Griensven, L.J., Visser, J. and Schaap, P.J. (1999) NAD^+-dependent glutamate dehydrogenase of the edible mushroom *Agaricus bisporus*: biochemical and molecular characterization. *Mol. Gen. Genet.*, **261**, 452-462.

Kohwi, Y. and Kohwi-Shigematsu, T. (1988) Magnesium ion-dependent triple-helix structure formed by homopurine-homopyrimidine sequences in supercoiled plasmid DNA. *Proc. Natl. Acad. Sci. USA*, **85**, 3781-3785.

Kohwi, Y. and Kohwi-Shigematsu, T. (1991) Altered gene expression correlates with DNA structure. *Genes&Dev.*, **5**, 2547-2554.

Kohwi-Shigematsu, T. and Kohwi, Y. (1991) Detection of triple-helix related structures adopted by poly(dG)-poly(dC) sequences in supercoiled plasmid DNA. *Nucleic Acids Res.*, **19**, 4267-4271.

Kondoh, O., Muto, A., Kajiwara, S., Takagi, J., Saito, U. and Shishido, K. (1995) A fruiting body-specific cDNA, *mfbAc*, from the mushroom *Lentinus edodes* encodes a high-molecular-weight cell-adhesion protein containing an Arg-Gly-Asp motif. *Gene*, **154**, 31-37.

Kuriki, Y. (1987) Response to temperature shifts of expression of the *amp* gene on pBR322 in *Escherichia coli* K-12. *J. Bacteriol.*, **169**, 2294-2297.

Lang-Hinrichs, C., Berndorff, D., Seefeldt, C. and Stahl, U. (1989) G418 resistance in the yeast *Saccharomyces cerevisiae*: comparison of the neomycin resistance genes from Tn5 and Tn903. *Appl. Microbiol. Biotechnol.*, **30**, 388-394.

Lilley, D.M. (1980) The inverted repeat as a recognizable structural feature in supercoiled DNA molecules. *Proc. Natl. Acad. Sci. USA*, **77**, 6468-6472.

Lyamichev, V.I., Mirkin, S.M. and Frank-Kamenetskii, M.D. (1985) A pH-dependent structural transition in the homopurine-homopyrimidine tract in superhelical DNA. *J. Biomol. Struct. Dyn.*, **3**, 327-338.

Lyamichev, V.I., Mirkin, S.M., Kumarev, V.P., Baranova, L.V., Vologodskii, A.V. and Frank-Kamenetskii, M.D. (1989) Energetics of the B-H transition in supercoiled DNA carrying d(CT)x.d(AG)x and d(C)n.d(G)n inserts. *Nucleic Acids Res.*, **17**, 9417-9423.

Maniatis, T., Goodbourn, S. and Fischer, J.A. (1987) Regulation of inducible and tissue-specific gene expression. *Science*, **236**, 1237-1245.

Miller, J.H. (1972) *Experiments in Molecular Genetics.* Cold Spring Harbor Laboratory, Cold Spring Habor, New York.

Mirkin, S.M., Lyamichev, V.I., Drushlyak, K.N., Dobrynin, V.N., Filippov, S.A. and Frank-Kamenetskii, M.D. (1987) DNA H form requires a homopurine-homopyrimidine mirror repeat. *Nature*, **330**, 495-497.

Miyazaki, Y. (1998) Molecular biological and biochemical studies on the DNA-binding proteins involved in fruiting development of the basidiomycete *Lentinus edodes.* Ph. D Thesis, Tokyo Institute of Technology.

Miyazaki, Y., Tsunoka, O. and Shishido, K. (1997) Determination of the DNA-binding sequences of the Zn(II)2Cys6 zinc-cluster-containing PRIB protein, derived from the basidiomycete *Lentinus edodes* gene. *J. Biochem.*, **122**, 1088-1091.

Murchie, A.I. and Lilley, D.M. (1992) Supercoiled DNA and cruciform structures. *Methods Enzymol.*, **211**, 158-180.

Myers, A.M., Tzagoloff, A., Kinney, D.M. and Lusty, C.J. (1986a) Yeast shuttle and integrative vectors with multiple cloning sites suitable for construction of *lacZ* fusions. *Gene*, **45**, 299-310.

Myers, R.M., Tilly, K. and Maniatis, T. (1986b) Fine structure genetic analysis of a ß-globin promoter. *Science*, **232**, 613-618.

Oka, A., Sugisaki, H. and Takanami, M. (1981) Nucleotide sequence of the kanamycin resistance transposon Tn903. *J. Mol. Biol.*, **147**, 217-226.

Panayotatos, N. and Wells, R.D. (1981) Cruciform structures in supercoiled DNA. *Nature*, **289**, 466-470.

Pruss, G.J. (1985) DNA topoisomerase I mutants. Increased heterogeneity in linking number and other replicon-dependent changes in DNA supercoiling. *J. Mol. Biol.*, **185**, 51-63.

Pruss, G.J. and Drlika, K. (1986) Topoisomerase I mutants: the gene on pBR322 that encodes resistance to tetracycline affects plasmid DNA supercoiling. *Proc. Natl. Acad. Sci. USA*, **83**, 8952-8956.

Rose, M. and Botstein, D. (1983) Construction and use of gene fusions to *lacZ* (ß-galactosidase) that are expressed in yeast. *Methods Enzymol.*, **101**, 167-180.

Sambrook, J., Fritsch, E.F., Maniatis, T. (1989) *Molecular cloning, a laboratory manual, Second edition.* Cold Spring Harbor Laboratory Press, New York.

Sanger, F., Nicklen, S. and Coulson, A.R. (1977) DNA sequencing with chain-terminating inhibitors. *Proc. Natl. Acad. Sci. USA*, **74**, 5463-5467.

Schaap, P.J., Müller, Y., Baars, J.J., Op den Camp, H.J., Sonnenberg, A.S., van Griensven, L.J. and Visser, J. (1996) Nucleotide sequence and expression of the gene encoding $NADP^+$- dependent glutamate dehydrogenase (*gdhA*) from *Agaricus bisporus*. *Mol. Gen. Genet.*, **250**, 339-347.

Schuren, F.H. and Wessels, J.G. (1990) Two genes specifically expressed in fruiting dikaryons of *Schizophyllum commune*: homologies with a gene not regulated by mating-type genes. *Gene*, **90**, 199-205.

Shimizu, M., Hanvey, J.C. and Wells, R.D. (1989) Intramolecular DNA triplexes in supercoiled plasmids. I. Effect of loop size on formation and stability. *J. Biol. Chem.*, **264**, 5944-5949.

Shimizu, M., Hanvey, J.C. and Wells, R.D. (1990) Multiple non-B-DNA conformations of polypurine·polypyrimidine sequences in plasmids. *Biochemistry*, **29**, 4704-4713.

Shimizu, M., Kubo, K., Matumoto, U. and Shindo, H. (1994) The loop sequence plays crucial roles for isomerization of intramolecular DNA triplexes in supercoiled plasmids. *J. Mol. Biol.*, **235**, 185-197.

Shishido, K. (1979) Location of S1 nuclease-cleavage sites on circular, superhelical DNAs between polyoma virus and simian virus 40. *Agric. Biol. Chem.*, **43**, 1093-1102.

Shishido, K. and Ando, T. (1982) Single-strand-specific nucleases. In *Nucleases*. (Linn, S.M. and Roberts, R.J. eds.) Cold Spring Harbor Laboratory Press, Cold Spring Harbor, NY, pp. 155-185.

Shishido, K., Ishii, S. and Komiyama, Y. (1989) The presence of the region on pBR322 that encodes resistance to tetracycline is responsible for high levels of plasmid DNA knotting in *Escherichia coli* DNA topoisomerase I deletion mutant. *Nucleic Acids Res.*, **17**, 9749-9759.

Shishido, K., Komiyama, N. and Ikawa, S. (1987) Increased production of a knotted form of plasmid pBR322 DNA in *Escherichia coli* DNA topoisomerase mutants. *J. Mol. Biol.*, **195**, 215-218.

Sikorski, R.S. and Hieter, P. (1989) A system of shuttle vectors and yeast host strains designed for efficient manipulation of DNA in *Saccharomyces cerevisiae*. *Genetics*, **122**, 19-27.

Skrzynia, C., Binninger, D.M., Alspaugh II, J.A. and Pukkila, P.J. (1989) Molecular

characterization of *TRP1*, a gene coding for tryptophan synthetase in the basidiomycete *Coprinus cinereus*. *Gene*, **81**, 73-82.

Smale, S.T. and Baltimore, D. (1989) The "initiator" as a transcription control element. *Cell*, **57**, 103-113.

Southern, E.M. (1975) Detection of specific sequences among DNA fragments separated by gel electrophoresis. *J. Mol. Biol.*, **98**, 503-517.

Sternglanz, R., DiNardo, S., Voelkel, K.A., Nishimura, Y., Hirota, Y., Becherer, K., Zumstein, L. and Wang, J.C. (1981) Mutations in the gene coding for *Escherichia coli* DNA topoisomerase I affect transcription and transposition. *Proc. Natl. Acad. Sci. USA*, **78**, 2747-2751.

Tsao, Y.P., Wu, H.-Y. and Liu, L.F. (1989) Transcription-driven supercoiling of DNA: direct biochemical evidence from *in vitro* studies. *Cell*, **56**, 111-118.

Ulmer, D.C., Leisola, M.S.A. and Fiechter, A. (1984) Possible induction of the ligninolytic system of *Phanerochaete chrysosporium*. *J. Biotechnol.*, **1**, 13-24.

Watson, N. (1988) A new revision of the sequence of plasmid pBR322. *Gene*, **70**, 399-403.

Weinreb, A., Collier, D.A., Birshtein, B.K. and Wells, R.D. (1990) Left-handed Z-DNA and intramolecular triplex formation at the site of an unequal sister chromatid exchange. *J. Biol. Chem.*, **265**, 1352-1359.

Wells, R.D., Collier, D.A., Hanvey, J.C., Shimizu, M. and Whohlrab, F. (1988) The chemistry and biology of unusual DNA structures adopted by oligopurine·oligopyrimidine sequences. *FASEB J.*, **2**, 2939-2949.

Wendland, J. and Kothe, E. (1996) Allelic divergence at B α 1 pheromone receptor genes of *Schizophyllum commune*. *FEMS Lett.*, **145**, 451-455.

Wu, H.-Y., Shyy, S.H., Wang, J.C. and Liu, L.F. (1988) Transcription generates positively and negatively supercoiled domains in the template. *Cell*, **53**, 433-440.

Yanisch-Perron, C., Vieira, J. and Messing, J. (1985) Improved M13 phage cloning vectors and host strains: nucleotide sequences of the M13mp18 and pUC19 vectors. *Gene*, **33**, 103-119.

Zaret, K.S. and Sherman, F. (1982) DNA sequence required for efficient transcription termination in yeast. *Cell*, **28**, 563-573.

Zolan, M.E. and Pukkila, P.J. (1986) Inheritance of DNA methylation in *Coprinus cinereus*. *Mol. Cell. Biol.*, **6**, 195-200.

List of Papers

Papers for Dissertation

1. Yamazaki, T., Hasebe, T., Shouguchi, J., Amano, H., Kajiwara, S. and Shishido, K. (1997) Structure and function in *Escherichia coli* of plasmids containing pyrimidine/purine-biased stretch originated from the 5'-flanking region of the basidiomycete *ras* gene. *J. Biochem.* **122**, 696-702

2. Ogawa, K., Yamazaki, T., Hasebe, T., Kajiwara, S., Watanabe, A., Asada, Y. and Shishido, K. (1998) Molecular breeding of the basidiomycete *Coprinus cinereus* strains with high lignin-degradation activity using novel heterologous protein expression vector. *Applied Microbiol. Biotechnol.* **49** (3), 285-289

3. Yamazaki, T., Hasebe, T., Kajiwara, S., Shishido, K. (2000) Structure and function of a pyrimidine/purine-biased sequence from the 5'-flanking region of the basidiomycete *Lentinus edodes* gene *priA*., *Mol. Gen. Genet.*, **263**, 262-270

4. Yanai, K., Yonekura, K., Usami, H., Hirayama, M., Kajiwara, S., Yamazaki, T., Shishido, K. and Adachi, T. (1996) The integrative transformation of *Pleurotus ostreatus* using bialaphos resistance as a dominant selectable marker. *Biosci. Biotech. Biochem.* **60** (3), 472-475

5. Yamazaki, T., Yasuda, T., Miyazaki, Y., Okada, K., Kajiwara, S., Shishido, K. A promoter activity in *Saccharomyces cerevisiae* of the 3'-noncoding region of the basidiomycetous mushroom gene. submitted.

Other Papers

1. Ishibashi, O., Yamazaki, T. and Shishido, K. (1996) A fruiting body-specific novel cDNA, *mfbBc*, containing continuous 5'-CCA(A/C)CA direct repeats within the coding region, derived from the basidiomycete *Lentinula edodes. Mycoscience* **37** 227-232

2. Shishido, K., Ogawa, K., Kikuchi, M., Yamazaki, T., Hasebe, T., Kajiwara, S., Watanabe, A., Asada, Y., Sugio, A. and Nakamura, S. (1998) Construction of novel heterologous protein expression vectors and use for molecular breeding of *Coprinus cinereus* strains with high lignin- and xylan-degradading activities, In *Proceedings of the fourth meeting on the genetics and cellular biology of basidiomycetes* (Van Griensven, L. and Vesser, J., eds.), Mushroom Experimental Station, Netherlands, 76-82

3. Shishido, K., Ogawa, K., Matsuda, S., Kikuchi, M., Yamazaki, T., Kajiwa Tsukamoto, A. and Sugiura, J. (1999) Heterologous protein expression vectors and molecular breeding of basidiomycetous fungi strains with high lignin- and xylan-degrading activities, In *Proceedings of 20th Fungal Genetics Conference* (March 23-28, 1999, Asilomar Conference Center, Pacific Grove, California), p. 18

4. Kikuchi, M., Ogawa, K., Yamazaki, T., Kajiwara, S., Sugio, A., Nakamura, S. and Shishido, K. (1999) Secretional Expression of *Bacillus subtilis* Xylanase Gene in the Basidiomycete *Coprinus cinereus. FEMS Microbiol. Lett.* **178** 277-282

Acknowledgements

I would like to express my deep gratitude to Professor Kazuo Shishido, Ph. D, Department of Life Science, Graduate School of Bioscience and Biotechnology, Tokyo Institute of Technology, for his support, advice, encouragement, and patience during the whole course of the work.

I am extremely grateful to Associate Professor Susumu Kajiwara, Ph. D, Department of Life Science, Graduate School of Bioscience and Biotechnology, Tokyo Institute of Technology, for his significant comments and helpful advice in valuable discussions.

I am deeply grateful to Ms. Mutsuko Hayashi-Komatsu, Technical Official of Department of Life Science, Graduate School of Bioscience and Biotechnology, Tokyo Institute of Technology, for her assistance and attentiveness.

I wish to thank all members of our laboratory at Tokyo Institute of Technology, for their helpful encouragement and assistance.

I am extremely thankful to all my families and friends...

January, 2000